PhD THESIS

Presented at

UNIVERSITÉ DU QUÉBEC À CHICOUTIMI

IN PARTIAL FULFILLMENT OF REQUIREMENTS FOR

THE DEGREE OF DOCTOR OF PHILOSOPHY IN ENGINEERING

BY

Pierre, TCHAKOUA TAKOUTSING

A NEW APPROACH FOR ELECTRIC MODELING OF VERTICAL AXIS WIND

TURBINE ROTORS IN VIEW TO THE CONSTRUCTION OF A GLOBAL

ELECTRIC MODEL FOR THE WIND ENERGY CONVERSION SYSTEM

Québec, Canada

THÈSE DE DOCTORAT

Présentée

À L'UNIVERSITÉ DU QUÉBEC À CHICOUTIMI

COMME EXIGENCE PARTIELLE DE L'OBTENTION DU GRADE

DE DOCTEUR EN PHILOSOHIE EN INGÉNIERIE

PAR

Pierre, TCHAKOUA TAKOUTSING

NOUVELLE APPROCHE DE MODÉLISATION ÉLECTRIQUE DES ROTORS

D'ÉOLIENNES À AXE VERTICAL EN VUE DE LA CONSTRUCTION D'UN

MODÈLE ÉLECTRIQUE GLOBAL DE LA CHAINE DE CONVERSION

ÉOLIENNE

Québec, Canada

Abstract

The combine effects of climate changes, the continue and considerable increase of energy demand in the world, the instability of fossil fuel prices as well as the energetic dependence of some countries who are not fuel producers leads to important development of renewable energies. More again, the energy bill in its dizzying rise causes the prices increase for raw materials, goods and even basic necessities. It is therefore imperative to go in for diversification of energy sources on the one hand and means to produce energy at a relatively low cost on the other hand.

This thesis proposes a novel approach for aerodynamic modelling of Darrieus type vertical axes wind turbines (VAWTs). Indeed, it is a contribution to the build-up of a global electric model for vertical axis wind turbine conversion system with a view to improve monitoring, diagnosis and maintenance.

The goal of this research work is double: firstly, to propose an innovative approach for aerodynamic modelling of VAWTs and secondly, based on this approach, to build a new equivalent electric model for the study, analysis and aerodynamic optimisation of Darrieus type VAWTs. More broadly, this work aims to contribute to the development of new tools, techniques and methods to improve the design, optimization, diagnosis, prognosis and monitoring of Darrieus VAWTs to better ensure their maintenance. The purpose is to provide the scientific community and the wind turbine industry with new tools that can ameliorate the reliability and thus increase performance and efficiency of Darrieus type VAWTs.

An equivalent electric circuit model for three-blade DT-VAWT rotors was builded. The new model that we named the Tchakoua model is based on a recently developed

approach for modelling DT-VAWT rotors using the equivalent electrical circuit analogy. The proposed model was built from the mechanical description given by the Paraschivoiu double-multiple streamtube model and was based on an analogy between mechanical and electrical circuits. Thus, the rotating blades and the blades' mechanical coupling to the shaft are modelled using the mechanical-electrical analogy, and the wind flow is modelled as a source of electric current.

Model simulations were conducted using MATLAB for a three-bladed rotor architecture, characterized by a NACA0012 profile, an average Reynolds number of 40,000 for the blade and a tip speed ratio of 5. The results obtained show strong agreement with findings from both aerodynamic and computational fluid dynamics (CFD) models in the literature.

Keywords: *Renewable energy, wind turbine; Darrieus turbines; vertical axis wind turbine; condition monitoring, diagnosis, maintenance, modelling; electric circuit model; aerodynamic characteristics; performance analysis; Tchakoua model*

RÉSUMÉ

Les effets conjugués du réchauffement climatique, l'augmentation considérable et continue de la demande énergétique mondiale, la volatilité des prix des énergies fossiles, la dépendance énergétique de certains pays non producteurs de pétrole, font que les énergies renouvelables bénéficient actuellement d'un essor très important. De plus, la facture énergétique dans sa hausse vertigineuse entraîne les matières premières, les biens de consommation et même les produits de première nécessité. Il est donc impératif de réfléchir à la diversification des sources d'énergie d'une part et aux moyens de produire de l'énergie à un coup relativement bas d'autre part.

Cette thèse propose un modèle électrique équivalent pour les rotors d'éoliennes à axes vertical. Elle constitue une contribution à la construction d'un modèle électrique global de la chaine de conversion éolienne.

L'objectif de cette recherche est d'une part de proposer une nouvelle approche de modélisation des éoliennes à axe vertical; et d'autre part d'élaborer, sur la base de cette approche, un nouveau modèle pour l'étude, l'analyse et l'optimisation aérodynamique des éoliennes à axe vertical de type Darrieus. De façon plus large, ce travail vise à contribuer au développement de nouveaux outils, techniques et méthodes devant permettre d'améliorer la conception, l'optimisation, le diagnostic, le pronostic et la surveillance des éoliennes à axe vertical de type Darrieus afin de mieux assurer leur maintenance. La finalité étant de mettre à la disposition de la communauté scientifique et de l'industrie de l'éolienne de nouveaux outils pouvant permettre d'accroître la performance aérodynamique ainsi que le rendement énergétique des éoliennes à axe vertical de type Darrieus.

Un modèle électrique équivaut pour rotor d'éolienne de type Darrius tri-pales a été développé. Ce nouveau modèle que nous avons nommé le 'Tchakoua model' est basé sur une nouvelle approche de modélisation des rotors d'éoliennes à axe vertical utilisant des circuits électriques équivalents. Le modèle a été construit sur la base de description à double disque actuateur à multiple tubes de vent faite par Paraschivoiu et est basé sur l'analogie circuits mécaniques et circuits électriques appliquée à l'aérodynamique. Ainsi, les pales et le couplage mécanique à l'arbre lent sont modélisées en utilisant l'analogie mécanique-électrique tandis que l'écoulement de vent est modélisé comme source de courant.

Les simulations ont été effectuées avec le logiciel MATLAB pour un rotor tripal caractérisé par un profil NACA0012, un nombre de Reynold moyen de 40000 et une vitesse spécifique de 5. Une validation croisée de ces résultats avec les données issues des modèles aérodynamiques ou même des modèles numériques de dynamique des fluides montre de bonnes concordances.

Mots clés : *Énergie éolienne, éolienne de Darrieus, éolienne à axe vertical, surveillance, diagnostic, maintenance, modélisation, circuit électrique équivalent, caractéristiques aérodynamiques, Tchakoua Model*

Dedication

To those who gave me life.

To my dear wife.

To my children.

Acknowledgements

I hereby express my gratitude to all those who contributed in any way to the successful completion of this work. I am grateful to my thesis director Professor Fouad Slaoui (UQAC/UQAT) for the opportunity I was given to work on an interesting topic, my co-directors Professor Mohand Ouhrouche (UQAC) who have both been very instrumental in various parts of the project. Their technical advices and encouragements were invaluable. Thank you for allowing me in the harmonious and rich environment of your research groups and your professional networks.

I would like to express gratitude to my examiner Professors Issouf Fofana, Nahi Kandil and Mamadou Doumbia for accepting to evaluate this work and for providing guidance, encouragement, valuable suggestions and constructive advice on this thesis.

I really appreciate Dr Francois Nzokou, Dr Aimé Sylvain Fotso Talla, for providing valuable comments and suggestions.

I would also like to thank Professor Ernesto Benini, Gabriel Ekemb, Tommy-Andy Theubou, Ayang Albert for good collaboration. Thanks for countless hours, early runs to the laboratories and sleepless nights going through everything, from Matlab codes, data analysis, report writing and even correspondence with various Editors. I indeed learned a lot from you.

My gratitude also goes to my friends Donald Poirier and Mark Hislop, my beloved sister Marie Pascale Makougoum, my dear brothers Fokou Francis and Mukam Emmanuel, my uncles Anselme Tchamssik and Ngatsing Emmanuel, my aunts Chantal Majomo, Honorine Mache, my sister inlaw Jougne Larrissa, my late friend and brother Wilfried Yopa, not forgetting my parents in law, Fotsing Camille and Madjou Colette. You were all invaluable supports. Thank you for encouraging me when I felt like quitting. Although some of you were weakened by sickness or going trough difficult moments, you still loved and encouraged me even when I spent months without communicating with you.

My ultimate gratitude goes to my parents, Takoutsing Joseph and Mayo Francoise. You always told me not to forget that education is the most robust key to open the doors of professional and personal accomplishment. Both of you are the key of this success. It is because you taught me virtues of hardworking and perseverance, finally, I can accomplish this work.

My most heartfelt acknowledgement must go to my sweetheart Magakou Fotsing Merline Romance for her endless patience, love and support. Romy, may you find here an expression of my love.

Finally, to my son Tchakoua Nenda Fresnel Betz and daughter Tchakoua Maya Yopaela Kline, thank you for your love, which made this work so joyful. Both of you are inexhaustible sources of hope and determination.

Pierre Tchakoua Takoutsing

Table des matières

LIST OF TABLES

LIST OF FIGURES

LIST OF ABREVIATIONS

A_e Area of a blade element (m^2)

c Chord of the blade (m)

C_{eq} Equivalent or total coefficient

C_L Lift coefficient

C_D Drag coefficient

C_N Normal coefficient

C_T Tangential coefficient

F_N Normal force (N)

F_T Tangential force (N)

F_L Lift force (N)

F_D Drag force (N)

H Half of rotor's height (m)

$i_w(t)$ Instantaneous current that represents the incident wind flow ($A^* = N/m^2$)

I_T Current at the primary side of the transformer ($A^* = N/m^2$)

I_S Current at the secondary side of the transformer ($A^* = N/m^2$)

N_b Number of blades

q Relative dynamic pressure flow (N/m^2)

r Local radius of the blade (m)

R_D Drag resistance ($\Omega^* = m^2$)

R_L Lift resistance ($\Omega^* = m^2$)

R_W Resistance to wind flow ($\Omega^* = m^2$)

R_e Reynolds number ($\Omega^* = m^2$)

R Rotor radius (m)

S_B	Apparent power produced by the blade $(VA* = N^2/m^3)$
S_T	Total apparent power produced by the rotor $(VA* = N^2/m^3)$
T_B	Blade torque (N.m)
T_R	Rotor torque (N.m)
$v = 1.45 \times 10^{-5}$	Kinematic viscosity of air (m)
$V_R = V_S$	Total voltage across the blade $(V* = N.m)$
V_N	Normal voltage across the blade $(V* = N.m)$
$V_T = V_B$	Tangential voltage across the blade $(V* = N.m)$
$V_T = V_B$	Tangential voltage across the blade $(V* = N.m)$
W_0	Incoming wind speed (m/s)
W_b	Linear velocity of the blade (m/s)
W_r	Relative wind speed seen by the blade (m/s)
W_{rb}	Incident wind on the wind turbine rotor (m/s) (relative wind speed seen by the blade when aligning the blade motion with the negative real axis)
x_b	Blade shift position
X_L	Lift reactance $(\Omega* = m^2)$
X_D	Drag reactance $(\Omega* = m^2)$
z	Local height of the blade from H (m)
Z_D	Drag impedance $(\Omega* = m^2)$
Z_B	Total impedance of the blade $(\Omega* = m^2)$
$Z_N = R_B$	Normal impedance of the blade $(\Omega* = m^2)$
$Z_T = X_B$	Tangential impedance of the blade $(\Omega* = m^2)$
Z_L	Lift impedance $(\Omega* = m^2)$
α	Angle of attack or angle of the wind with respect to the X axis (deg)

δ	Pitch angle of the blade (deg)
φ	Angle of the relative wind speed (deg)
η	Angle of the blade relative to the vertical axis (deg)
θ_b	Azimuthal angle of the blade (deg)
λ	Blade tip speed ratio
ρ	Fluid density (kg/m^3)
Ψ	Modulus of the instantaneous current (A* = N/m^2)
ω	Rotational speed of the rotor (rad/s)
CFD	Computational fluid dynamics
DT-VAWTs	Darrieus-type vertical axis wind turbines
OM	Operations and maintenance
SCADA	Supervisory control and data acquisition
VAWTs	Vertical axis wind turbines
WECS	Wind energy conversion system
WTCM	Wind turbine condition monitoring

Chapter I

GENERAL INTRODUCTION

This chapter discusses the background of the work covered in this thesis, the challenges it tackled, its targeted objectives and an overview of its resulting scientific contributions.

1.1. INTRODUCTION

Electric energy is essential for the economic development in all countries of the world. It relative importance increases with technical progress, industrialization and the need for comfort in modern societies. The estimated share of renewable energy in global power generation (including hydropower) reached 24.5% in 2016 [1]. Indeed, in a world context marked by global climate warming, considerable and continuing increase in world energy demand, volatility of fossil fuel prices, energy dependency of certain non-oil producing countries, etc., renewable energies are growing steadily.
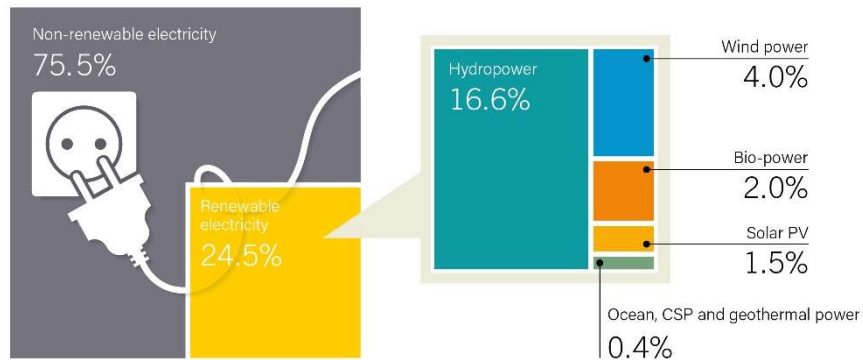
Figure I-1   Share of renewable energy in global power generation in 2016 [1].

Figure I-1 shows the structure of electricity generation and that of renewable electricity production in the world in 2016. As it can be seen, apart from hydroelectricity, wind energy sector represents the first renewable energy source. This tendency will be consolidated further for, with an average growth of 28% per year over the last 10 years, because wind energy is the most expanding renewable energy source in terms of installed capacity. In addition, according to GWEC (Global Wind Energy Council) forecasts, wind energy production could reach 2110 GW in 2030, which would then represent about 20% of the world's electricity consumption and could create up to 2.4 million new jobs [2], [3].

1.2. THESIS MOTIVATIONS

In recent years, there has been a renewed interest in vertical axis wind turbines (VAWTs). Indeed, VAWTs have several advantages compared to horizontal axis wind turbines (HAWTs). Among other advantages, VAWTs are insensitive to the wind speed and, consequently, do not require any orientation system with respect to wind direction [4], [5]. They are also less noisy than HAWTs, which make them more suitable for installation in urban environments. For these wind turbines, the gearbox and the generator can be placed at ground level, which makes maintenance easier and, as a result, reduces operating costs [6]. Also, VAWTs have greater resistance to strong winds. Finally, the wind speed slow down for VAWTs is lesser compare to that of HAWTs, therefore, VAWTs can be installed close to each other in a wind farm [7] . However, VAWTs have a major flaw that explains why they are not used on a large scale: their yield is much lower than that of HAWTs [8].

4.3.1. Socio-economic motivations

The reputation of wind industry amongst populations and communities in Quebec province is not of it best. Here are some of the reasons often mentioned:

- Wind energy is often more expensive than hydroelectricity produced by Hydro-Québec;

- Wind farms are important sources of noise pollution;

- The aesthetic aspect; indeed, the integration of wind turbines into the landscape and the appreciation of their appearance are major criteria in the acceptance of this mode of energy production;

- WTs contribute to the decimation of birds and bats populations.

3

Yet Quebec's wind energy potential is enormous and estimated between 8000 and 12000MW [9]. Moreover, the economic impact of wind energy production on communities is not negligible. In fact, in addition to the royalties paid, the wind sector provides many good jobs and therefore significantly contribute to stimulate local economy.

So as to make the most of this huge potential, the Québec government intends to encourage the production of electric power by private companies as well as cogeneration with the Hydro Québec network. In addition, it's about for Quebec, on one hand to continue to offer electricity at the lowest price in North America and, on the other hand, to have supplementary energy sources in order to overcome significant increase in energy demand observed during peak consumption (during episodes of extreme cold for example). Achieving these objectives and at the same time responding to community concerns require the implementation of reliable and low-cost technologies as well as the development of local expertise in the design, construction and maintenance of wind turbines.

Québec's new energy strategy forecasts a significant increase of the installed wind power by 2030 [9]. Wind turbines could be used for power compensation in long electric transmission lines. In addition, hybrid energy systems including wind turbines could be used to power villages, industrial projects or mines in the Far North of the province. It is in this perspective that the Cap d'Ours wind turbine was developed.

a) Brief presentation of the Cap d'Ours wind turbine

The 'Cap d'Ours' wind turbine is a 200-kW vertical axis wind turbine that was built by the Dermond company in 2004. It operated for about two years, producing electrical energy in a satisfactory quantity. 'Cap d'Ours' wind turbine is installed on a site located not far (a few hundred meters) from the main campus of UQAT in Rouyn-Noranda. The design

and construction of this wind turbine with special features was carried out as part of an innovative project. The Dermond company foresaw then to produce 12 of the wind turbine per year. These wind turbines where expected to be used, among other things, to supply the isolated communities of Nunavik with electricity.

In 2005, 'Cap d'Ours' wind turbine stopped operating and since then, it has never been restarted. It should be noted that the 'Cap d'Ours' wind turbine has been for many years at the mercy of bad weather and vandals. During this period, many equipment's of the structure were vandalized (destroyed and/or taken away) by looters. The wind turbine has lost several parts among its important equipment's. In addition, lack of maintenance and climatic hazards have contributed to weakening some aspects of its metal structure.

Figure I-2 Overview of the Cap d'Ours wind turbine.

Designed to withstand wind speeds greater than 220 km/h, the Cap d'Ours wind turbine turns out to be an ideal prototype for Canada's Far North, where winds are particularly strong [10]. Blais Industries, which is a Rouyn-Noranda-based company is owner of the Cap d'Ours wind turbine since the bankruptcy of the Dermond company in 2007. Recently Blais Industries agreed to put the impressive structure at the disposal of UQAT researchers. The company intends to use this wind turbine as a prototype for the development of wind turbine technology more appropriate for installation in Far North mining sites. To help achieve this goal, the UQAT School of Engineering is conducing various research projects that will contribute to optimize the structure, as well as reduce noise and vibrations during operation.

4.3.2. **Scientific motivations : problem statement**

In recent years, many research works have been conducted on the improvement of aerodynamic performance of VAWs. However, very few researchers dedicate their work to solve the problem of the lack of a more conducive rotor model for the conceptual optimization, the monitoring as well as the diagnosis and maintenance of Darrieus wind turbine rotors. This despite the growth of installed wind power worldwide and the renewed interest in VAWTs pose the thorny problem of research and staff training in the areas of optimization, diagnosis and maintenance of the wind turbines.

Wind turbines are equipment that can experience many hazards during their useful life. They are designed to work for a period of about 20 years [11], [12], [13]. Like all other mechanical systems, wind turbines are subject to many defects at the beginning and at the end of their life. In Canada, the wind energy industry very often practices reactive maintenance (repair when it breaks) [14]; the preventive maintenance is then limited to the instructions of the maintenance manual of the wind turbine manufacturer. Meanwhile, the

development of preventive maintenance strategies, as well as more efficient methods of diagnosis and troubleshooting, could significantly reduce the shortfall associated with maintenance operations of wind turbines; that is 10 to 20% of the revenues generated by the total production of the wind turbine during its lifetime [15]. Indeed, the application of a maintenance strategy that wisely combines preventive and reactive maintenance would certainly improve the reliability, availability and maintainability of wind turbines while reducing maintenance costs [16], [17].

Wind turbines are exposed to very harsh and variable climatic conditions, including: a binding weather alternating calm, violent winds, tropical heat, lightning, Siberian cold, rain, hail and snow. These extreme and variable conditions increase the mechanical stress on the structure of the wind turbine; thus, causing vibrations, risks of torsional resonances, numerous failures, and sometimes even the complete breakage of the wind turbine [18].
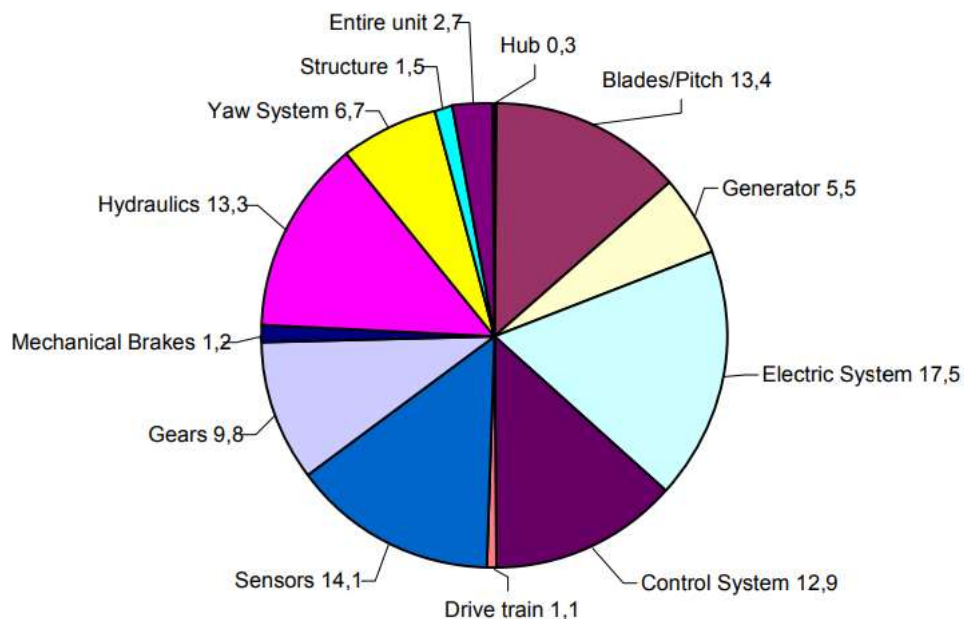
Figure I-3   Percentage of failures in a Swedish wind farm [19].

To these defects, can be added failures such as the deterioration of the sensors, the loss of efficiency of the actuators which control the blades, the short circuits of the WT windings, etc. The unfortunate consequences are, of course, the frequent shutdowns of production, the rapid aging of production equipment and the high cost of maintenance, all of which increases operating expenses. Figure I-3 shows the failure distribution of wind turbines with a nominal power greater than 490 kW between 2000 and 2004 in Sweden [19]. Theses statistics show that in a wind farm, electric system components are those who suffer more regularly from defects meanwhile, 13.4% of faults occurs on blades. On the other hand, rotor is one of the most expensive part of the wind turbine. Figure I-4 illustrates the breakdown of capital expenditure for onshore wind project [20], the component percentages are highlighted. It comes that rotor can represent up to 20% of the investment in a wind turbine. It is therefore essential to maintain rotors including blades, bearings and shaft as faultless as possible. This will reduce the maintenance downtimes and therefore ameliorate both reliability of energy production and profitability of the project.
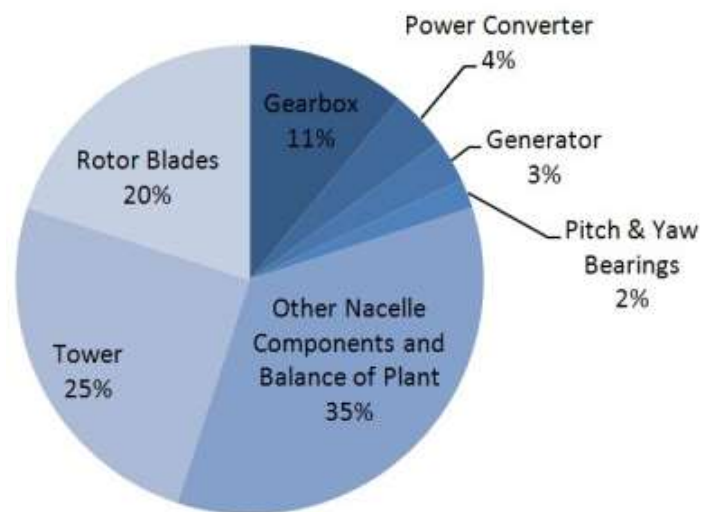
Figure I-4   Capital expenditures for onshore wind project [20]

It's becoming imperative for wind industry to develop appropriates advanced predictive maintenance methods that will quickly identify potential failures on rotors and correct them before complete part deterioration. A global electric model for the entire wind energy conversion system can be of great utility for achieve this goal.

1.3. THESIS GENERAL OBJECTIVES AND SCOPE

Considering all social, economic and scientific motivations mentioned above, we have chosen, within the framework of this doctoral thesis, to work on: contribution to the modeling and diagnosis of a vertical axis aerogenerator for maintenance.

In general, this work aims to contribute to the development of new tools, techniques and methods to improve the design, optimization, diagnosis, prognosis and monitoring of Darrieus vertical axis wind turbines to better ensure their maintenance. The goal is to enrich the scientific community and the wind turbine industry with new tools that can help to increase the aerodynamic performance and energy efficiency of Darrieus type AVEs. The development of an equivalent electric rotor model will therefore be the focus of our work. This model will be use in future research work to propose new methods for optimization, diagnosis and maintenance of wind turbines.

1.4. SPECIFIC OBJECTIVES AND LINK BETWEEN CHAPTERS

Achieving the general objective goes through several specific objectives. More specifically, this research work aims to:

1- Propose a new approach to modeling WTs rotors;

2- Develop, based on this approach, a new model for the study, analysis and aerodynamic optimization of Darrieus type VAWTs.

The thesis is subdivided into five chapters. Chapter I is a general introduction to the work. As well, it discusses the challenges tackle by this work. The motivations, objectives and limitations of the work. Chapter II is a review of WT condition monitoring techniques. State of the art, trends as well as challenges are addressed. It aimed to highlight the strengths and weaknesses of the different methods according to corresponding the state of the art. This allowed us to determine the need to develop an equivalent model of roto wind turbine that could improve the detection of defects occurring on the rotor. Chapter III establishes the foundations of a theoretical as well as the physical and mathematical concepts of an equivalent electric model capable of simulating the aerodynamic behavior of wind turbine rotors. The equivalent electric model for a single blade has thus been developed. Simulations and cross-validation were performed in MATLAB. Subsequently, using the validated model of a single blade, we perform in chapter IV the modulization of the mechanical link between the blades and the slow shaft of the rotor. Association all, we obtain the electric equivalent model of the whole three blades rotor for a Darrius type VAWT. Finally, chapter V conclude the thesis and gives some recommendations for future research works in continuity to this thesis.

1.5. THESIS LIMITATIONS

Once the scope of the project is defined, some limitation arises in order to fulfill the scope of the project. These limitations are as fallows:

- The model will be developed in the linear regime;

- The wind will be considered continuous and constant;

- The rotor mechanical coupling of three blades to the shaft is ideal.

1.6. CREDITS

The main part of this thesis consists of three chapters that where written in 'paper' style in order to favour publication of the results and ideas presented in this thesis. Chapters two, three and four are published in the journal Energies. All papers have been written by the author of this thesis, and all ideas presented are genuinely his. Supervisor of this thesis Fouad Slaoui Hasnaoui and cosupervisors Mohand Ouhrouche guided and helped the author to stay focused on the objectives of the study throughout the core of this thesis. René wamkeue, Gabriel Ekemb, Ernesto Benini and Tommy Andy Tameghe participated by assisting the author in results analysis and interpretation.

References

[1] Observ'ER, «La production d'électricité d'origine renouvelable dans le monde,» *Collection chiffres et statistiques. Neuvième inventaire-Edition,* 2007.

[2] «Renewables 2012 Global Status Report,» 2012.

[3] «Small Wind World Report 2012,» 2012.

[4] S. Shamsoddin et F. Porté-Agel, «Large Eddy Simulation of Vertical Axis Wind Turbine Wakes,» *Energies,* vol. 7, n° %12, pp. 890-912, 2014.

[5] F. Scheurich, «Modelling the aerodynamics of vertical-axis wind turbines,» 2011.

[6] F. Scheurich et R. E. Brown, «Modelling the aerodynamics of vertical-axis wind turbines in unsteady wind conditions,» *Wind Energy,* vol. 16, n° %11, pp. 91-107, 2013.

[7] M. R. Castelli, G. Grandi et E. Benini, «Numerical Analysis of the Performance of the DU91-W2-250 Airfoil for Straight-Bladed Vertical-Axis Wind Turbine Application,» chez *World Academy of Science, Engineering and Technology*, 2012.

[8] R. Lanzafame, S. Mauro et M. Messina, «2D CFD Modeling of H-Darrieus Wind Turbines using a Transition Turbulence Model,» *Energy Procedia,* vol. 45, pp. 131-140, 2014.

[9] G. Lafrance, «Oui aux renouvelables alternatifs,» Mémoire déposé dans le cadre de la Commission sur les enjeux énergétiques du Québec, 2013.

[10] G. Westerholm, «The wind energy frontier: Urban retail markets,» *Refocus,* vol. 5, n° %14, pp. 42-45, 2004.

[11] E. Echavarria, B. Hahn, G. J. W. et T. Tomiyama, «Reliability of Wind Turbine Technology Through Time,» *Journal of Solar Energy Engineering,* vol. 130, p. 31005, August 2008.

[12] B. Hahn, «RELIABILITY ASSESSMENT OF WIND TURBINES IN GERMANY,» *In Proceedings Europeen Wind Energy Conference, Nice, France,* pp. 1-5, March 1999.

[13] B. Hahn, M. Durstewitz et K. Rohrig, «Reliability of Wind Turbines,» *Wind Energy,* pp. 329-332, 2007.

[14] B. Steve et Golbeck, «Maintenance d'éoliennes et surveillance d'état,» 2014. [En ligne]. Available: http://windsksolutions.com. [Accès le Juin 2013].

[15] C. A. Walford, Wind turbine reliability: understanding and minimizing wind turbine operation and maintenance costs, United States. Department of Energy, 2006.

[16] E. Byon, L. Ntaimo et Y. Ding, «Optimal maintenance strategies for wind turbine systems under stochastic weather conditions,» *Reliability, IEEE Transactions on,* vol. 59, pp. 393-404, 2010.

[17] R. F. Orsagh, H. Lee, M. Watson, C. S. Byington et J. Power, «Advance Vibration Monitoring for Wind turbine Health Management».

[18] Y. Amirat, M. Benbouzid, S. Member, B. Bensaker et R. Wamkeue, «Condition Monitoring and Fault Diagnosis in Wind Energy Conversion Systems: A Review,» *Electric Machines \& Drives Conference, 2007. IEMDC'07. IEEE International. Proceeding,* vol. 2, pp. 1434-1439, 2007.

[19] J. Ribrant, «Reliability performance and maintenance - A survey of failures in wind power systems,» 2005/2006.

[20] C. Moné, A. Smith et B. M. a. M. Hand, «2013 Cost of Wind Energy,» *National Renewable Energy Laboratory: Golden CO,* 2015.

Chapter II

LITERATURE REVIEW

WIND TURBINE CONDITION MONITORING: STATE-OF-THE-ART REVIEW, NEW TRENDS, AND FUTURE CHALLENGES

Pierre Tchakoua, René Wamkeue, Mohand Ouhrouche, Fouad Slaoui-Hasnaoui, Tommy Andy Tameghe and Gabriel Ekemb

Résumé

Avec la forte croissance de l'énergie éolienne, la réduction des coûts d'exploitation et de maintenance ainsi que l'amélioration de la fiabilité sont devenues les principales priorités dans les stratégies de développement de projets éoliens. En plus du développement de modèles d'éoliennes plus évolués afin d'assurer une plus grande continuité dans la production d'énergie électrique, l'application de techniques de surveillance fiables et moins onéreuses est une approche efficace pour l'atteinte de ces objectifs. Cet article planche sur la revue et la classification des différentes méthodes et des techniques de surveillance d'éoliennes et ceci en mettant l'accent sur les nouvelles tendances et les défis à venir. Après avoir mis en lumière les principales techniques de surveillance, de diagnostic et de maintenance utilisées dans l'industrie éolienne, une description des relations entre ces différents concepts et les théories connexes a été effectuée ainsi que l'examinassion des nouvelles tendances et des défis futurs. Ce travail de recherche permet de mettre en exergue les forces et les faiblesses de l'industrie éolienne d'aujourd'hui et de définir les priorités de recherche qui permettront à l'industrie de relever les défis de l'évolution technologique et de la croissance du marché dans l'industrie éolienne.

Abstract

As the demand for wind energy continues to grow at exponential rates, reducing operation and maintenance (OM) costs and improving reliability have become top priorities in wind turbine (WT) maintenance strategies. In addition to the development of more highly evolved WT designs intended to improve availability, the application of reliable and cost-effective condition-monitoring (CM) techniques offers an efficient approach to achieve this goal. This paper provides a general review and classification of wind turbine condition monitoring (WTCM) methods and techniques with a focus on trends and future challenges. After highlighting the relevant CM, diagnosis, and maintenance analysis, this work outlines the relationship between these concepts and related theories and examines new trends and future challenges in the WTCM industry. Interesting insights from this research are used to point out strengths and weaknesses in today's WTCM industry and define research priorities needed for the industry to meet the challenges in wind industry technological evolution and market growth.

2.1. INTRODUCTION

Energy conversion and efficiency improvement have become a worldwide priority to secure an energy supply and address the challenges of climate change, greenhouse gas emission reduction, biodiversity protection, and renewable technology development. In 2011, renewable sources accounted for nearly 50% of the estimated globally added electric capacity evaluated at 208 GW [1]. Among all renewable energy sources, wind energy is the fastest-growing sector in terms of installed capacity. As shown in Figure II-1, the cumulative installed wind power capacity reached 283 GW in 2011, which represents nearly 3% of global electricity production. Furthermore, the contribution of wind power to the world total generation capacity is expected to reach 8% by 2018 [1–3].

	2012	2013	2014	2015	2016	2017
Cumulative [GW]	282.6	322.4	367.7	418.7	474.9	536.13
Cumulative capacity growth rate [%]	18.70	14.10	14.00	13.90	13.40	12.89
Annual installed capacity ([GW]	44.8	39.6	45.3	51	56.2	61.2
Annual installed capacity growth rate [%]	10.80	-11.60	14.40	12.60	10.20	8.90
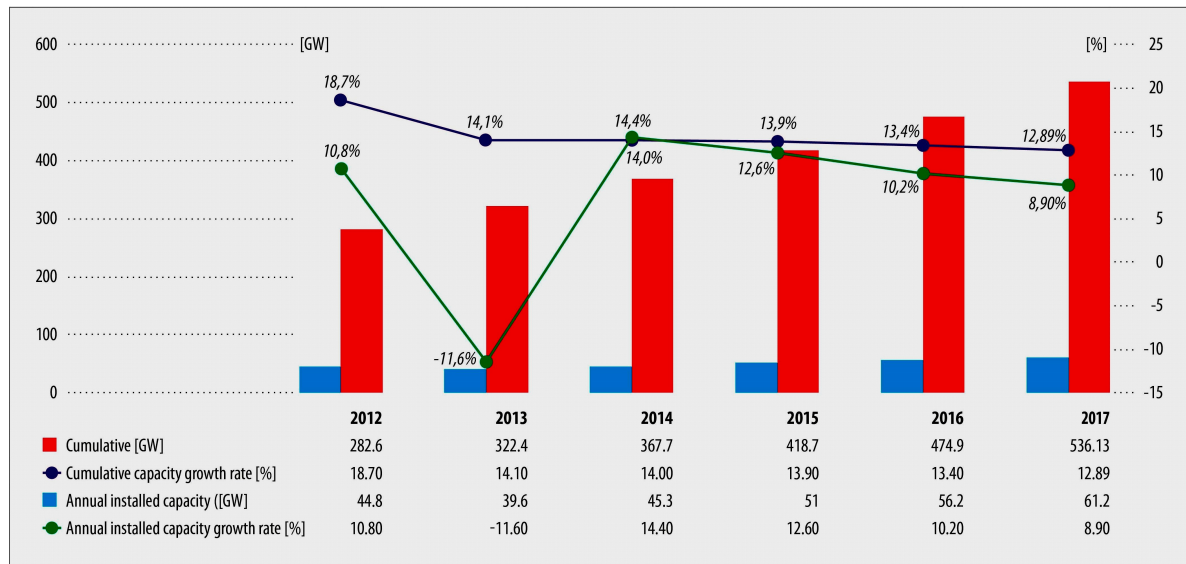
Figure II-1   Wind energy world market forecast for 2013–2017 [1]. Reprinted/Reproduced with permission from [1]. Copyright 2013, Global Wind Energy Council (GWEC).

Wind turbines (WTs) are unmanned, remote power plants. Unlike conventional power stations, WTs are exposed to highly variable and harsh weather conditions, including calm to severe winds, tropical heat, lightning, arctic cold, hail, and snow. Due to these external variations, WTs undergo constantly changing loads, which result in highly variable

operational conditions that lead to intense mechanical stress [4]. Consequently, the operational unavailability of WTs reaches 3% of the lifetime of a WT. Moreover, operation and maintenance (OM) costs can account for 10%–20% of the total cost of energy (COE) for a wind project, and this percentage can reach 35% for a WT at the end of life. A preventive-centered maintenance strategy that avoids machine shutdown can considerably reduce these costs [5–7]. Therefore, WTs require a high degree of maintenance to provide a safe, cost-effective, and reliable power output with acceptable equipment life. The state-of-the-art method for determining the maintenance strategy in the WT industry is reliability-centered maintenance (RCM), which consists of preventive maintenance based on performance and/or parameter monitoring and subsequent actions. In this strategy, condition-monitoring (CM) is used to determine the optimum point between corrective and scheduled maintenance strategies [8–11]. The recurrent and commonly used condition-monitoring techniques (CMTs) are: (i) vibration/acoustic-controlled and OM techniques for the turbine; and (ii) optical strain gauges for the blades.

The WTs are typically designed to operate for a period of 20 years [12,13]. As with other mechanical systems, time-based maintenance assumes that the failure behavior of WTs is predictable. Fundamentally, three failure patterns describe the failure characteristics of WT mechanical systems [14].

The bathtub curve shown in Figure II-2 illustrates the hypothetical failure rate versus time in a mechanical system [15–18], where $\beta < 1$ represents a decreasing failure rate, $\beta = 1$ represents a constant failure rate, and $\beta > 1$ represents an increasing failure rate.
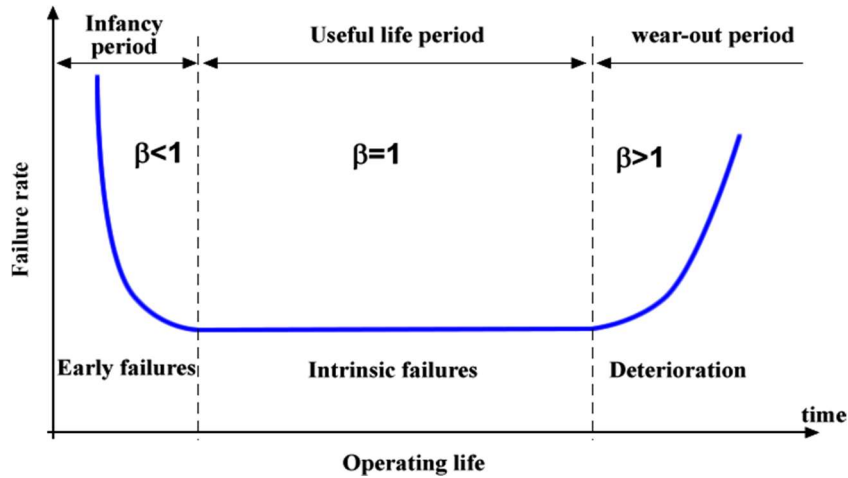
Figure II-2 The "bathtub" curve illustrating the reliability of technical systems.

Guo et al. [19] developed a three-parameter Weibull failure rate function for WTs, and their results corroborate the bathtub curve. Echavarria et al. [12] published results of a remarkable 15-year research study on the frequency of failures versus increasing operational age for various WT power ratings (Figure II-3).
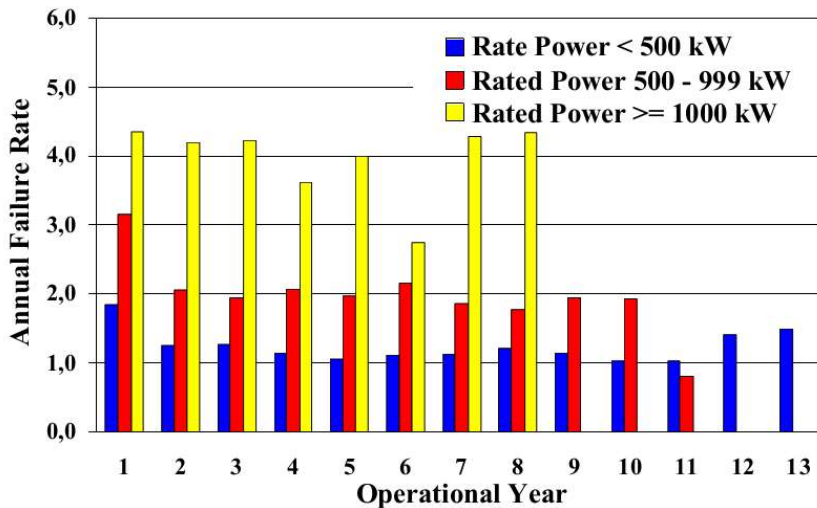
Figure II-3 Number of incidents per wind turbine (WT) per operational year; WTs are categorized by rated power [12]. Reprinted/Reproduced with permission from [12]. Copyright 2008, American Society of Mechanical Engineers.

The frequency of failures in WTs also varies with the scale and type. Spinato et al. [18,20] carried out a failure analysis based on onshore WT types, as specified in the Schleswig Holstein Landwirtschaftskammer (LWK) database. The work displayed a general

18

trend of an increasing failure rate with turbine size. Because turbine capacity continues to grow, we can assume that it will be difficult to decrease the initial failure rate. Several research studies considered the distribution of WT failures in the main components [13,20,21]. Haln et al. [13] reported a survey of 1500 WTs over 15 years and found that five component groups, i.e., electrical system, control system, hydraulic system, sensors, and rotor blades, are responsible for 67% of failures in WTs, as shown by the pie chart in Figure II-4.
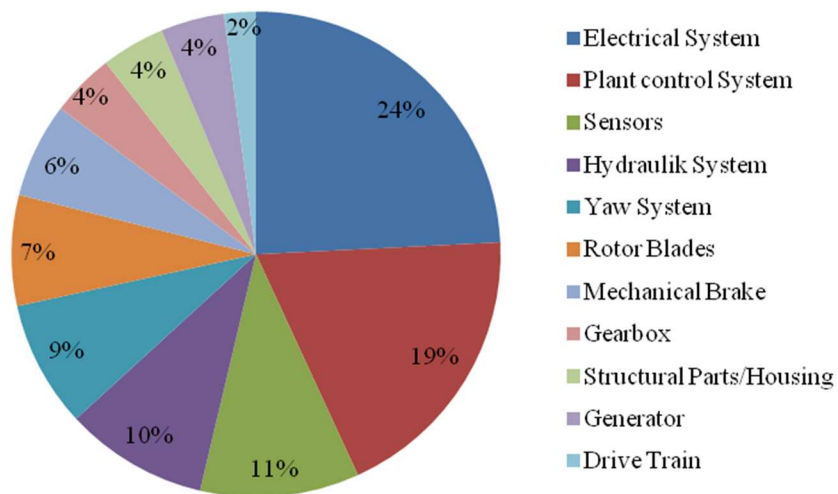
Figure II-4   Share of the main components of the total number of failures [13]. Reprinted/Reproduced with permission from [13]. Copyright 2007, Springer Science + Business Media.

To establish the impact of component failure on WT reliability, research centered on the availability of WTs was presented in [8,22–25]. The results published by Fischer et al. [8] indicated that 75% of the annual downtime is caused by only 15% of the failures in WTs. This result corroborates the conclusions of Haln et al. [13], regarding the average failure rate and average downtime per component. The results of this study are also in agreement with the conclusions of Crabtree et al. [24], regarding the comparison of failure rates and downtime for different WT subassemblies based on surveys of European wind-energy conversion systems (WECSs). The chart in Figure II-5 summarizes the failure rate and

downtime of different WT subassemblies. The reliability and downtime data of the Egmond aan Zee wind farm in Germany also produced similar results, i.e., the gearbox failure rate is low, but the downtime and resultant costs are high. As a result, the percentage of electricity production lost due to gearbox downtime is the highest of all subassemblies [24].

A statistical analysis of WT faults demonstrates that their reliability and availability depend on multiple factors, i.e., age, size, weather, wind speed, and subassembly failure rates. However, applying efficient CMTs can greatly increase the reliability of WTs.
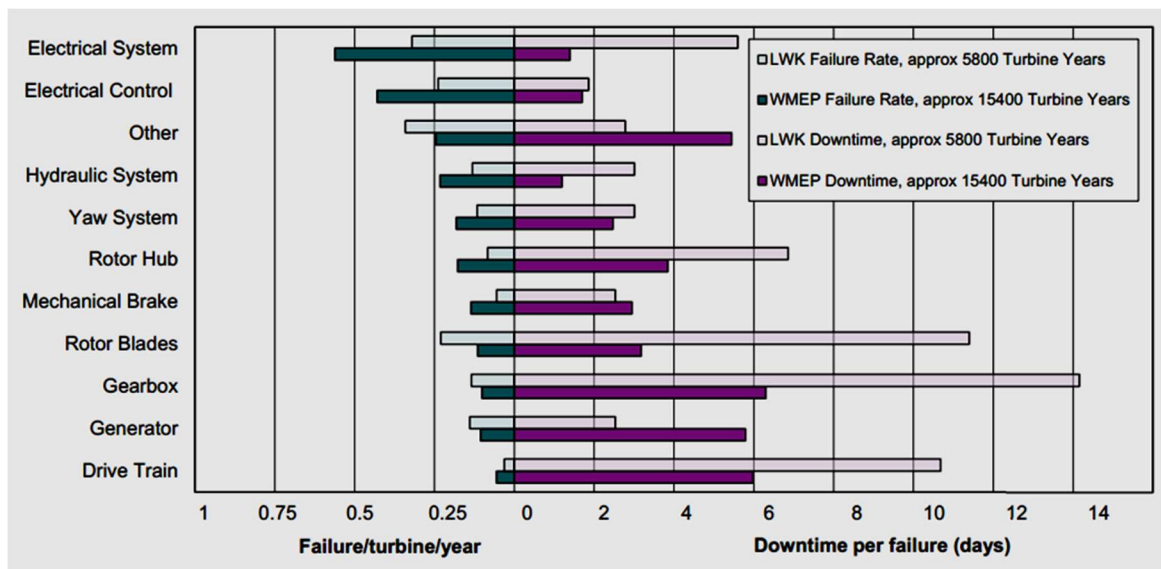
Figure II-5 Failure rates and downtime from two large surveys of European WTs over 13 years [13]. Reprinted/Reproduced with permission from [13]. Copyright 2007, Springer Science + Business Media.

In the literatures, few articles have provided a review of wind turbine condition monitoring (WTCM) and/or fault diagnosis [7,21,26–29]. The goal of this paper is to provide a review of methods and techniques for WTCM with a classification of: (i) intrusive and nonintrusive techniques; and (ii) destructive techniques and non-destructive techniques. This work also focuses on trends and future challenges in the WTCM industry. The paper is organized as follows: Section 2 is dedicated to CM-related concepts and definitions and outlines the relationships among CM, fault diagnosis, and fault prognostic and maintenance

strategies; Section 3 presents a review of techniques and methods used in WECSs and CM, subdividing them into subsystem techniques and overall system techniques as well as destructive and non-destructive techniques; Section 4 discusses the new trends and future challenges that will enable the industry to address the WT challenges of the future, including reducing operational costs and improving reliability; finally, Section 5 provides conclusions to the work.

2.2. CONCEPTS AND DEFINITIONS

2.2.1. Maintenance Approaches

As in most industries, maintenance approaches in the WT industry can be widely classified into three main groups [30,31]:

- Reactive or corrective maintenance (run to failure);

- Preventive maintenance (time-based);

- Predictive maintenance (condition-based).

The COE estimation for a WECS is given by Equation (1) [6,32–35], where ICC is the initial capital investment cost; FRC is the annual fixed charge rate; E is the annual energy production in kW h; and OM is the annual OM cost:

$$COE = \frac{ICC \cdot FCR + OM}{E} \tag{1}$$

where ICC and FCR are fixed parameters; and OM is a variable parameter that can affect the COE during the lifetime of the project. Therefore, the profit from wind energy is highly dependent on the ability to control and reduce this variable cost. The OM cost of equipment will notably depend on the maintenance strategy adopted by the user.

The cost associated with traditional maintenance strategies is presented in Figure II-6 [30]. In a preventive maintenance strategy, the prevention cost will be quite high, whereas the repair cost will be low because many potential failures will not occur. In other words, preventive maintenance will considerably reduce the number of failures that occur but will be expensive. In a reactive maintenance strategy, a greater number of faults will occur and will lead to a high cost of repair and low cost of prevention. As shown on the graph, a combination of preventive and reactive maintenance strategies can improve the reliability, availability, and maintainability of WTs while simultaneously reducing the maintenance cost [4,6,30,36].
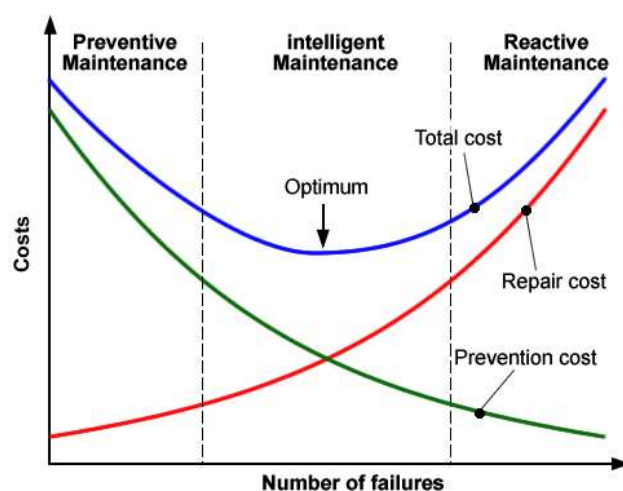
Figure II-6   Costs associated with traditional maintenance strategies [30].

2.2.2. Condition Monitoring, Diagnosis, and Maintenance Theories

Reliability is the ability of a device to perform the required functions under the given conditions for a given time [4,37]. The reliability of a WT is critical for extraction of the maximum energy available from wind. Reliability can be highly improved by the implementation of adequate condition-monitoring systems (CMSs) and fault detection systems (FDSs), and availability is a fundamental measure of reliability. Holen et al. [38] defined availability as the probability that a component or system is capable of functioning

at time t, given by Equation (2), where MTTF is the mean time to failure and MTTR is the mean time to recovery:

$$A = \frac{MTTF}{MTTF + MTTR}$$ (2)

A CMS is a tool used to ensure and measure the reliability of any running system [39]. Wiggelinkhuizen et al. [40] suggested that for WECSs, significant changes are indicative of a developing failure. The continuous component states (i.e., WT health) are evaluated using a collection of techniques, i.e., vibration analysis (VA), acoustics, oil analysis (OA), strain measurement (SM), and thermography [27]. Data are sampled at regular time intervals using sensors and measurement systems. Using data processing and analyses, CMSs can determine the states of the key WECS components. By processing the data history, faults can be detected (diagnosis) or predicted (prognostic) and the appropriate maintenance strategy can be chosen.

Maintenance includes any actions appropriate for retaining equipment in or restoring it to a given condition [31]. Maintenance is required to ensure that the components continue to perform the functions for which they were designed. The basic objectives of the maintenance activity are to: (i) deploy the minimum resources required; (ii) ensure system reliability; and (iii) recover from breakdowns [41]. The applied maintenance strategy can be preventive if a predicted failure is avoided or corrective when a detected failure is repaired [42].

A description of and models for CMSs can be found in [27,39,43,44]. This description can be combined with concepts definitions provided in [14,31,45–48], which address maintenance techniques and methods. The diagram relating technical concepts and words used in the domain of WTCM and fault diagnosis emerges from the aforementioned

combination. As shown in Figure II-7, CM is performed in three main steps: data acquisition using sensors, signal processing using various data processing techniques, and feature extraction via the retrieval of parameters that will aid in establishing the current status of the monitored equipment. Using both: (i) current information sources; and (ii) information on the system's past status obtained from stored data, the system's present state is obtained via online monitoring such that a fault can be detected or predicted. After a fault is diagnosed, corrective maintenance is carried out. Two approaches to corrective maintenance can be distinguished, i.e., palliative maintenance, which consists of provisional solutions to failures, and curative maintenance for standing solutions to failures. If a fault is predicted, preventive maintenance is carried out before the fault can occur. In this case, four different approaches can be used: time-based or scheduled maintenance, current-state based or conditional maintenance, parameter-projection-based or forecasting maintenance, and status-based or proactive maintenance.
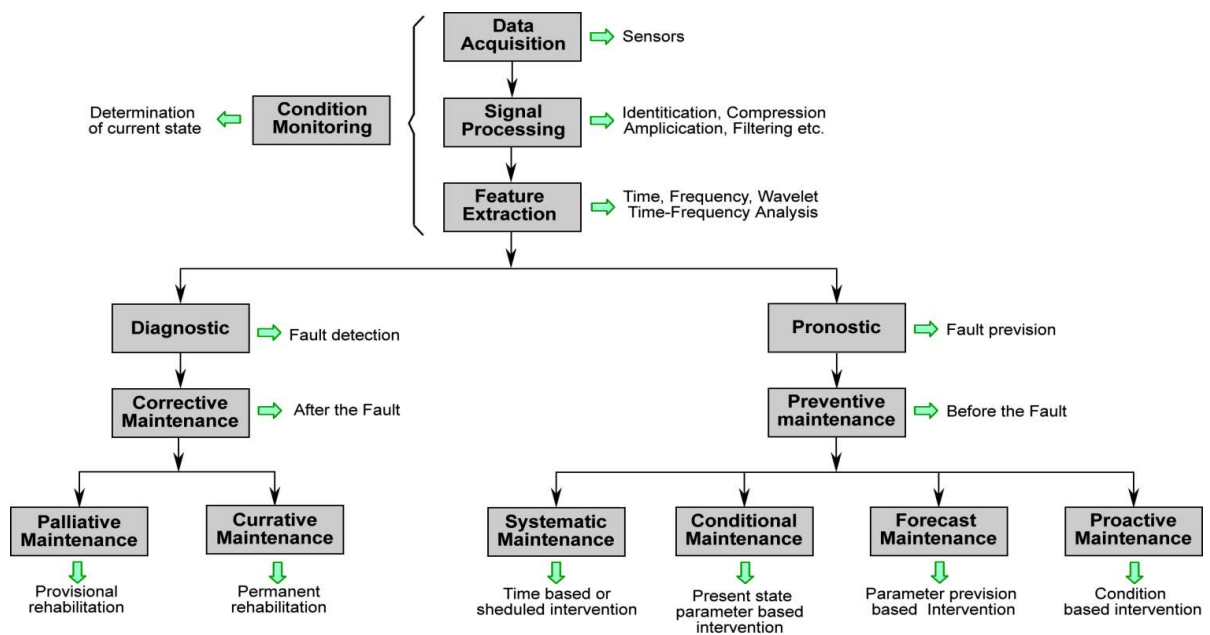
Figure II-7 Overview of condition-monitoring (CM) and maintenance processes for WTs.

2.3. REVIEW OF CONCEPTS AND METHODS FOR WTCM

According to the Swedish standard SS-EN 13306 [49], monitoring can be defined as an activity performed either manually or automatically that is intended to observe the actual state of an item. The key function of a successful CMS should be to provide a reliable indication of the presence of a fault within the WECS and to indicate the location and severity of the situation [25]. For this purpose, a CMS is required for early warning sign detection. CM is based on data acquisition and signals processing and can be implemented using various approaches with different levels of technology [46].

A complete CMS is composed of many subsystems, each monitoring a particular component of the wind generator [50]. Due to the considerable level of overlap between functions of different subsystems, certain CM subsystems will monitor many components of the WT. The approach proposed in this review differentiates CMTs applied on WT subsystems from CMTs applied on the overall WT system.

2.3.1. Wind Turbines Subsystems or Intrusive Condition Monitoring Techniques

The subsystem-level CM of WTs is based on subcomponents related to local parameters [27,28,51] and enables the acquisition of information on specific components and thus the precise localization of eventual failures. The typical main components of a utility-scale WT are presented in Figure II-8, and an example of a function model for the monitoring of a WECS based on the subsystem approach is presented in Figure II-9.
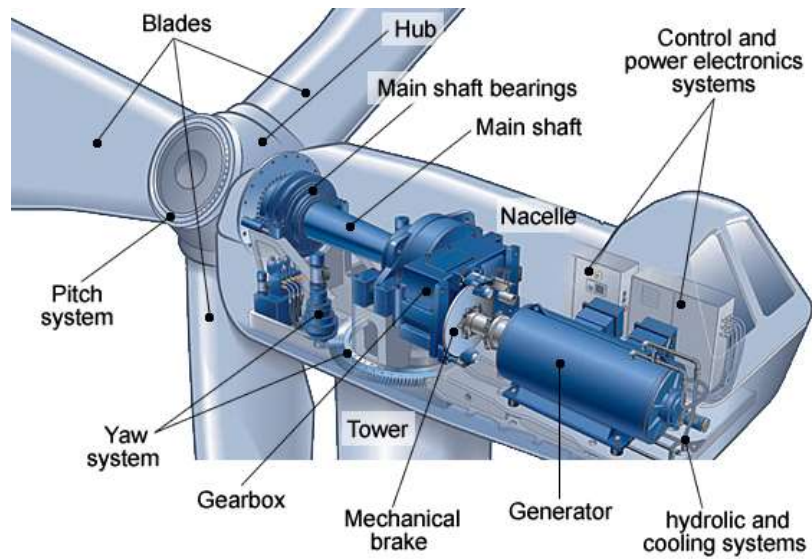
Figure II-8 Typical main components of a utility-scale WT [51].

Subsystem CM can be classified into two main subcategories, namely, those based on destructive test (DT) and those based on non-destructive test (NDT) [52].

Subsystem CM based on DT uses:

- VA;

- OA;

- SM;

- Electrical effects;

- Shock pulse method;

- Physical condition of materials;

- Self-diagnosis sensors;

- Other techniques.

- Subsystem CM based on NDT uses:

- Ultrasonic testing techniques (UTTs);

- Visual inspection (VI);

- Acoustic emission;

-   Thermography;

-   Performance monitoring;

-   Radiographic inspection.
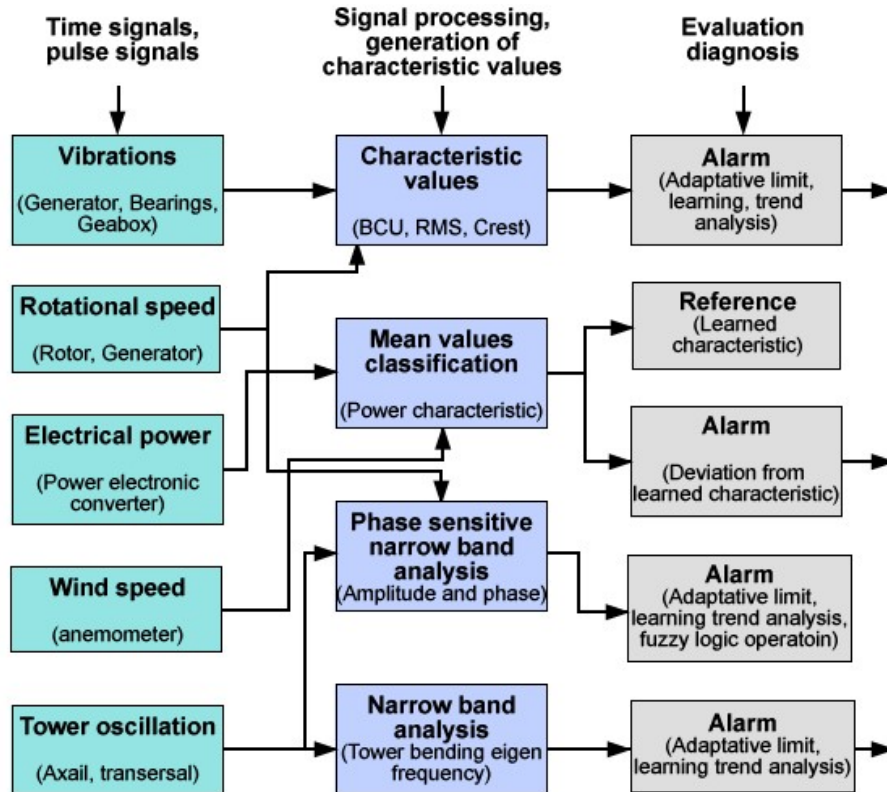
Figure II-9 Function model for monitoring of a wind-energy conversion system (WECS) [53]. BCU: boundary controlling unstable; and RMS: root mean square. Reprinted/Reproduced with permission from [53]. Copyright 2008, Blekinge Institute of Technology.

2.3.2. Subsystem Condition Monitoring Techniques Based on Destructive Techniques

As stated in [54], a DT is "a form of mechanical test (primarily destructive) of materials whereby certain specific characteristics of the material can be evaluated quantitatively". DTs are generally realized more easily and yield additional data that are easier to interpret than those from NDTs [55,56]. As applied to WECSs, DTs are dynamic or static and can provide useful information related to the material's design considerations, equipment performance, structural health, and useful life.

a) *Voltage Analysis (VA)*

VA is the most well-known technology for rotating equipment CM. As shown in Figure II-10, VA is the most efficient technology for early prediction and detection of failures in mechanical equipment [32]. Applied sensor technology is selected by considering the frequency range and operating conditions [57]. Position transducers, velocity sensors, accelerometers, and spectral emission energy sensors are used for low-, middle-, high-, and very-high-frequency ranges, respectively. Fast Fourier transformation is the signal processing technique commonly used in VA to convert a time-domain signal into a frequency-domain signal [58].
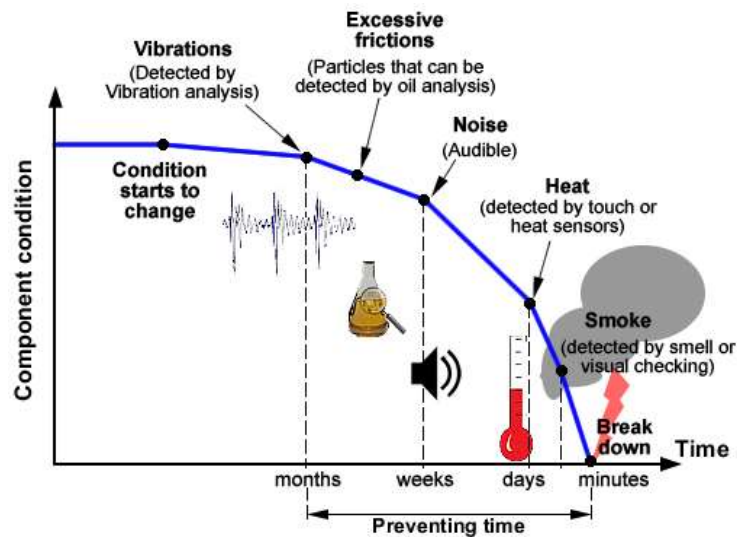
Figure II-10 Typical development of a mechanical failure.

As a subsystem monitoring technique, VA is applied to such WT components as shafts, bearings, gearboxes, and blades. In WTs or wind farms, CM via the VA's extreme false alarm levels can provide information on the incorrectness of vibration signals from the recording process (e.g., in the case of a faulty sensor). To minimize the risk of anomalies, which is increased in a wind farm due to the greater number of WTs, Jablosky et al. [59] developed an algorithm for the automatic validation of vibration signals in the distributed

monitoring system of a wind farm. Based on amplitude validation, the vibration data are validated via an original implementation of Parseval's theorem, in addition to the novel idea of a so-called "N-point" rule, which is a simple yet powerful in automatic signal error detection.

The WTCM techniques with VA are standardized in ISO10816 [60], which define the positioning and use of sensors. VA methods are easy to implement in existing equipment and have a high level of interpretation, making it easy to locate the exact faulty component. Nevertheless, this approach implies the use of additional hardware and software, which increases the production costs. Additionally, it is difficult to use sensors to detect low-frequency faults [28].

b) *Oil Analysis (OA)*

Oil debris monitoring has been proven as a viable CMT for the early detection and tracking of damage in bearing and gear elements in WT gearboxes [61]. Indeed, 80% of gearbox problems can be attributed to the bearings, which subsequently lead to damage to the gearing [62].

In most cases, oil is pumped through the component in a closed-loop system, and metal debris from cracked gearbox wheels or bearings is caught by a filter. The amount and type of metal debris can indicate the health of the component. OA has three main purposes [61]: (i) to monitor the lubricant; condition and reveal whether the system fluid is healthy and fit for further service or requires a change; (ii) to ensure the oil quality (e.g., contamination by parts, moisture); and (iii) to safeguard the components involved (part characterization). Six main tests are generally employed in the OA process: [57,63–65]:

- Viscosity analysis;

- Oxidation analysis;

- Water content or acid content analysis;

- Particle count analysis;

- Machine wear analysis;

- Temperature.

OA techniques can be divided into two categories: real-time continuous monitoring and offline oil sample analysis [66]. These processes are typically executed off line by taking samples. However, online real-time oil debris monitoring may be desirable for applications in which failure modes develop rapidly or when accessibility is limited. In this case, it is advisable to install several sensors in the gearbox lubrication loop to analyze different characteristics. This approach will increase the reliability and accuracy of the analyses [53,64].

The technology for on-line detection can be broadly divided into three subcategories depending on the sensing techniques applied [4]: electromagnetic sensing, flow or pressure-drop sensing, and optical debris sensing. In terms of cost, size, accuracy, and development, suitable oil monitoring technologies are online ferrography, selective fluorescence spectroscopy, scattering measurements, Fourier transform infrared (IR) spectroscopy, photo acoustic spectroscopy, and solid-state viscometry [62,64]. Du and Zhe [67] developed a high-throughout, high-sensitivity inductive sensor for the detection of micro-scale metallic debris in nonconductive lubrication oil. The device is able to detect and differentiate ferrous and non-ferrous metallic debris in lubrication oil with high efficiency.

Although OA is the only method for detecting cracks in the internal gearbox, this approach has two main limitations. First, it cannot detect failures outside the gearbox, and

second, use of this equipment for online monitoring is highly expensive. For these reasons, offline monitoring of oil samples is often used [28,68].

c) Temperature Measurement (TM)

Monitoring the temperature of the observed component is one of the most common methods of CM [56]. TM aids in detecting the presence of any potential failure related to temperature changes in the equipment. In the wind energy industry, TM is applied on such components as bearings, fluids (oil), and generator windings, among others [53,69]. Optical pyrometers, resistant thermometers, and thermocouples are a subset of the sensors used in TM [70]. Unlike thermography, TM provides information on the ongoing deterioration process in the component from excessive mechanical friction due to faulty bearings and gears, insufficient lubricant properties, and loose or bad electrical connections [53].

TM is reliable because every piece of equipment has a limited operational temperature. However, temperature develops slowly and is not sufficient for early and precise fault detection [71]. Additionally, the measured temperature can also be influenced by the surroundings. Therefore, TM is rarely used alone but often as a secondary source of information. In this case, the primary source could be vibration monitoring [32,71].

d) Structural Monitoring (SM)

SM is a renowned technique for structural health monitoring (SHM) and is becoming increasingly important in the WT industry, where it is applied to blades and towers; SM is commonly used in laboratory settings for blade lifetime testing [16,51,72,73]. Measurements are gathered with sensors, i.e., so-called metal foil strain gauges, and the finite element method is commonly used to process the acquired data [73,74]. Strain gauges can be placed randomly on the blade, and the distribution varies according to the number of transducers.

However, strain gauges are not robust over the long term, and more robust sensors might offer an interesting application area [51,57].

Currently, certain WT manufacturers incorporate fiber-optic sensors into the blades to reduce connections with the data logger and permit little to no weakening of the signal over a considerable distance. With the latest fiber optic sensing technologies, monitoring of stresses on the blades during rotation is easier and more accurate [27,75–77]. Kreuzer [73], Bang et al. [74] and Schroeder et al. [78] investigated the development of a high-speed-fiber Bragg-grating-based sensor array system for strain-based deflection shape estimation of WT structures.

e) *Optical Fiber Monitoring (OFM)*

OFM is growing as a reliable and cost-effective technique for WT SHM [71]. A network of sensors can be embedded in the blade structure to enable the measurement of five parameters that are critical to SHM. The five parameters include: (i) SM for monitoring the blade loading and vibration level; (ii) TM for likely over-heating; (iii) acceleration measurement for monitoring the pitch angle and rotor position; (iv) crack detection measurements; and (v) lightning detection for measuring the front steepness, maximum current, and specific energy [79–82].

The optical fibers must be mounted on the surface or embedded into the body of the monitored WT components. Therefore, OFM is complicated and expensive in real-world applications compared with other CM and fault detection methods [83,84]. However, due to technological progress, it is expected that the cost of OFM for WT SHM will decrease considerably in the future.

2.3.3. Subsystem Condition Monitoring Techniques Based on Non-Destructive Techniques (NDTs)

Malhotra *et al.* [54] defined NDT as "an examination, test, or evaluation performed on any type of test object without changing or altering it in any way". This is often done in order to determine the absence or presence of conditions or discontinuities that may have an effect on the usefulness or serviceability of the monitored object. NDTs may also be conducted to measure other tested object characteristics, *i.e.*, size, dimension, configuration, or structures, including alloy content, hardness, and grain size. Nevertheless, these approaches are largely applied to localized areas. Thus, NDT technologies require more accurate prior knowledge of probable damage locations as well as the use of dedicated sensors [56].

a) *Visual Inspection (VI)*

Based on human sensory capabilities, VI or observation is undoubtedly one of the oldest CMT and can serve as a supplement to other CMTs. VI includes the detection of sounds emitted by a functioning system, touch (temperature and vibration checking), and VI (e.g., deformation and aspects). This approach is generally used to monitor such components as rotor blades, nacelles, slip rings, yaw drives, bearings, generators, and transformers [53,85].

In several cases, VI is of great importance in identifying a problem that was not identified by other CMTs. Such cases may include loose parts, connections, terminals, and components; visibly worn or broken parts; excessive temperatures that reflect through the structure or housing, oil leakages, corrosion, chattering gears, or hot bearing housings [85–87]. Nevertheless, VI is limited to the identification of damages that are visible on the surface

of a structure. Moreover, VI is labor intensive and highly subjective because the results depend on the experience and judgment of the inspector [88].

Today, the industry is implementing remote VI technologies to inspect gearboxes, WT blades, and other critical components [89]. AIT Inc. has developed a video boroscope or videoscope used to inspect the interior areas that are not accessible and can be efficient in revealing hairline cracks, corrosion, pitting, rubbing, and other defects [85]. Moreover, the AutoCopter™ Corporation [87] has developed a flying remote VI device that enables inspection of WTs, thus increasing reliability and the number of daily inspections while eliminating the risk of personal injury.

b) *Acoustic Emission (AE)*

AE phenomena are based on the release of energy in the form of transitory elastic waves within a material via a dynamic deformation process [90]. Typically, sources of AE within a material are [91,92] crack initiation and propagation, breaking of fibers, and matrix cracking and fretting between surfaces at de-bonds or de-laminations. Unlike VA, AE can detect failures characterized by high-frequency vibrations ranging from 50 kHz to 1 MHz [93]. Piezoelectric transducers and optic fiber displacement sensors are often employed in this approach [94]. The most commonly measured AE parameters for diagnosis are amplitude, root mean square (RMS) value, energy, kurtosis, crest factor, counts, and events [95].

This method is typically applied for fault detection in gearboxes, bearings, shafts, and blades, and its advantages include a large frequency range and a relatively high signal-to-noise ratio. The main drawback of AE is its cost. Furthermore, only a few types of faults occur in the high-frequency range. Another limitation of AE is the attenuation of the signal

during propagation. Therefore, an AE sensor must be located as close to its source as possible [96], which may pose a practical constraint in applying AE to certain wind machines.

Research was carried on the combined use of AE and VA data [97–99]. Soua et al. [99] presented the results of a combined vibration and AE monitoring effort that was performed over a continuous period of five years on an operating WT. Good results were obtained for the detection of defects, most notably in the gearbox, using special digital processing techniques, such as similarity analysis. Tan et al. [96] carried out a comparative experimental study on the diagnostic and prognostic capabilities of AE, VA, and spectrometric OA for spur gears and observed that based on the analysis of RMS levels, only the AE technique was more sensitive in detecting and monitoring faults than either the vibration or spectrometric OA.

c) Ultrasonic Testing Techniques (UTTs)

UTTs are extensively used by the wind energy industry for structural evaluation of WT towers and blades [27,92]. This method relies on elastic wave propagation and reflection within the material. Three different techniques can be used for this investigation: pulse-echo (Figure II-11), through transmission, and pitch-catch [100,101]. Laser interferometric sensors, air-coupled transducers, electromagnetic acoustic transducers, or contact transducers are a subset of the sensors that can be used as the scanning sensor for acoustic wave field imaging, which is another UTT [72,102].
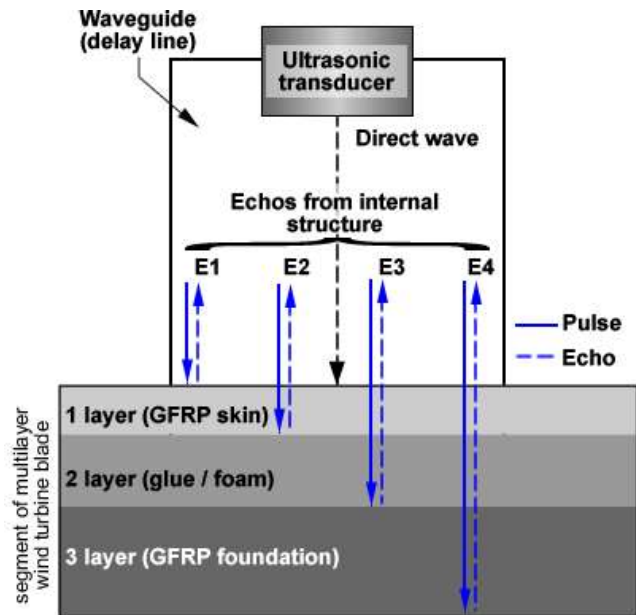
Figure II-11 Principle of the pulse-echo technique used for the investigation of WT blades [100,103]. GFRP: glass fiber reinforced plastic. Reprinted/Reproduced with permission from [100]. Copyright 2008, Kaunas University of Technology.

Implementation of UTTs implies one or more of the following measurements: time of flight or delay, path length, frequency, phase angle, amplitude, acoustic impedance, and angle of wave deflection [104]. Thus, signal-processing algorithms, including such time-frequency techniques as the Wigner-Ville distribution, Hilbert-Huang transform, and wavelet transform [100,105], can be used to extract additional information on internal defects.

Ultrasonic testing via wave propagation characteristics allows for the estimation of the location and nature of the detected failure. This approach provides a quick, reliable, and effective method for determining the material properties of the principal turbine components [106]. Ultrasound scanning allows personnel to see below the surface and check the laminate for dry glass fibers and de-lamination [107]. Unlike other NDT techniques (i.e., thermographic techniques), acoustic techniques are not as affected by temperature or air humidity [108].

d)   Thermography Analysis (TA)

TA provides a wide range of diagnostic and monitoring applications in different equipment and machines, i.e., bearings, gear boxes, conveyor systems, drivers, motors, and electric generators. IR thermography is recognized as one of the most versatile and effective CM tools for use in the WT industry for control and diagnoses of electric parts and mechanical equipment [109,110]. This method is based on the fact that all working components emit heat and when a component in the system starts to malfunction, its temperature increases beyond the normal values [56]. IR temperature transmitters and high-resolution IR cameras are the sensors applied in TA, and results are typically interpreted visually [27,111].

Today, TA is primarily used for periodical manual inspection and can be used as a local or global technique because it is possible to assess the damage at the component or system level, depending on the resolution of the camera. However, TA is not appropriate for early fault detection because temperature develops slowly, as mentioned earlier [111,112]. Another important difficulty with TA for WTCM is that monitoring should be performed offline [111]. However, cameras and diagnostic software that are suitable for on-line process monitoring are currently entering the market [57].

e) *Radiographic Inspection*

Radiography (both film and digital) uses the well-known effects of an X-ray source on one side of a specimen and an X-ray-sensitive receptor on the other side. Although this method does provide useful information on the structural condition of the WT component under inspection, radiographic imaging using X-rays is rarely used in WECS industry [27]. The technique is highly efficient in detecting crack and de-lamination in the blade/rotor and tower structures.

f) **Other Non-Destructive Wind Turbine Condition Monitoring Techniques**

Other techniques are not widespread but are also used in the maintenance of WTs. In many cases, their performance is heavily influenced by the costs or excessive specialization, making them impractical in some situations. Examples are SMs in blades, voltage and current analysis, shock pulse methods, and magnetic flux leakage.

2.3.4. Wind Turbine Global System or Nonintrusive Condition Monitoring Techniques

Conventional subsystems CMTs (i.e., vibration, lubrication oil, and generator current signal analysis) require the deployment of a variety of sensors and computationally intensive analysis techniques [113]. The use of additional sensors and equipment increases costs and hardware complexity of the WECS. Furthermore, sensors and equipment are inevitably subject to failure, causing additional problems with system reliability and additional OM costs [114]. For these reasons, it is of interest to develop overall CMTs. These techniques are nonintrusive, low cost, and reliable.

Unlike subsystem CMTs, global systems CMTs enable the extraction of fault features with low calculation time from direct or indirect drives and fixed- or variable-speed WTs. In addition, these techniques can all be used in online and thus increase the WT reliability while reducing the downtime and OM costs [113–115]. Certain overall WTCM approaches include performance monitoring, power curve analyses, electrical signature, and supervisory control and data acquisition (SCADA) system data analysis.

a) **Performance Monitoring or the Process Parameter Technique**

In WT performance monitoring, parameter readings of the capacity factors of the plant, power, wind velocity, rotor speed, and blade angle are compared with the values in operator manuals or manufacturer performance specifications to determine whether the

system is performing at optimum efficiency. The relationships among power, wind velocity, rotor speed, and blade angle can be used for safeguarding purposes, and an alarm is generated in the case of large deviations. The detection margins are large to prevent false alarms [51,53]. Today, more intelligent usage of the signals based on parameter estimation and trending is not a common practice in the WT industry [51].

b) *Power Signal Analysis*

Power quality is a high-interest area for WTCM because quality could degrade as a result of wind speed turbulence and switching events. From a global viewpoint, the mechanical power (torque times speed) measured on the WT drive shaft and the total three-phase electrical power measured from the terminals of the generator are the input and output of a WT system, respectively. Both energy flows are disturbed by WT abnormalities caused by mechanical or electrical faults [115]. Significant variations in the WT drive train torque are generally signs of abnormalities. Faults in the drive train cause either a torsional oscillation or shift in the $\left(\dfrac{T}{\omega}\right)$ ratio. By monitoring this ratio, certain fault conditions can be detected. For example, torque oscillations can be detected in a blade or rotor imbalance condition in the WT [71,116].

Peak power output, reactive power, voltage fluctuations, and harmonics greatly influence the power quality [117–120]. As an example, for a healthy WT, the output current is assumed to be sinusoidal:

$$i_H(t) = a\cos(\omega_1 t) \tag{3}$$

Where ω_1 is the pulsation for a healthy WT.

A failure will cause a vibration in the shaft rotation at a certain frequency that can be detected using vibration sensors. The new shaft rotating speed is given by [121,122]:

$$\omega_F(t) = \omega_1 + c\cos(\omega_2 t) \tag{4}$$

ω_2 is the pulsation in the broken down WT that is due to the vibration caused by the failure.

Therefore, the instantaneous phase for a faulty WT can be obtained:

$$\theta_F(t) = \int_0^t \omega_F(t)dt = \omega_1 t + \gamma\sin(\omega_2 t) \tag{5}$$

The current for the faulty WT can then be written as:

$$i_F(t) = a\cos\left[\omega_1 t + \gamma\sin(\omega_2 t)\right] = a\cos(\omega_1 t)\cos(\gamma\sin(\omega_2 t)) - a\sin(\omega_1 t)\sin(\gamma\sin(\omega_2 t)) \tag{6}$$

If we assume $(c \ll \omega)$, thus $(\gamma \ll 1)$. As a result, $\cos(\gamma\sin(\omega_2 t)) \approx 1$ and $\sin(\gamma\sin(\omega_2 t)) = \gamma\sin(\omega_2 t)$.

We will finally obtain:

$$i_F(t) = a\cos(\omega_1 t) - a\gamma\sin(\omega_1 t)\sin(\omega_2 t) = a\cos(\omega_1 t) - \frac{a\gamma}{2}\cos((\omega_1 - \omega_2)t) + \frac{a\gamma}{2}\cos((\omega_1 + \omega_2)t) \tag{7}$$

where $i_H(t)$ and $i_F(t)$ are the instantaneous currents for healthy and faulty WT, respectively; ω_1 is the angular shaft rotation speed for a healthy WT; ω_2 is the angular shaft rotation speed generated by the fault; ωF is the shaft rotation speed for a faulty WT; a is the amplitude of the instantaneous current for a healthy WT; c is the amplitude of the current due to the WT fault; and $\gamma = c/\omega$. a, c and γ are constants values. Frequency demodulation is used for feature extraction from Equation (7).

A mechanical failure can also lead to amplitude modulation of the output current. For a three-phase generator, the stator current ik(t) (k = 1,2,3) can be described in a discrete form as [121,123]:

$$i_k(n) = a_k(n) \cdot \cos(\omega n - \Phi_k) \tag{8}$$

where $n = 0, ..., N-1$ is the sample index (N being the total number of received samples); and $\Phi_k = 2k\pi/3$ is the phase parameter. The angular frequency ω is equal to $2\pi f/Fe$, where f and Fe are the supply and sampling frequencies, respectively. The amplitude ak(n) is related to the fault as follows:

- For a healthy WT, ak(n) is constant and there is no amplitude modulation;

- For a faulty WT, ak(n) is time variant and the current signal is modulated in amplitude.

- Amplitude demodulation can be used for feature extraction using various techniques, such as the Concordia transform or Hilbert transform.

Wakui and Yokoyama [124] developed a sensorless wind-speed performance-monitoring method for stand-alone vertical-axis WTs using numerical analyses in a dynamic simulation model. Yang et al. [113,125,126] and Watson et al. [122] proposed a wind turbine condition monitoring technique (WTCMT) that uses the generator output power and rotational speed to derive a fault detection signal. The technique is based on a detection algorithm using a continuous-wavelet-transform-based adaptive filter to track the energy in the prescribed time-varying fault-related frequency bands in the power signal. A probabilistic model of the power curve based on copulas was developed by Gill et al. [127], for CM purposes. Copula analysis is likely to be useful in WTCM, particularly in early recognition of incipient faults, such as blade degradation, yaw, and pitch errors.

c) **WTCM Based on Signature Analysis (SA)**

SA is a simpler but more inclusive WTCM technique. Intensive research efforts have been focused on the use of SA to predict or detect electrical and mechanical faults in WECSs. Different signals can be detected (i.e., voltages, power, currents, or stray flux), and SA can be used to detect various faults (i.e., broken rotor bars, bearing failures, air gap eccentricity, and unbalanced rotors and blades) [50,128]. Yazidi et al. [129] proposed a monitoring system for WTs with double-fed induction generators based on stator and rotor current signatures. Different tests were performed in this work, and relevant results were obtained. The proposed CMS was efficient for detection of rotor and stator asymmetry in a double-fed induction machine connected to a back-to-back converter. A similar investigation was carried out by Douglas et al. [130].

Yang et al. [131] proposed a CMT based on both electrical and mechanical signatures. In addition to its versatile function, i.e., its ability to detect both mechanical and electrical faults, this technique removes the negative influence of variable wind in the machine CM. This work also investigated the possibility of detecting a WT mechanical fault (e.g., rotor imbalance fault and drive train mechanical fault) via power signal analysis.

d) *Wind Turbine Condition Monitoring Based on SCADA Data Analysis*

In most modern WTs, SCADA systems are now common. The WTCM using SCADA data analysis is cost effective (data collection and sensor networks already in place) and reliable because it relies on the interpretation of SCADA data [132]. The SCADA system collects information extensively from key WT subassemblies using sensors fitted to the WT, i.e., anemometers, thermocouples, and switches. The operational data reflect either turbine status or measurements of signals, such as wind speed and direction, temperatures, currents, or pressures. This information can effectively reflect the real-time condition of a WECS, and by analyzing SCADA data, the relationship between different signals can be observed and

the health of WT components deduced [133]. Neural networks and fuzzy logic are other examples of the common tools for data analysis. An overview of WTCM based on SCADA data analysis is presented in Figure II-12.
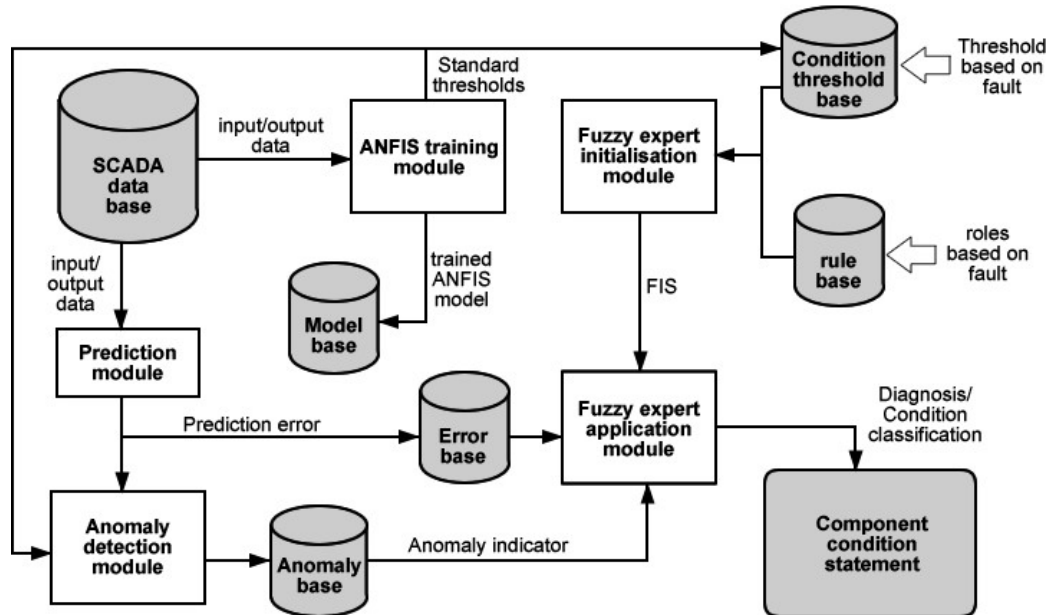
Figure II-12 Overview of wind turbine condition monitoring (WTCM) based on supervisory control and data acquisition (SCADA) data analysis. FIS: fuzzy interference system.

Several recent studies on SCADA data for WECS CM can be found in the literatures [132,134–137]. A wind turbine condition monitoring system (WTCMS) based on SCADA using normal behavior models and fuzzy logic was presented in [135]. This CMS is designed to detect trends and patterns in SCADA data and predict possible failures. Another recent research study by Li et al. [136] focused on improving the fuzzy synthetic condition assessment of a WT generator system. The results indicated that the evaluation of dynamic limits and deterioration degree functions for the characteristic variables for WECSs could be improved by analyzing SCADA data with the improved fuzzy synthetic model.

However, the WT SCADA system does not collect all of the information necessary to conduct a full CM of a WT because it was not initially designed for CM purposes.

43

Furthermore, although SCADA techniques are widely applied to WT, the data rate of once every 5–10 min is too slow for most rotating machine fault diagnoses [116,131,133]. Another concern is that the values of SCADA data vary over wide ranges under varying operational conditions, and it is difficult to detect an incipient fault from raw SCADA data without an appropriate data analysis tool [137].

This section provides a status update on different methods and techniques used for WTCM. Table II-1 presents an overview on the state of the art for WTCMSs, including possible failures and corresponding monitoring techniques for various WT components and subsystems. The following section focuses on new trends in WTCM with respect to the wind industry's evolution, and implications for challenges in the research area will be discussed based on these tendencies.

Table II-1   *Overview of possible failures and monitoring techniques for various WTs components and subsystems. OA: oil analysis; AE: acoustic emission; SM: strain measurement; VI: visual inspection; SPM: shock pulse method; and OM: operation and maintenance.*

WT subsystems	Components	Possible failures	Component or subsystem monitoring	
Rotor	Blades	Deterioration, cracking, and adjustment error	Ultrasound, and active thermography	Torque, AM, SM, and VI
	Bearings	Spalling, wear, defect of bearing shells and rolling element	Vibration, OA, AE, shock pulse methods, and performance monitoring	
	Shaft	Fatigue, and crack formation	Vibration	
Drive train	Main shaft bearing	Wear, and high vibration	Vibration, SPM, temperature, and AE	Torque, power signal analysis, thermography, AE, and performance monitoring
	Mechanical brake	Locking position	Temperature	

	Gearbox	Wearing, fatigue, oil leakage, insufficient lubrication, braking in teeth, displacement, and eccentricity of toothed wheels	Temperature, vibration, SPM, particles in oil, and AE
	Generator	Wearing, electrical, problems, slip rigs, winding damage, rotor asymmetries, bar break, overheating, and over speed	Generated effect, temperature, vibration, SPM, OM, torque, power signal analysis, electrical effects, process parameters, performance monitoring, and thermography
Auxiliary systems	Yaw system	Yaw motor problem, brake locked, and gear problem	Motor current
	Pitch system	Pitch motor problem	OM
	Hydraulic system	Pump motor problems, and oil leakage	OM, process parameter, performance monitoring
	Sensors	Broken, and wrong indication	Thermography
Electrical system	Control system	Short circuit, component fault, and bad connection	Current consumption, and temperature	Thermography, and VI
	Power electronics	Short circuit, component fault, and bad connection	Current consumption, and temperature
	High Voltage	Contamination, and arcs	Arc guard, temperature
Tower	Nacelle	Fire, and yaw error	Smoke, heat, flame detection	Vibration, shock pulse method, SM, and VI
	Tower	Crack formation, fatigue, vibration, and foundation weakness	-
System transformer		Problem with contamination, breakers, disconnectors, and isolators	Thermography

2.4. NEW TRENDS AND FUTURE CHALLENGES IN WIND TURBINE CONDITION MONITORING SYSTEMS (WTCMS)

The state-of-the-art maintenance strategy in the wind machine industry is defined by the implementation of on-line continuous CMS. The authors of [133,138] conducted respective surveys of: (i) commercially available CMSs for WT; and (ii) commercially available SCADA data analysis tools for WT health monitoring. The survey in [138] elaborated on the methods used by 20 suppliers and concluded that nearly all of them focus on the same subassemblies, i.e., blades, main bearings, gearbox internals, gearbox bearings, and generator bearings.

Furthermore, VM, OM, and fiber optic monitoring are the most frequently used monitoring techniques. The study in [133] addressed 17 SCADA data analysis tools for WTCM. Among the 17 products, three were developed by WT manufacturers, two by renewable energy consultancies, up to nine by industrial software companies, two by an electrical equipment provider, and only one by a WT operating company.

2.4.1. New Trends in Wind Turbine Condition Monitoring Systems

The current trend in the wind energy industry is the use of larger WTs in remote locations, which are increasingly situated offshore for optimal wind conditions. Both the size and location factors have led to maintenance challenges that are unique compared with those of traditional power generation systems [66]. To cope with this reality, WTCMS manufacturers must improve the existing monitoring techniques and/or develop more appropriate techniques. The future goal in CMS is to continue to minimize the efforts required from operators through the use of intelligent software algorithms and automated analysis.

The WT industry is moving toward intelligent machine health management (IMHM), which is a fourth-generation maintenance strategy. The final objective is to provide WECSs that are capable of understanding and making decisions without human intervention. This goal implies the use of intelligent condition-based maintenance systems based on RCM mechanisms. Thus, the following tendencies can be mentioned with respect to the new tendencies in the WTCM industry [52].

e) *Toward Smart Monitoring*

The purpose of this effort is to develop a CMS that is self-contained. Such systems could be operated by trained personnel but would not require specialists for the interpretation of results because a smart monitoring system will be able to perform classification and prediction operations [139]. Therefore, the number of turbines that a technician is able to oversee might double. Moreover, smart WTCMSs will integrate built-in hardware auto-diagnostics that continuously check all sensors, cabling, and electronics for any faults, signal interruption, shorts, or power failures. Any malfunctions trigger an alarm. Indeed, false warnings and false alarms occur on a regular basis with actual CMSs [119,140–143]. The use of smart monitoring will aid in avoiding such situations.

Automation of CM and diagnostic systems will also be an important development as WT operators acquire a larger number of turbines and manual inspection of data becomes impractical. Furthermore, it is essential that methods for reliable, automatic diagnosis are developed with consideration of multiple signals to improve detection and increase operator confidence in alarm signals [25,138].

f) *Necessity of Remote and E-Monitoring*

Considering: (i) the tendency toward the use of offshore WTs; and (ii) the fact that wind parks are geographically dispersed and often located in remote areas, cost considerations make it necessary to re-evaluate the traditional monitoring setup. Thus, remote CM of WECSs is gaining popularity in the industry and can be implemented as either standalone or networked systems. Remote CM involves monitoring the condition of a component at a location far away from the immediate vicinity of the component in question. E-monitoring and CM using the Internet improves remote monitoring by providing worldwide remote capabilities. Because browsers reside on many platforms, internet-based CMSs can be accessed by multiple users working on any type of operating system [144–146]. In short, wireless technologies will help to optimize the cost and efficiency of WTCMSs.

g) *In-Service SHM*

Given the increased size of modern turbines and their growing cost and fabrication sophistication, i.e., high-tech, complex, and constructed with composite materials, SHM is becoming increasingly important to both operators and insurers [143]. The necessity for continuous in-service SHM is a reality because these complex structures are fragile. For example, if any blade fails, the rotor can become unbalanced and might lead to the destruction of the entire WT [147]. Therefore, it is important to acquire early indications of structural or mechanical problems that will allow operators to better plan for maintenance, possible operation of the machine in a de-rated condition rather than taking the turbine off-line, or, in the case of an emergency, shutdown of the machine to avoid further damage.

The development of real-time, remote, wireless, and smart SHM is playing an increasingly important role. Such monitoring systems designed for the continuous assessment of structural performance and safety should be comprehensive and include

functions for self-diagnostics and management of the SHM system [88,148,149]. Similar SHM techniques are already used in certain industries, such as aeronautics, where they are applied for the SHM of aircraft composite structures [150,151]. Additionally, there is a tendency to require ambient energy harvesting for powering wireless sensors [152,153]. However, a major limitation in the field of energy harvesting is the fact that the energy generated by harvesting devices is far too small to directly power most electronics. Therefore, (i) efficient, innovative, and adapted methods of storing electric energy; and (ii) more energy-efficient sensors are the key technologies that will allow energy harvesting to become a source of power for electronics and wireless sensors [154–156].

Two different approaches are emerging in the field of WTSHM. The first and more practical approach is the development of appropriate non-contact and remote NDT/inspecting technologies for in-service WTSHM because non-contact and remote NDTs have overwhelming advantages in terms of on-line testing and inspection. The second approach consists of equipping the WT with a SHM system consisting of a network of sensors, data acquisition units, and an on-site server installed in the WT maintenance room. The sensors (accelerometers, displacement transducers, and temperature sensors) are placed at different levels inside and outside the steel tower and on the foundation of the WT. In this last case, microchip path antennas are increasingly used for sensing, ambient energy harvesting, and data transmission [157–160].

h) *Integration and Interaction of Monitoring and Control Systems*

Today's standard CMSs essentially still operate in stand-alone mode, i.e., independent of the WT controller. The CMSs are increasingly integrated with control functions and included in maintenance concepts [161]. The full integration of CM capabilities within the WT control system is beneficial with regard to three different aspects:

(i) cost benefits; (ii) technical benefits; and (iii) quality benefits. An overview of the benefits of controller-integrated CMSs was presented in [162,163] and can be summarized as follows:

Cost benefits:

- Lower hardware costs due to industrial mass production and fewer components;

- Lower installation and cabling costs due to integration in the existing control cabinet and communication with the main controller via bus systems;

- Fewer required parts because no additional voltage transformers, communication modules, uninterruptible power supply (UPS), or similar devices are needed;

- Reduced analysis because fewer false alarms occur.

Technical benefits:

- No measurement if interference signals are present;

- Higher-quality raw data for analysis;

- Fewer false alarms;

- Reduced scatter leads to improved fault detection;

- Integration of further signals (e.g., temperature, pressure, and current) enables integrated signal/system monitoring.

Quality benefits:

- Reliable hardware from established industrial suppliers;

- Mass production with high-quality standards.

i) *Estimation of the Remaining Component Life Service*

The limited accessibility of offshore wind farms requires new maintenance and repair strategies. In fact, offshore wind farms are likely to be unreachable for several months out of a year, especially if sited in the North Sea and polar regions [164,165]. Thus, maintenance

and repair activities must be carried out during seasons in which the turbines are accessible. Components that are likely to fail during periods of inaccessibility must be replaced. This approach is referred to as a "condition-dependent and predictive maintenance and repair strategy" [38,166]. Such a strategy requires comprehensive knowledge of the actual condition and the remaining lifetime of the turbine components. Such knowledge can be provided by CMSs. For those components, a count of their lifetime fatigue load can provide information on the condition and remaining lifetime. However, current CMSs are not able to assure that a given component will not fail, nor can they prevent a failure.

2.4.2. Future Research Challenges in WTCMTs

Although CM technologies face various challenges in WT applications, they are still necessary and valuable. As with any technology, there is room for improvement such that these systems can be better utilized to benefit the wind industry. Based on the provided discussion on new trends in WTCM, selected key points that must be addressed by further research are listed as follows:

- Determine the most cost-effective measurement or monitoring strategy.

- Automate the "experts" in data interpretation to automate actionable recommendations.

- Develop reliable and accurate prognostic techniques.

- Improve the use of SCADA system data (normally only stored at 10-min intervals) to provide a more reliable, flexible, and efficient tool for automatic WT monitoring and control [133].

- Develop smart, wireless, and energy-efficient sensors that will offer opportunities for placing sensors in difficult-to-reach locations, electrically noisy environments, and mobile applications in which wires cannot be installed.

- Focus on providing the newest and industry-proven signal processing algorithms for extracting the key features of a signal to predict machine component health.

- Combine numerical simulation analysis with testing, inspecting, and monitoring technologies. The finite element method is one such interesting tool that has traditionally been used in the development of WT blades, primarily to investigate the global behavior in terms of eigenfrequencies, tip deflections, and global stress/strain levels [167]. An advantage of using the finite element method is that complex load cases that represent actual wind conditions can be analyzed once the model is set up and calibrated. Moreover, this method will considerably reduce the cost of testing, inspecting, and monitoring for WTs, especially SHM.

- Develop innovative, adapted, and efficient methods of harvesting and storing electric energy for autonomous and wireless sensors.

Other technological advances that must be developed in WTCMs include advancements in diagnostic and prognostic software, acceptance of communication protocols, and developments in maintenance software applications and computer networking technologies [146]. Although these future research areas may appear challenging to address, they also represent great opportunities for CM to boost the success of the wind industry by reducing the COE and increasing its competitiveness.

2.5. CONCLUSIONS

WT technology has greatly advanced in a relatively short time span. Among the technologies successfully transferred from applications in other industries, CMSs enable early detection and diagnosis of potential component failures and serve as a platform for implementing CM practices.

This paper performed an inventory and classification of WTCMTs and has highlighted the fact that a combination of preventive and reactive maintenance strategies can improve reliability, availability, and maintainability of WTs while reducing maintenance costs. An overview of CM and the maintenance process in the WT industry enabled the presentation of a global diagram linking the various concepts, and a comprehensive review of WTCM techniques and methods was carried out.

For new trends in WTCM, the wind energy industry's tendency to use larger WTs in remote locations implies the need for remote, intelligent, and integrated CMSs. In particular, efforts should be directed toward improving the capacity of CMSs for failure prognostics and determination of remaining equipment life. Finally, this work addressed certain important and challenging areas of research that should be explored for the industry to better cope with the major innovations that are likely to occur in the WTCM industry.

Acknowledgments

Author Contributions

Pierre Tchakoua Takoutsing is the main author of this work. This paper provides a further elaboration of some of the results associated to his Ph.D. dissertation. René Wamkeue and Mohand Ouhrouche have supervised the Ph.D. work and thus have supported Pierre Tchakoua Takoutsing's research in terms of both scientific and technical expertise. Fouad Slaoui-Hasnaoui, Tommy Andy Tameghe and Gabriel Ekemb participated in designing the

structure of the contributions to fit them into a review of concepts and methods for WTCM.

All authors have been involved in the manuscript preparation.

Nomenclature

WT   Wind turbine

RCM   Reliability-centered maintenance

CM   Condition monitoring

OM: Operation and maintenance

WTCM   Wind turbine condition monitoring

WTCMS   Wind turbine condition-monitoring system

WECS   Wind energy conversion system

COE   Cost of energy

CMS   Condition-monitoring system

CMT   Condition-monitoring technique

FDS   Fault detection system

DT   Destructive test

NDT   Non-destructive tests

VA   Vibration analysis

OA   Oil analysis

TM   Temperature monitoring

SM   Strain measurement

OFM   Optical-fiber monitoring

SHM   Structural health monitoring

VI   Visual inspection

AE   Acoustic emission

UTT   Ultrasonic testing techniques

TA   Thermography analysis

SCADA   Supervisory control and data acquisition

SA   Signature analysis

Conflicts of Interest

The authors declare no conflict of interest.

References

1. Fried, L.; Sawyer, S.; Shukla, S.; Qiao, L; *Global Wind Report 2012—Annual Market Update*; Global Wind Energy Council (GWEC), http://www. gwec. net, 2013.

2. Zhang, P. *Small Wind World Report 2012*; World Wind Energy Association (WWEA): Bonn, Germany, 2012.

3. *Renewables 2012: Global Status Report*; REN21: Paris, France, 2012.

4. Ribrant, J. Reliability Performance and Maintenance—A Survey of Failures in Wind Power Systems. Master's Thesis, School of Electrical Engineeringm, KTH Royal Institute of Technology, Stockholm, Sweden, 2005–2006.

5. Hines, V.; Ogilvie, A.; Bond, C. *Continuous Reliability Enhancement for Wind (CREW) Database: Wind Turbine Reliability Benchmark Report*; Sandia National Laboratories: Albuquerque, N.M., USA, 2013.

6. Walford, C.A. *Wind Turbine Reliability: Understanding and Minimizing Wind Turbine Operation and Maintenance Costs*; Sandia Report No. SAND2006-1100; Sandia National Laboratories: Albuquerque, N.M., USA, 2006.

7. Tchakoua, P.; Wamkeue, R.; Tameghe, T.A.; Ekemb, G. A Review of Concepts and Methods for Wind Turbines Condition Monitoring. In Proceedings of the 2013 World Congress on Computer and Information Technology (WCCIT), Sousse, Tunisia, 22–24 June 2013; pp. 1–9.

8. Fischer, K.; Besnard, F.; Bertling, L. Reliability-centered maintenance for wind turbines based on statistical analysis and practical experience. *IEEE Trans. Energy Convers.* **2012**, *27*, 184–195.

9. McMillan, D.; Ault, G. Condition monitoring benefit for onshore wind turbines: Sensitivity to operational parameters. *IET Renew. Power Gener.* **2008**, *2*, 60–72.

10. Amayri, A.; Tian, Z.; Jin, T. Condition Based Maintenance of Wind Turbine Systems Considering Different Turbine Types. In Proceedings of the 2011 International

Conference on Quality, Reliability, Risk, Maintenance, and Safety Engineering (ICQR2MSE), Xi'an, Shannxi, China, 17–19 June 2011; pp. 596–600.

11. Besnard, F.; Bertling, L. An approach for condition-based maintenance optimization applied to wind turbine blades. *IEEE Trans. Sustain. Energy* **2010**, *1*, 77–83.

12. Echavarria, E.; Hahn, B.; van Bussel, G.J.; Tomiyama, T. Reliability of wind turbine technology through time. *J. Sol. Energy Eng.* **2008**, *130*, doi:10.1115/1.2936235.

13. Hahn, B.; Durstewitz, M.; Rohrig, K. Reliability of Wind Turbines. In *Wind Energy*; Springer: Berlin/Heidelberg, Germany, 2007; pp. 329–332.

14. Ahmad, R.; Kamaruddin, S. An overview of time-based and condition-based maintenance in industrial application. *Comput. Ind. Eng.* **2012**, *63*, 135–149.

15. Andrawus, J.A.; Watson, J.; Kishk, M. Wind turbine maintenance optimisation: Principles of quantitative maintenance optimisation. *Wind Eng.* **2007**, *31*, 101–110.

16. Andrawus, J.A. Maintenance Optimisation for Wind Turbines. Ph.D. Thesis, Robert Gordon University, Aberdeen, UK, April 2008.

17. Hahn, B. Reliability Assessment of Wind Turbines in Germany. In Proceedings of the 1999 Europeen Wind Energy Conference, Nice, France, 1–5 March 1999.

18. Tavner, P.J.; Xiang, J.; Spinato, F. Reliability analysis for wind turbines. *Wind Energy* **2007**, *10*, 1–18.

19. Guo, H.; Watson, S.; Tavner, P.; Xiang, J. Reliability analysis for wind turbines with incomplete failure data collected from after the date of initial installation. *Reliab. Eng. Syst. Saf.* **2009**, *94*, 1057–1063.

20. Spinato, F.; Tavner, P.J.; van Bussel, G.J.W.; Koutoulakos, E. Reliability of wind turbine subassemblies. *IET Renew. Power Gener.* **2008**, *3*, 387–401.

21. Amirat, Y.; Benbouzid, M.E.H.; Member, S.; Bensaker, B.; Wamkeue, R. Condition Monitoring and Fault Diagnosis in Wind Energy Conversion Systems: A Review. In Proceedings of the IEEE International Electric Machines & Drives Conference, IEMDC '07, Antalya, Turkey, 3–5 May 2007;Volume 2, pp. 1434–1439.

22. Ribrant, J.; Bertling, L. Survey of Failures in Wind Power Systems with Focus on Swedish Wind Power Plants during 1997–2005. In Proceedings of the 2007 IEEE

Power Engineering Society General Meeting, Tampa, FL, USA, 24–28 June 2007; pp. 1–8.

23. Villa, L.F.; Renones, A.; Pera, J.R.; de Miguel, L.J. Statistical fault diagnosis based on vibration analysis for gear test-bench under non-stationary conditions of speed and load. *Mech. Syst. Signal Process.* **2012**, *29*, 436–446.

24. Crabtree, C.J.; Feng, Y.; Tavner, P.J. Detecting Incipient Wind Turbine Gearbox Failure: A Signal Analysis Method for On-line Condition Monotoring. In Proceedings of European Wind Energy Conference (EWEC 2010), Warsaw, Poland, 20–23 April 2010; pp. 154–156.

25. Crabtree, C.J. Condition Monitoring Techniques for Wind Turbines. Ph.D. Thesis, Durham University, Durham, UK, February 2011.

26. Aziz, M.A.; Noura, H.; Fardoun, A. General Review of Fault Diagnostic in Wind Turbines. In Proceedings of the 2010 18th Mediterranean Conference on Control & Automation (MED), Marrakech, Morocco, 23–25 June 2010; pp. 1302–1307.

27. García, F.P.; Tobias, A.M.; Pinar, J.M.; Papaelias, M. Condition monitoring of wind turbines: Techniques and methods. *Renew. Energy* **2012**, *46*, 169–178.

28. Hameed, Z.; Hong, Y.S.; Cho, Y.M.; Ahn, S.H.; Song, C.K. Condition monitoring and fault detection of wind turbines and related algorithms: A review. *Renew. Sustain. Energy Rev.* **2009**, *13*, 1–39.

29. Lu, B.; Li, Y.; Wu, X.; Yang, Z. A Review of Recent Advances in Wind Turbine Condition Monitoring and Fault Diagnosis. In Proceedings of the IEEE Power Electronics and Machines in Wind Applications, PEMWA 2009, Lincoln, NE, USA, 24–26 June 2009; pp. 1–7.

30. Orsagh, R.F.; Lee, H.; Watson, M.; Byington, C.S.; Power, J. *Advance Vibration Monitoring for Wind turbine Health Management*; Impact Technologies, LLC: Rochester, NY, USA, 2006.

31. Dhillon, B.S. *Engineering Maintenance: A Modern Approach*; CRC Press: Boca Raton, FL., USA, 2002.

32. Madsen, B.N. Condition Monitoring of Wind Turbines by Electric Signature Analysis. Master's Thesis, Technical University of Denemark, Copenhagen, Denmark, October 2011.

33. Wang, L.; Yeh, T.-H.; Lee, W.-J.; Chen, Z. Benefit evaluation of wind turbine generators in wind farms using capacity-factor analysis and economic-cost methods. *IEEE Trans. Power Syst*. **2009**, *24*, 692–704.

34. Al-Ahmar, E.; Hachemi, M.E.; Turri, S. Wind energy conversion systems fault diagnosis using wavelet analysis. *Int. Rev. Electr. Eng.* **2008**, *3*, 646–652.

35. De Oliveria, W.S.; Fernandes, A.J. Cost-effectiveness analysis for wind energy projects. *Int. J. Energy Sci.* **2012**, *2*, 15–21.

36. Byon, E.; Ntaimo, L.; Ding, Y. Optimal maintenance strategies for wind turbine systems under stochastic weather conditions. *IEEE Trans. Reliab*. **2010**, *59*, 393–404.

37. Blischke, W.R.; Karim, M.R.; Prabhakar Murthy, D.N. *Warranty Data Collection and Analysis*; Springer: London, UK, 2011.

38. Nilsson, J.; Bertling, L. Maintenance management of wind power systems using condition monitoring systems—Life cycle cost analysis for two case studies. *IEEE Trans. Energy Convers*. **2007**, *22*, 223–229.

39. Hameed, Z.; Ahn, S.H.; Cho, Y.M. Practical aspects of a condition monitoring system for a wind turbine with emphasis on its design, system architecture, testing and installation. *Renew. Energy* **2010**, *35*, 879–884.

40. Wiggelinkhuizen, E.J.; Verbruggen, T.W.; Braam, H.; Rademakers, L.W.M.M.; Xiang, J.; Watson, S.; Giebel, G.; Norton, E.; Tipluica, M.C.; MacLean, A.; *et al.* CONMOW: Condition Monitoring for Offshore Wind Farms. In Proceedings of the European Wind Energy Conference (EWEC2007), Milan, Itlay, 7–10 May 2007.

41. *Renewable Energy Technologies: Cost Analysis Series*; The International Renewable Energy Agency (IRENA): Abu Dhabi, United Arab Emirates, 2012; Volume 1.

42. Arunraj, N.S.; Maiti, J. Risk-based maintenance—Techniques and applications. *J. Hazard. Mater.* **2007**, *142*, 653–661.

43. Sheng, C.; Li, Z.; Qin, L.; Guo, Z.; Zhang, Y. Recent progress on mechanical condition monitoring and fault diagnosis. *Procedia Eng.* **2011**, *15*, 142–146.

44. Jardine, A.K.S.; Lin, D.; Banjevic, D. A review on machinery diagnostics and prognostics implementing condition-based maintenance. *Mech. Syst. Signal Process.* **2006**, *20*, 1483–1510.

45. Utne, I.B.; Brurok, T.; Rodseth, H. A structured approach to improved condition monitoring. *J. Loss Prev. Process Ind.* **2012**, *25*, 148–188.

46. Bengsston, M. On Condition Based Maintenance ant Its Implimentation in Industrial Settings. Ph.D. Thesis, Mälardalen University, Västerås, Sweden, 2007.

47. Bengtsson, M.; Olsson, E.; Funk, P.; Jackson, M. Technical Design of Condition Based Maintenance System—A Case Study using Sound Analysis and Case-Based Reasoning. In Proceedings of the 8th Congress on Maintenance and Reliability Conference, MARCON 2004, Knoxville, TN., USA, 2-5 May 2004.

48. Simeón, E.A.; Álvares, A.J. An Expert System for Fault Diagnostics in Condition Based Maintenance. *ABCM Symp. Ser. Mechatron.* **2010**, *4*, 304–313.

49. *Maintenance Terminology*; SS-EN 13306; Swedish Standards Institute: Stockholm, Sweden, 2011.

50. Popa, L.M.; Jensen, B.-B.; Ritchie, E.; Boldea, I. Condition Monitoring of Wind Generators. In Proceedings of the 38th IAS Annual Meeting, Conference Record of the Industry Applications Conference, Salt Lake City, UT, USA, 12–16 October 2003; Volume 3, pp. 1839–1846.

51. Verbruggen, T. *Wind Turbine Operation & Maintenance based on Condition Monitoring WT-Ω*; ECN-C--03-047; Energieonderzoek Centrum Nederland (ECN): Petten, The Netherlands, 2003.

52. Tchakoua, P.; Wamkeue, R.; Slaoui-Hasnaoui, F.; Tameghe, T.A.; Ekemb, G. New Trends and Future Challenges for Wind Turbines Condition. In Proceedings of the 2013 International Conference on Control Automation and Information Sciences (ICCAIS), Nha Trang, Vietnam, 25–28 November 2013; pp. 238–245.

53. Saeed, A. Online Condition Monitoring System for Wind Turbine. Master's Thesis, Blekinge Institute of Technology, Karlskrona, Sweden, 2008.

54. Malhotra, V.M.; Carino, N.J. *Handbook on Nondestructive Testing of Concrete*; CRC Press: Boca Raton, FL., USA, 2004.

55. Gamidi, S.H. Non Destructive Testing of Structures. Master's Thesis, Indian Institute of Technology, Bombay, Libya, November 2009.

56. Hellier, C.J. *Handbook of Nondestructive Evaluation*; McGraw-Hill Professional Publishing: New York, NY., USA, 2003.

57. Elforjani, M.A. Condition Monitoring of Slow Speed Rotating Machinery Using Acoustic Emission Technology. Ph.D. Thesis, Cranfield University, Cranfield, UK, June 2010.

58. Khan, M.M.; Iqbal, M.T.; Khan, F. Reliability and Condition Monitoring of a Wind Turbine. In Proceedings of the 2005 Canadian Conference on Electrical and Computer Engineering, Saskatoon, SK,Canada, 1–4 May 2005; pp. 1978–1981.

59. Jablonsky, A.; Barszcz, T.; Bielecka, M. Automatic validation of vibration signals in wind farm distributed monitoring systems. *Measurement* **2011**, *44*, 1954–1967.

60. *Mechanical Vibration—Evaluation of Machine Vibration by Measurements on Non-Rotating Parts—Part 1: General Guidelines*; ISO 10816-1:1995; International Organization for Standardization (ISO): Geneva, Switzerland, 1995.

61. Barrett, M.P.; Stover, J. Understanding Oil Analysis: How it Can Improve the Reliability of Wind Turbine Gearboxes. *Gear Technology* **2013**, 104-111.

62. Dupuis, R. Application of Oil Debris Monitoring For Wind Turbine Gearbox Prognostics and Health Management. In Proceedings of the Annual Conference of the Prognostics and Health Management Society 2010, Portland, OR, USA, 10–16 October 2010.

63. Goncalves, A.C.; Campos, J.B. Predictive maintenance of a reducer with contaminated oil under an excentrical load through vibration and oil analysis. *J. Braz. Soc. Mech. Sci. Eng.* **2011**, *33*, 1–7.

64. Hamilton, A.; Quail, F. Detailed state of the art review for the different on-line/in-line oil analysis techniques in context of wind turbine gearboxes. *J. Tribol.* **2011**, *133*, doi:10.1115/1.4004903.

65. Walford, C.; Roberts, D. *Condition Monitoring of Wind Turbines: Technology Overview, Seeded-Fault Testing, and Cost-Benefit Analysis*; Technical Report 1010149; Global Energy Concepts, LLC: Kirkland, WA, USA, 2006.

66. Sheng, S.; Veers, P. *Wind Turbine Drivetrain Condition Monitoring—An Overview*; Mechanical Failures Prevention Group: Applied Systems Health Management Conference 2011, Virginia Beach, VA, USA, 10–12 May 2011.

67. Du, L.; Zhe, J. A high throughput inductive pulse sensor for online oil debris monitoring. *Tribol. Int.* **2011**, *44*, 175–179.

68. Hasan, I.; Rahaman, M.I. Intelligent Diagnostics and Predictive Maintenance Sensor System for Electrical Fault Diagnosis of Wind Turbine System. In Proceedings of the Global Engineering, Science and Technology Conference 2012, Dhaka, Bangladesh, 28–29 December 2012.

69. Park, J.-Y.; Lee, J.-K.; Oh, K.-Y.; Lee, J.-S.; Kim, B.-J. Design of Simulator for 3MW Wind Turbine and its Condition Monitoring System. In Proceedings of the International MultiConference of Engineers and Computer Scientists, IMECS 2010, Kowloon, Hong Kong, 17–19 March 2010; Volume II, pp. 930–933.

70. Jayaswal, P.; Wadhwani, A.; Mulchandani, K. Machine fault signature analysis. *Int. J. Rotat. Mach.* **2008**, *2008*, doi:10.1155/2008/583982.

71. Gong, X. Online Nonintrusive Condition Monitoring and Fault Detection for Wind Turbines. Ph.D. Thesis, Department of Electrical Engineering, University of Nebraska–Lincoln, Lincoln, NE, USA, August 2012.

72. Ciang, C.C.; Lee, J.-R.; Bang, H.-J. Structural health monitoring for a wind turbine system: A review of damage detection methods. *Meas. Sci. Technol.* **2008**, *19*, doi:10.1088/0957-0233/
19/12/122001.

73. Kreuzer, M. *Strain Measurement with Fiber Bragg Grating Sensors*; S2338–1.0 e; HBM GmbH: Darmstadt, Germany, 2006.

74. Bang, H.-J.; Kim, H.-I.; Lee, K.-S. Measurement of strain and bending deflection of a wind turbine tower using arrayed FBG sensors. *Int. J. Precis. Eng. Manuf.* **2012**, *13*, 2121–2126.

75. Lee, J.M.; Hwang, Y. A novel online rotor condition monitoring system using fiber Bragg grating (FBG) sensors and a rotary optical coupler. *Meas. Sci. Technol.* **2008**, *19*, doi:10.1088/0957-0233/19/6/065303.

76. Kang, L.-H.; Kim, D.-K.; Han, J.-H. Estimation of dynamic structural displacements using fiber Bragg grating strain sensors. *J. Sound Vib.* **2007**, *305*, 534–542.

77. Turner, A.; Graver, T.W. Structural monitoring of wind turbine blades using fiber optic Bragg grating strain sensors. *Exp. Mech. Emerg. Energy Syst. Mater.* **2011**, *5*, 149–154.

78. Schroeder, K.; Ecke, W.; Apitz, J.; Lembke, E.; Lenschow, G. A fibre Bragg grating sensor system monitors operational load in a wind turbine rotor blade. *Meas. Sci. Technol.* **2006**, *17*, doi:10.1088/0957-0233/17/5/S39.

79. Kramer, S.G.; Leon, F.P.; Appert, B. Fiber Optic Sensor Network for Lightning Impact Localization and Classification in Wind Turbines. In Proceedings of the 2006 IEEE International Conference on Multisensor Fusion and Integration for Intelligent Systems, Heidelberg, Germany, 3–6 September 2006; pp. 173–178.

80. Rademakers, L.W.M.M.; Vebruggen, T.W.; van der Werff, P.A.; Korterink, H.; Richon, D.; Rey, P.; Lancon, F. Fiber Optic Blade Monitoring. In Proceedings of the European Wind Energy Conference, London, UK, 22–25 November 2004; pp. 22–25.

81. Eum, S.; Kageyama, K.; Murayama, H.; Uzawa, K.; Ohsawa, I.; Kanai, M.; Igawa, H. Process/Health Monitoring for Wind Turbine Blade by Using FBG Sensors with Multiplexing Techniques. In Proceedings of the 19th International Society for Optics and Photonics, Perth, Australia, 14–18 April 2008; Volume 7004, doi:10.1117/12.786240.

82. Shin, C.; Chen, B.; Cheng, J.; Liaw, S. Impact response of a wind turbine blade measured by distributed FBG sensors. *Mater. Manuf. Process.* **2010**, *25*, 268–271.

83. Guemes, A.; Fernandez-Lopez, A.; Soller, B. Optical fiber distributed sensing-physical principles and applications. *Struct. Health Monit.* **2010**, *9*, 233–245.

84. Merzbacher, C.; Kersey, A.; Friebele, E. Fiber optic sensors in concrete structures: A review. *Smart Mater. Struct.* **1996**, *5*, doi:10.1088/0964-1726/5/2/008.

85. Moragues Pons, J. Practical Experiments on the Efficiency of the Remote Presence: Remote Inspection in an Offshore Wind Turbine. Master's Thesis, Norwegian University of Science and Technology, Trondheim, Norway, 21 June 2012.

86. Sheppard, R.; Puskar, F.; Waldhart, C. SS: Offshore Wind Energy Special Session: Inspection Guidance for Offshore Wind Turbine Facilities. In Proceedings of the Offshore Technology Conference, Houston, TA, USA, 3–6 May 2010.

87. Effren, D. *Automated Turbine Inspection*; AutoCopter™ Corporation: Charlotte, NC, USA, 2011.

88. Smarsly, K.; Law, K.H. Advanced Structural Health Monitoring Based on Multi-Agent Technology. In *Computation for Humanity: Information Technology to Advance Society*; Taylor & Francis Group: Boca Raton, FL, USA, 2012.

89. McGugan, M.; Larsen, G.C.; Sorensen, B.F.; Borum, K.K.; Engelhardt, J. *Fundamentals for Remote Condition Monitoring of Offshore Wind Turbines*; Danmarks Tekniske Universitet, Risø Nationallaboratoriet for Bæredygtig Energi, 2008.

90. Balageas, D.; Fritzen, C.-P.; Güemes, A. *Structural Health Monitoring*; ISTE Ltd: London, United Kingdom, 2006.

91. Schubel, P.; Crossley, R.; Boateng, E.; Hutchinson, J. Review of structural health and cure monitoring techniques for large wind turbine blades. *Renew. Energy* **2013**, *51*, 113–123.

92. Hyers, R.; McGowan, J.; Sullivan, K.; Manwell, J.; Syrett, B. Condition monitoring and prognosis of utility scale wind turbines. *Energy Mater.* **2006**, *1*, 187–203.

93. Watson, M.; Sheldon, J.; Amin, S.; Lee, H.; Byington, C.; Begin, M. A Comprehensive High Frequency Vibration Monitoring System for Incipient Fault Detection and Isolation of Gears, Bearings and Shafts/Couplings in Turbine Engines and Accessories. In Proceedings of the ASME Turbo Expo 2007: Power for Land, Sea, and Air, Montreal, QC, Canada, 14–17 May 2007; Volume 5, pp. 885–894.

94. Lading, L.; McGugan, M.; Sendrup, P.; Rheinlander, J.; Rusborg, J. *Fundamentals for Remote Structural Health Monitoring of Wind Turbine Blades-A Preproject, Annex B: Sensors and Non-Destructive Testing Methods for Damage Detection in Wind Turbine Blades*; Riso National Laboratory: Roskilde, Denmark, 2002.

95. Mba, D.; Rao, R.B. Development of acoustic emission technology for condition monitoring and diagnosis of rotating machines; bearings, pumps, gearboxes, engines and rotating structures. *Shock Vib. Dig.* **2006**, *38*, 3–16.

96. Tan, C.K.; Irving, P.; Mba, D. A comparative experimental study on the diagnostic and prognostic capabilities of acoustics emission, vibration and spectrometric oil analysis for spur gears. *Mech. Syst. Signal Process.* **2007**, *21*, 208–233.

97. Loutas, T.; Kalaitzoglou, J.; Sotiriades, G.; Kostopoulos, V. The Combined Use Of Vibration, Acoustic Emission And Oil Debris Sensor Monitored Data Coming From

Rotating Machinery For The Development Of A Robust Health Monitoring System. Availble online: http://maritime-conferences.com/asranet2010-conference/asranet2008/53%20Kostopoulos,%20V.pdf (accessed on 22 February 2011).

98. Loutas, T.; Sotiriades, G.; Kalaitzoglou, I.; Kostopoulos, V. Condition monitoring of a single-stage gearbox with artificially induced gear cracks utilizing on-line vibration and acoustic emission measurements. *Appl. Acoust.* **2009**, *70*, 1148–1159.

99. Soua, S.; Lieshout, P.V.; Perera, A.; Gan, T.-H.; Bridge, B. Determination of the combined vibrational and acoustic emission signature of a wind turbine gearbox and generator shaft in service as a pre-requisite for effective condition monitoring. *Renew. Energy* **2013**, *51*, 175–181.

100. Raisutis, R.; Jasiuniene, E.; Sliteris, R.; Vladisauskas, A. The review of non-destructive testing techniques suitable for inspection of the wind turbine blades. *Ultrasound* **2008**, *63*, 26–30.

101. Rose, J.L. Ultrasonic guided waves in structural health monitoring. *Key Eng. Mater.* **2004**, *270*, 14–21.

102. Lee, J.-R.; Takatsubo, J.; Toyama, N.; Kang, D.-H. Health monitoring of complex curved structures using an ultrasonic wavefield propagation imaging system. *Meas. Sci. Technol.* **2007**, *18*, doi:10.1088/0957-0233/18/12/017.

103. Jasiuniene, E.; Raisutis, R.; Sliteris, R.; Voleisis, A.; Jakas, M. Ultrasonic NDT of wind turbine blades using contact pulse-echo immersion testing with moving water container. *Ultrasound* **2008**, *63*, 28–32.

104. Giurgiutiu, V.; Cuc, A. Embedded non-destructive evaluation for structural health monitoring, damage detection, and failure prevention. *Shock Vib. Dig.* **2005**, *37*, 83–105.

105. Tsai, C.-S.; Hsieh, C.-T.; Huang, S.-J. Enhancement of damage-detection of wind turbine blades via CWT-based approaches. *IEEE Trans. Energy Convers.* **2006**, *21*, 776–781.

106. Drewry, M.A.; Georgiou, G.A. A review of NDT techniques for wind turbines. *Insight-Non-Destr. Test. Cond. Monit.* **2007**, *49*, 137–141.

107. Cheng, L.; Tian, G.Y. Comparison of nondestructive testing methods on detection of delaminations in composites. *J. Sens.* **2012**, *2012*, doi:org/10.1155/2012/408437.

108. Jüngert, A. Damage Detection in Wind Turbine Blades Using Two Different Acoustic Techniques. In Proceedings of the 7th fib Ph.D. Symposium, Stuttgart, Germany, 11–13 September 2008.

109. Beattie, A.G.; Rumsey, M. *Non-Destructive Evaluation of Wind Turbine Blades Using an Infrared Camera*; SAND98-2824C; Sandia National Laboratory: Albuquerque, NM, USA, 1998.

110. Liu, W.; Tang, B.; Jiang, Y. Status and problems of wind turbine structural health monitoring techniques in China. *Renew. Energy* **2010**, *35*, 1414–1418.

111. Bodil, A.; Mats, D.; Magnus, U. *Feasibility Study of Thermal Condition Monitoring and Condition Based Maintenance in Wind Turbines*; Elforsk Report 11:19; ELFORSK: Stockholm, Sweden, 2011.

112. Ge, Z.; Du, X.; Yang, L.; Yang, Y.; Li, Y.; Jin, Y. Performance monitoring of direct air-cooled power generating unit with infrared thermography. *Appl. Therm. Eng.* **2011**, *31*, 418–424.

113. Yang, W.; Tavner, P.J.; Crabtree, C.J.; Wilkinson, M. Cost-effective condition monitoring for wind turbines. *IEEE Trans. Ind. Electron.* **2010**, *57*, 263–271.

114. Yang, W.; Jiang, J.; Tavner, P.; Crabtree, C. Monitoring Wind Turbine Condition by the Approach of Empirical Mode Decomposition. In Proceedings of the International Conference on Electrical Machines and Systems, ICEMS 2008, Wuhan, Hubei, China, 17–20 October 2008; pp. 736–740.

115. Yang, W.; Tavner, P.; Crabtree, C.; Wilkinson, M. Research on a Simple, Cheap but Globally Effective Condition Monitoring Technique for Wind Turbines. In Proceedings of the 18th International Conference on Electrical Machines, ICEM 2008, Vilamoura, Portugal, 6–9 September 2008; pp. 1–5.

116. Wilkinson, M.R.; Spinato, F.; Tavner, P.J. Condition Monitoring of Generators & Other Subassemblies in Wind Turbine Drive Trains. In Proceedings of the IEEE International Symposium on Diagnostics for Electric Machines, Power Electronics and Drives, SDEMPED 2007, Cracow, Poland, 6–8 September 2007; pp. 388–392.

117. Costinas, S.; Diaconescu, I.; Fagarasanu, I. Wind Power Plant Condition Monitoring. In Proceedings of the 3rd WSEAS Int. Conf. on Energy Planning, Energy Saving,

Environmental Education (EPESE '09), Canary Islands, Spain, 1–3 July 2009; pp. 71–76.

118. Fuchs, E.; Masoum, M.A.S. *Power Quality in Power Systems and Electrical Machines*; Elsevier Academic Press: Burlington, MA., USA, 2008.

119. Yang, W.; Tavner, P.J.; Crabtree, C.J. An Intelligent Approach to the Condition Monitoring of Large Scale Wind Turbines. In Proceedings of the European Wind Energy Conference and Exhibition (EWEC2009), Marseille, France, 16–19 March 2009.

120. Cook, K. A Power Quality Monitoring System for a 20 kW Ocean Turbine. Master's Thesis, Florida Atlantic University, Dania Beach, FL, USA, August 2010.

121. Qiao, W. *Recovery Act: Online Nonintrusive Condition Monitoring and Fault Detection for Wind Turbines*; Award Number DE-EE0001366; University of Nebraska–Lincoln, Lincoln, NE, USA, 2012.

122. Watson, S.J.; Xiang, B.J.; Yang, W.; Tavner, P.J.; Crabtree, C.J. Condition monitoring of the power output of wind turbine generators using wavelets. *IEEE Trans. Energy Convers.* **2010**, *25*, 715–721.

123. Amirat, Y.; Choqueuse, V.; Benbouzid, M. Condition Monitoring of Wind Turbines Based on Amplitude Demodulation. In Proceedings of the 2010 IEEE Energy Conversion Congress and Exposition (ECCE), Atlanta, GA, USA, 12–16 September 2010; pp. 2417–2421.

124. Wakui, T.; Yokoyama, R. Wind speed sensorless performance monitoring based on operating behavior for stand-alone vertical axis wind turbine. *Renew. Energy* **2013**, *53*, 49–59.

125. Yang, W.X.; Tavner, P.J.; Crabtree, C.J. Bivariate empirical mode decomposition and its contribution to wind turbine condition monitoring. *J. Sound Vib.* **2011**, *330*, 3766–3782.

126. Yang, W.X.; Tavner, P.J.; Court, R. An online technique for condition monitoring the induction generators used in wind and marine turbines. *Mech. Syst. Signal Process.* **2012**, *38*, 103–112.

127. Gill, S.; Stephen, B.; Galloway, S. Wind turbine condition assessment through power curve copula modeling. *IEEE Trans. Sustain. Energy* **2012**, *3*, 94–101.

128. Yazidi, A.; Henao, H.; Capolino, G.; Artioli, M.; Filippetti, F.; Casadei, D. Flux Signature Analysis: An Alternative Method for the Fault Diagnosis of Induction Machines. In Proceedings of the 2005 IEEE Russia Power Tech, St. Petersburg, Russia, 27–30 June 2005; pp. 1–6.

129. Yazidi, A.; Capolino, G.; Filippetti, F.; Casadei, D. A New Monitoring System for Wind Turbines with Doubly-Fed Induction Generators. In Proceedings of the IEEE Mediterranean Electrotechnical Conference, MELECON 2006, Malaga, Spain, 16–19 May 2006; pp. 1142–1145.

130. Douglas, H.; Pillay, P.; Barendse, P. The Detection of Interturn Stator Faults in Doubly-Fed Induction Generators. In Proceedings of the Conference Record of the 2005 Industry Applications Conference, Fourtieth IAS Annual Meeting, Kowloon, Hong Kong, 2–6 October 2005; Volume 2, pp. 1097–1102.

131. Yang, W.; Tavner, P.; Wilkinson, M. Wind Turbine Condition Monitoring and Fault Diagnosis Using Both Mechanical and Electrical Signatures. In Proceedings of the IEEE/ASME International Conference on Advanced Intelligent Mechatronics, AIM 2008, Xian, Shannxi, China, 2–5 July 2008; pp. 1296–1301.

132. Butler, S.; O'Connor, F.; Farren, D.; Ringwood, J.V. A Feasibility Study into Prognostics for the Main Bearing of A Wind Turbine. In Proceedings of the 2012 IEEE International Conference on Control Applications (CCA), Dubrovnik, Croatia, 3–5 October 2012; pp. 1092–1097.

133. Chen, B. *Survey of Commercially Available SCADA Data Analysis Tools for Wind Turbine Health Monitoring*; School of Engineering and Computing Sciences, Durham University: Durham, UK, 2010.

134. Schlechtingen, M.; Santos, I.F. Condition Monitoring with Ordinary Wind Turbine SCADA Data—A Neuro-Fuzzy Approach. In Proceedings of the European Wind Energy Association (EWEA) Offshore 2011, Amsterdam, The Netherlands, 29 November–1 December 2011.

135. Schlechtingen, M.; Santos, I.F.; Achiche, S. Wind turbine condition monitoring based on SCADA data using normal behavior models: Part 1: System description. *Appl. Soft Comput.* **2013**, *13*, 259–270.

136. Li, H.; Hu, Y.; Yang, C.; Chen, Z.; Ji, H.; Zhao, B. An improved fuzzy synthetic condition assessment of a wind turbine generator system. *Int. J. Electr. Power Energy Syst.* **2013**, *45*, 468–476.

137. Yang, W.X.; Court, R.; Jiang, J.S. Wind turbine condition monitoring by the approach of SCADA data analysis. *Renew. Energy* **2013**, *53*, 365–376.

138. Crabtree, C.J. *Survey of Commercially Available Condition Monitoring Systems for Wind Turbines*; Durham University: Durham, UK, 2010.

139. Wang, W. An intelligent system for machinery condition monitoring. *IEEE Trans. Fuzzy Syst.* **2008**, *16*, 110–122.

140. Amirat, Y.; Choqueuse, V.; Benbouzid, M. Wind Turbines Condition Monitoring and Fault Diagnosis Using Generator Current Amplitude Demodulation. In Proceedings of the 2010 IEEE International Energy Conference and Exhibition (EnergyCon), Manama, Bahrain, 18–22 December 2010; pp. 310–315.

141. Zimroz, R.; Urbanek, J.; Barszcz, T.; Bartelmus, W.; Millioz, F.; Martin, N. Measurement of instantaneous shaft speed by advanced vibration signal processing-application to wind turbine gearbox. *Metrol. Meas. Syst.* **2011**, *18*, 701–712.

142. Ye, X.; Yan, Y.; Osadciw, L.A. Learning Decision Rules by Particle Swarm Optimization (PSO) for Wind Turbine Fault Diagnosis. In Proceedings of the Annual Conference of the Prognostics and Health Management Society 2010, Portland, OR, USA, 10–16 October 2010.

143. Boyle, D.; Magno, M.; O'Flynn, B.; Brunelli, D.; Popovici, E.; Benini, L. Towards Persistent Structural Health Monitoring through Sustainable Wireless Sensor Networks. In Proceedings of the 2011 Seventh International Conference on Intelligent Sensors, Sensor Networks and Information Processing (ISSNIP), Adelaide, SA, Australia, 6–9 December 2011; pp. 323–328.

144. Christensen, J.J.; Andersson, C.; Gutt, S. Remote Condition Monitoring of Vestas Turbines. In Proceedings of the of European Wind Energy Conference and Exhibition (EWEC2009), Marseille, France, 16–19 March 2009.

145. Miguelanez, E.; Lane, D. Predictive Diagnosis for Offshore Wind Turbines Using Holistic Condition Monitoring. In Proceedings of the OCEANS 2010, Seattle, WA, USA, 20–23 September 2010; pp. 1–7.

146. Higgs, P.A.; Parkin, R.; Jackson, M.; Al-Habaibeh, A.; Zorriassatine, F.; Coy, J. A Survey on Condition Monitoring Systems in Industry. In Proceedings of the ASME 7th Biennial Conference on Engineering Systems Design and Analysis, Manchester, UK, 19–22 July 2004; Volume 3, pp. 163–178.

147. Yang, B.; Sun, D. Testing, inspecting and monitoring technologies for wind turbine blades: A survey. *Renew. Sustain. Energy Rev.* **2013**, *22*, 515–526.

148. Lynch, J.P.; Loh, K.J. A summary review of wireless sensors and sensor networks for structural health monitoring. *Shock Vib. Dig.* **2006**, *38*, 91–130.

149. Smarsly, K.; Law, K.H.; Hartmann, D. Implementing a Multiagent-Based Self-Managing Structural Health Monitoring System on a Wind Turbine. In Proceedings of the 2011 NSF Engineering Research and Innovation Conference, Atlanta, GA, USA, 4–7 January 2011.

150. Diamanti, K.; Soutis, C. Structural health monitoring techniques for aircraft composite structures. *Prog. Aerosp. Sci.* **2010**, *46*, 342–352.

151. Giurgiutiu, V.; Zagrai, A.; Bao, J.J. Piezoelectric wafer embedded active sensors for aging aircraft structural health monitoring. *Struct. Health Monit.* **2002**, *1*, 41–61.

152. Seah, W.K.; Eu, Z.A.; Tan, H.-P. Wireless Sensor Networks Powered by Ambient Energy Harvesting (WSN-HEAP)-Survey and Challenges. In Proceedings of the 1st International Conference on Wireless Communication, Vehicular Technology, Information Theory and Aerospace & Electronic Systems Technology, Wireless VITAE 2009, Aalborg, Denmark, 17–20 May 2009; pp. 1–5.

153. Eu, Z.A.; Tan, H.-P.; Seah, W.K. Design and performance analysis of MAC schemes for wireless sensor networks powered by ambient energy harvesting. *Ad Hoc Netw.* **2011**, *9*, 300–323.

154. Fu, T.S.; Ghosh, A.; Johnson, E.A.; Krishnamachari, B. Energy-efficient deployment strategies in structural health monitoring using wireless sensor networks. *Struct. Control Health Monit.* **2013**, *20*, 971–986.

155. Park, G.; Rosing, T.; Todd, M.D.; Farrar, C.R.; Hodgkiss, W. Energy harvesting for structural health monitoring sensor networks. *J. Infrastruct. Syst.* **2008**, *14*, 64–79.

156. Ling, Q.; Tian, Z.; Yin, Y.; Li, Y. Localized structural health monitoring using energy-efficient wireless sensor networks. *IEEE Sens. J.* **2009**, *9*, 1596–1604.

157. Daliri, A.; Galehdar, A.; Rowe, W.S.; Ghorbani, K.; John, S. Utilising microstrip patch antenna strain sensors for structural health monitoring. *J. Intell. Mater. Syst. Struct.* **2012**, *23*, 169–182.

158. Daliri, A.; Galehdar, A.; John, S.; Rowe, W.; Ghorbani, K. Circular Microstrip Patch Antenna Strain Sensor for Wireless Structural Health Monitoring. In Proceedings of the World Congress on Engineering, WCE 2010, London, UK, 30 June–2 July 2010; Volume II, pp. 1173–1178.

159. Daliri, A.; Galehdar, A.; John, S.; Rowe, W.S.T.; Ghorbani, K. Slotted Circular Microstrip Patch Antenna Application in Strain Based Structural Health Monitoring. In Proceedings of the AIAC14 Fourteenth Australian International Aerospace Congress, Melbourne, Australia, 28 February–3 March 2011.

160. Taylor, S.G.; Farinholt, K.M.; Flynn, E.B.; Figueiredo, E.; Mascarenas, D.L.; Moro, E.A.; Park, G.; Todd, M.D.; Farrar, C.R. A mobile-agent-based wireless sensing network for structural monitoring applications. *Meas. Sci. Technol.* **2009**, *20*, doi:10.1088/0957-0233/20/4/045201.

161. Park, J.-Y.; Kim, B.-J.; Lee, J.-K. Development of Condition Monitoring System with Control Functions for Wind Turbines. *World Acad. Sci. Eng. Technol.* **2011**, *5*, 269–274.

162. Isko, V.; Mykhaylyshyn, V.; Moroz, I.; Ivanchenko, O.; Rasmussen, P. Remote Wind Turbine Generator Condition Monitoring with Mita-Teknik's WP4086 System. In Proceedings of the 2010 European Wind Energy Conference (EWEC) & Exhibition, Warsaw, Poland, 20–23 April 2010.

163. Koutroulis, E.; Kalaitzakis, K. Development of an integrated data-acquisition system for renewable energy sources systems monitoring. *Renew. Energy* **2003**, *28*, 139–152.

164. Feuchtwang, J.; Infield, D. The Offshore Access Problem and Turbine Availability-Probabilistic Modelling of Expected Delays to Repairs. In Procedings of the European

Offshore Wind (EOW) Conference & Exhibition, Stockholm, Sweden, 14–16 September 2009.

165. Karyotakis, A. On the Optimisation of Operation and Maintenance Strategies for Offshore Wind Farms. Ph.D. Thesis, University College London (UCL), London, UK, 2011.

166. Byon, E.; Ding, Y. Season-dependent condition-based maintenance for a wind turbine using a partially observed Markov decision process. *IEEE Trans. Power Syst.* **2010**, *25*, 1823–1834.

167. Jensen, F.M.; Falzon, B.; Ankersen, J.; Stang, H. Structural testing and numerical simulation of a 34 m composite wind turbine blade. *Compos. Struct.* **2006**, *76*, 52–61.

Chapter III

PROPOSING A NEW APPROACH FOR WIND TURBINES AERODYNAMICS MODELLING WITH APPLICATION TO DARRIEUS TYPE VERTICAL AXIS WIND TURBINES

A New Approach for Modeling Darrieus-Type Vertical Axis Wind Turbine Rotors Using Electrical Equivalent Circuit Analogy: Basis of Theoretical Formulations and Model Development

Pierre Tchakoua, René Wamkeue, Mohand Ouhrouche, Tommy Andy Tameghe and Gabriel Ekemb

Résumé

Les modèles sont essentiels dans le processus de conception en ingénierie car ils peuvent être utilisés aussi bien pour l'optimisation des paramètres de conception que pour la prédiction des performances. Ainsi, les modèles peuvent considérablement réduire les coûts de conception, de développement et d'optimisation. Cet article propose un nouveau modèle électrique équivalent pour les rotors d'éoliennes à axe vertical type Darrieus. Le modèle proposé a été construit à partir de la description mécanique donnée par le modèle à double disques et multiples tubes de vents donnés par Paraschivoiu et repose sur l'analogie entre circuits mécaniques et électriques. Ce travail présente les concepts physiques et les fondements théoriques sur lesquels est basé le développement du nouveau modèle. Après avoir présenté le principe de fonctionnement des éoliennes à axe vertical type Darrieus, les différentes étapes de développement du nouveau modèle sont graduellement présentées. À des fins d'évaluation, les caractéristiques aérodynamiques des pales et celles des composants électriques correspondants sont simulées et comparées.

Abstract

Models are crucial in the engineering design process because they can be used for both the optimization of design parameters and the prediction of performance. Thus, models can significantly reduce design, development and optimization costs. This paper proposes a novel equivalent electrical model for Darrieus-type vertical axis wind turbines (DTVAWTs). The proposed model was built from the mechanical description given by the Paraschivoiu double-multiple streamtube model and is based on the analogy between mechanical and electrical circuits. This work addresses the physical concepts and theoretical formulations underpinning the development of the model. After highlighting the working principle of the DTVAWT, the step-by-step development of the model is presented. For assessment purposes, simulations of aerodynamic characteristics and those of corresponding electrical components are performed and compared.

3.1. INTRODUCTION

The aerodynamic characteristics of vertical-axis wind turbines (VAWTs) are somewhat more complex than those of horizontal-axis configurations. Thus, industrial and academic research has primarily focused on horizontal-axis turbines over the past several decades. As a result, VAWTs are still relatively poorly understood [1].

3.1.1 The Growing Interest for Vertical-Axis Wind Turbines (VAWTs)

VAWTs have various advantages over horizontal-axis wind turbines (HAWTs). The main advantage is their omni-directionality; a VAWT can operate using wind incident from any direction and therefore does not require a yaw control system. Moreover, a VAWT gearbox and generator can be placed at ground level, making maintenance easier and reducing construction costs [1–3]. Finally, VAWTs are noiseless and do not slow wind down as much as HAWTs do, making VAWTs less detrimental to humans and birds. As a result, VAWTs can be placed close together in a wind farm [4]. These advantages make VAWTs better suited to local production of clean electric power in industrial and residential areas [5]; furthermore, these benefits have led to a renewed interest in VAWTs for small- and medium-scale power generation. For all of these reasons, VAWTs have experienced renewed interest in recent years [6–8]. Several universities and research institutions have conducted extensive research and developed numerous designs based on several aerodynamic computational models [3,6].

Being able to numerically predict wind turbine performance offers a tremendous benefit over classic experimental techniques; the major benefit is that computational studies are more economical than are such costly experiments. Various wind turbine computational models exist, each with their own strengths and weaknesses, which attempt to accurately

predict the performance of VAWTs [9]. These models are all based on the simple idea of being able to determine the relative velocity and, in turn, the tangential force component of the individual blades at various azimuthal locations [10].

3.1.2 The Necessity of a New Modeling Approach for Darrieus-Type Vertical-Axis Wind Turbines (VAWTs)

VAWTs are becoming ever more important in wind power generation thanks to their compactness and adaptability for domestic installations. However, it is well known that VAWTs have poor efficiency, especially compared to HAWTs. To improve the performance of VAWTs, industries and researchers are attempting to optimize the design of the rotors [11]. Thus, models are crucial because they can be used for parameter optimization, performance prediction before fabrication, condition monitoring and fault detection and prediction [12–14]. Various models can be found for VAWT simulation in the literature [15–22]. These models can be broadly classified into four categories: momentum models, vortex models, cascade models and computational fluid dynamic (CFD) models. Based on [17,23–30], a quick literature survey was performed on most used models. Table 1 presents the relevant features as well as the advantages and shortcoming for each model category. Table 1 shows that aerodynamic models remain unable to meet the demands of various applications, although the streamtube and vortex models have seen significant improvement. Meanwhile, CFD solutions remain computationally very expensive and are basically prohibitive for the routine engineering analyses of the local interaction mechanisms of wind turbines. Furthermore, none of the models with high reliability and accuracy can be efficiently coupled with models of the other mechanical and electrical parts of the wind turbine to form a global model for the wind energy conversion system (WECS).

The goal of this research is to establish the bases for the construction of a new model for Darrieus-type vertical axis wind turbines (DTVAWTs). This model is likely to be more user friendly for the electrical engineering community in particular. This is of great importance especially because wind energy is multidisciplinary domain with increasing resources from the field of electrical engineering. In addition, it will be possible to link the model to other mechanical and electrical part models to form a global model for the WECS. Such a global model will help users understand the effects of various aerodynamic phenomena and other structural faults on other blade components as well as the overall performance of the WECS. Finally, the new model is of great versatility and may therefore permit the study of various effects and phenomena, including dynamic stall effects, flow curvature effects, pitching circulation, added mass effects, interference among blades, and vibration effects.

The proposed model is an equivalent model based on the analogy between mechanical and electrical circuits. Our initial motivation is that the use of electrical circuit elements to model physical devices and systems has a long history of success. Additionally, knowledge of analogies and construction of an analogue model for a given system allows the study of a system in an environment other than that for which it is intended [31–33], thereby facilitating the study of specific phenomena of the system. Moreover, a model based on electrical components is accessible and quickly understood by researchers from almost all engineering fields. This last argument is of great importance because research and development in the wind turbine industry requires a variety of competencies from different fields of engineering. Furthermore, the equivalent electrical model can take advantage of existing resources by simultaneously capitalizing on their strengths and minimizing their respective drawbacks. In addition, such a model can be a good tool for the simulation of wind turbine rotor operation

77

in the case of physical damage or structural faults on one or more blades. Finally, because electric and other dynamic models for other parts of the wind turbine have been developed [34–41], this new model can be easily linked to existing models to obtain an overall wind turbine model.

This paper proposes a new approach for modeling Darrieus-type VAWT rotors using the electrical-mechanical analogy. This new model is likely to be more appropriate for the design, performance prediction and optimization of Darrieus rotors. Mechanical fault diagnosis and prognosis is also an important aspect because the model can be use to simulate the rotor's behavior for the case of a mechanical fault on one or more of the blades as well as on rotor-shaft coupling elements. This paper focuses on providing a proof-of-concept demonstration of the new model. Section 2 presents the working principle of Darrieus-type VAWTs. In Section 3, the basis of the mechanical-electrical analogy approach is discussed. Theoretical concepts underpinning the new model and the step-by-step development process are also described in this section. The results are presented and discussed in Section 4; simulations of aerodynamic characteristics and those of corresponding electrical components are presented for a single blade and for various parameters of the new model. Finally, Section 5 concludes the paper and gives prospects for future research work.

Table III-1 *Features, advantages and shortcoming of different aerodynamic models for vertical-axis wind turbine (VAWT) rotors.*

Model	Main features	Advantages	Shortcomings
Momentum or blade element model	- Combines momentum theory with blade element theory. - Uses the calculation of flow velocity through the turbine by equating the streamwise aerodynamic force on the blades with the rate of change of momentum of air. - Momentum models include the single streamtube model, multiple streamtube model and Double-multiple streamtube model.	- Can predict the overall performance of a lightly loaded wind turbine. It is thus useful for overall design. - Very fast computational prediction. - Can provide a good correlation between the performance prediction and the experimental data (double-multiple streamtube model).	- Invalid for large tip speed ratios and for high rotor solidities. - Does not provide any information as to the shape of the near wake, which is important when considering the placement of struts and other structures close to the turbine blades. - The effect of perpendicular perturbations in blade element momentum (BEM) methods can only be added as a correction. - Cannot predict wind velocity variations across the rotor. - Some convergence problems (double-multiple streamtube model).
Vortex model	- Potential flow models based on the calculation of the velocity field about the turbine through the influence of vorticity in the wake of the blades. - Vortex models include the free-wake vortex model and fixed-wake momentum theory.	- Can include the dynamic stall effect, pitching circulation and added mass effect. - Capable of providing information about the wake structure near the turbine because the velocity normal to the airflow is neglected. - High-precision prediction capabilities. - Can be used for highly loaded rotors at large tip speed ratios. - Naturally addresses perturbations both parallel and perpendicular to the streamwise velocity.	- Computationally too expensive. - Relies on significant simplifications (such as the potential flow being assumed in the wake, and the effect of viscosity in the blade aerodynamics is included through empirical force coefficients). - Convergence problems in some cases. - Computational accuracy greatly dependent on the potential flow model used in computations.

Table III-1 . Cont.

Model	Main features	Advantages	Shortcomings
Cascade model	- Consists in equidistantly placing the blades one behind another on a plane, the width of which is the circumference of the rotor. - The aerodynamic characteristics of each element of the blade are independently obtained using the local Reynolds number.	- Can predict the overall values of both low and high solidity turbines quite well. - Highly precise computation with no iterative convergence even at high tip speed ratios and high solidities. - Incorporates the effect of the local Reynolds number variation at different azimuth angles, zero-lift-drag coefficients, finite aspect ratios and flow curvature effect in the calculation process. - Dynamic stall and flow curvature with blade pitching can be considered. - Achieves smooth convergence even at high tip speed ratios and high solidity VAWT with quite reasonable accuracy.	- Reasonable computation time.
Computational fluid dynamics (CFD) model	- CFD simulation of VAWT is performed by solving the Unsteady Reynolds Averaged Navier Stokes (URANS) equation. - According to the discrete principle, CFD models can be generally classified into three branches: the Finite Difference Method (FDM), the Finite Element Method (FEM) and the Finite Volume Method (FVM).	- Provides a more precise aerodynamic prediction for VAWTs (reliability and accuracy). - Can visualize the flow near airfoils in detail. - Can accelerate the design process and reduce the overall cost of design. - Effective solutions for the analysis of local flow fields around blades, particularly for dynamic stall and wake flow. - Attractive solution for performance optimization	- Computationally intensive. - Basically prohibitive for the routine engineering analyses of wind turbines.

3.2. THEORY: WORKING PRINCIPLE OF DARRIEUS-TYPE VERTICAL-AXIS WIND TURBINES (VAWTS)

A vertical-axis wind turbine is of Darrieus-type when it is driven by aerodynamic lift [26,42]. The Darrieus turbine consists of two or more aerofoil-shaped blades attached to a rotating vertical shaft. The wind blowing over the aerofoil contours of the blade creates aerodynamic lift and actually pulls the blades along. In this section, general mathematical expressions that describe the aerodynamic models of Darrieus-type VAWTs are presented.

Let us consider a curved blade Darrieus-type VAWT as shown in Figure III-1. The given aerofoil is characterized by its height $2H$, rotor radius R, number of blades $N_b = 3$ and blade chord c. Consider a given point on any of the blades. r and z are the local radius and height, respectively. When the rotor is subject to an instantaneous incoming wind speed $W_0(t)$, it turns at a rotational speed $\omega(t)$.
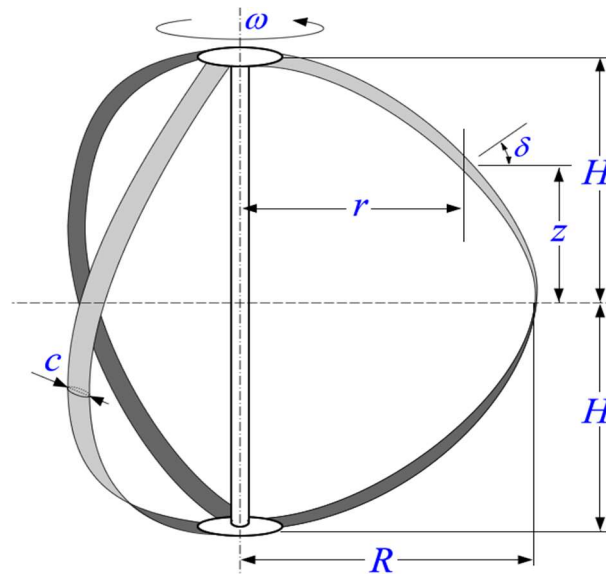
Figure III-1   Curved, three-blade, Darrieus-type VAWT.

Figure III-2 shows the aerodynamic forces and the three velocity vectors acting on Darrieus-type VAWT blade elements at a random position [25,43]. F_L and F_D are the lift

and drag force, respectively. As the blade rotates, the local angle of attack α varies with the relative velocity W_r. The incoming wind speed W_0 and the rotational velocity of the blade ω govern the orientation and magnitude of W_r [23,42]. In turn, the forces F_L and F_D acting on the blade vary. The magnitude and orientation of the lift and drag forces as well as the resultant force vary. The resultant force can be decomposed into a normal force F_N and a tangential force F_T.

The tangential force component then drives the rotation of the wind turbine and produces the torque necessary to generate electricity [24].
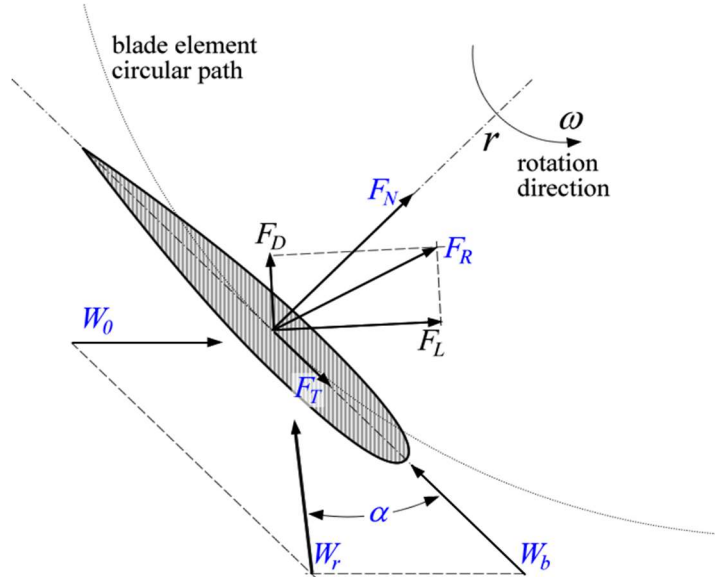
Figure III-2 Velocity and force components for a Darrieus-type VAWT (DTVAWT).

Elementary normal and tangential forces applied to a blade element are, respectively, given by [44]:

$$dF_N = C_N \left(\frac{1}{2} \rho W^2 \frac{c}{\cos \delta} \right) dz \tag{1}$$

$$dF_T = C_T \left(\frac{1}{2} \rho W^2 \frac{c}{\cos \delta} \right) dz \tag{2}$$

where δ is the pitch angle of the blade, defined as $\delta = \tan^{-1} \left(\dfrac{H}{2z} \right)$; c is the blade chord

(m); and C_N and C_T are the normal and tangential force coefficients, respectively, which are given by:

$$C_N = C_L \cos\varphi + C_D \sin\varphi, \quad C_T = C_L \sin\varphi - C_D \cos\varphi \tag{3}$$

where C_L and C_D are the blade lift and drag coefficients, respectively. These coefficients are related to the blade profile and are obtained from empirical data and made available by the blade manufacturer. C_L and C_D are experimentally determined and depend on the incidence angle α and the Reynolds number $R_e = \dfrac{R\omega c}{W}$ [45]. The lift and drag coefficients are given by the following relations [42]:

$$C_L = \frac{R_x}{\dfrac{\rho}{2} \cdot l \cdot W^2} \tag{4}$$

$$C_D = \frac{R_z}{\dfrac{\rho}{2} \cdot l \cdot W^2} \tag{5}$$

If we assume that the relative dynamic pressure flow q and the blade element area A_e can be expressed as $q = \dfrac{1}{2} \rho W^2$ and $A_e = c \cdot dz$, then [46]:

$$dF_N = \frac{C_N q A_e}{\cos \delta} \tag{6}$$

$$dF_{\text{T}} = \frac{C_{\text{T}}qA_e}{\cos\delta} \tag{7}$$

The components of the force acting along the x and y Cartesian directions are also called the lift and drag forces. The elementary lift and drag forces are given by [44]:

$$dF_{\text{L}} = qc\left(-C_{\text{N}}\sin\theta_{\text{b}} + C_T\frac{\cos\theta_{\text{b}}}{\cos\delta}\right)dz \tag{8}$$

$$dF_{\text{D}} = qc\left(C_{\text{N}}\cos\theta_{\text{b}} - C_T\frac{\sin\theta_{\text{b}}}{\cos\delta}\right)dz \tag{9}$$

As described in [43,47], the total lift and drag forces, F_{L} and F_{D}, for a single blade can then be calculated by integrating dF_{L} and dF_{D} with respect to the height $(-H \leq z \leq H)$ and the azimuthal revolution $(0 \leq \theta_{\text{b}} \leq 2\pi)$. We then obtain:

$$F_{\text{L}} = \frac{c}{2\pi}\int_{z=-H}^{H}\int_{\theta=0}^{2\pi} q\left(-C_{\text{N}}\sin\theta_{\text{b}} + C_T\frac{\cos\theta_{\text{b}}}{\cos\delta}\right)d\theta_{\text{b}}\,dz \tag{10}$$

$$F_{\text{D}} = \frac{c}{2\pi}\int_{z=-H}^{H}\int_{\theta=0}^{2\pi} q\left(C_{\text{N}}\cos\theta_{\text{b}} + C_T\frac{\sin\theta_{\text{b}}}{\cos\delta}\right)d\theta_{\text{b}}\,dz \tag{11}$$

For a rotor with N_{b} blades, the average lift and drag forces for the rotor are defined as:

$$F_{\text{Lr}} = \frac{N_{\text{b}}c}{2\pi}\int_{z=-H}^{H}\int_{\theta=0}^{2\pi} q\left(-C_{\text{N}}\sin\theta_{\text{b}} + C_T\frac{\cos\theta_{\text{b}}}{\cos\delta}\right)d\theta_{\text{b}}\,dz \tag{12}$$

$$F_{\text{Dr}} = \frac{N_{\text{b}}c}{2\pi}\int_{z=-H}^{H}\int_{\theta=0}^{2\pi} q\left(C_{\text{N}}\cos\theta_{\text{b}} + C_T\frac{\sin\theta_{\text{b}}}{\cos\delta}\right)d\theta_{\text{b}}\,dz \tag{13}$$

The torque of the Darrieus rotor is produced solely by the tangential component of the applied force [23,43,48]. Thus, from the elementary tangential force of the rotor, we can obtain the elementary torque of the rotor at a given position. For a blade element of length $dz/\cos\delta$, we obtain:

$$dT_B = \frac{C_T qrc}{\cos\delta} dz \tag{14}$$

The torque varies as a function of the azimuthal angle and the rotor height [48]. The total torque can then be obtained by successively integrating the elementary torque with respect to the variables θ and z. For a rotor with N_b blades, we have:

$$T_R = N_b T_B = \frac{c\omega}{2\pi} \int\limits_{z=-xH}^{xH} \int\limits_{0}^{2\pi} \frac{qC_T r}{\cos\delta} d\theta_b dz \tag{15}$$

The average power generated by the rotor shaft is defined as:

$$P = \omega T_R = \frac{Nc\omega}{2\pi} \int\limits_{z=-xH}^{xH} \int\limits_{0}^{2\pi} \frac{qC_T r}{\cos\delta} d\theta_b dz \tag{16}$$

The power coefficient of the rotor can then be obtained as:

$$C_p = \frac{P}{P_{max}} = \frac{81}{64} \frac{1}{2\pi} \frac{Nc\omega}{\rho V_\infty^3 RH} \int\limits_{z=-xH}^{xH} \int\limits_{0}^{2\pi} \frac{qC_T r}{\cos\delta} d\theta_b dz \tag{17}$$

3.3. METHOD AND MODEL CONSTRUCTION

Based on the aerodynamic model described in the precedent section, this section is devoted to the presentation of the building process of an equivalent electrical model. Our methodology is based on the complex plane representation of various model subassemblies and an analogy between electrical and mechanical systems.

3.3.1. The Mechanical-Electrical Analogy Approach

The main value of analogies lies in the way in which mathematics unifies these diverse fields of engineering into one subject. Tools developed for solving problems in one field can be used to solve problems in another. This is an important concept because some fields, particularly electrical engineering, have developed rich sets of problem-solving tools that are fully applicable to other engineering fields [49]. There are simple and straightforward analogies between electrical and mechanical systems. Furthermore, analogies between mechanical systems and electrical and fluid systems are effective and are in common use.

Two valid techniques of modeling mechanical systems with electrical systems or drawing analogies between the two types of systems can found in the literature, with each method having its own advantages and disadvantages [50–54]. The first technique is intuitive; in this technique, current corresponds to velocity (both are motion), and voltage corresponds to force (both provide a "push"). The second technique is the through/across analogy, which uses voltage as an analogy for velocity and current as an analogy for force. The two schools of thought for modeling mechanical systems with electrical systems are presented in Table 2 [49]. Both are valid. However, the through/across analogy results in a counterintuitive definition of impedance [49,51,52,55]. The analogy for impedance that is universally applied is the one from the intuitive analogy listed in the corresponding section of Table II-1. For this reason, the intuitive analogy will be used in the present study.

Table III-2   *System analogy used in developing the new model.*

| | Topology-Preserving Set (book's Analogy) | | | Intuitive Analogy Set | | | | |
| | ↔ Intuitive Stretch | | | ↔ Topology Change | | | | |
Description	Trans Mech	Rot Mech	Electrical	Thermal	Fluid	Trans Mech	Rot Mech	Description
"through" variable	f (force)	τ (torque)	i (current)	ϕ (heat flux)	q (flow)	v (velocity)	ω (angular velocity)	Motion
"across" variable	v (velocity)	ω (angular velocity)	v (voltage)	T, θ	p (pressure)	f (force)	τ (torque)	Push (force)
Dissipative element	$v = \frac{1}{B} f$	$\omega = \frac{1}{B_r} \tau$	$v = iR$	$\theta = \phi R$	$p = qR$	$f = vB$	$\tau = \omega B_r$	Dissipative element
Dissipation	$f^2 \frac{1}{B} = \frac{v^2}{1/B}$	$\tau^2 \frac{1}{B} = \frac{\omega^2}{1/B}$	$i^2 R = v^2/R$	N/A	$q^2 R = p^2/R$	$v^2 R = f^2/R$	$\omega^2 B_r = \tau^2/B_r$	Dissipation
Through-variable storage element	$v = \frac{1}{K} \frac{df}{dt}$ or $\int v\,dt = \frac{1}{K} f$	$\omega = \frac{1}{K_r} \frac{d\tau}{dt}$ or $\int \omega\,dt = \frac{1}{K_r} \tau$	$v = L \frac{di}{dt}$	N/A	$p = I \frac{dq}{dt}$	$f = M \frac{dv}{dt}$ (one end must be "grounded")	$\tau = J \frac{d\omega}{dt}$ (one end must be "grounded")	Motion storage element
Energy	$E = \frac{1}{2} \frac{1}{K} f^2$	$E = \frac{1}{2} \frac{1}{K_r} \tau^2$	$E = \frac{1}{2} Li^2$		$E = \frac{1}{2} I q^2$	$E = \frac{1}{2} Mv^2$	$E = \frac{1}{2} J \omega^2$	Energy
Impedance	Standard definition is at right		$V(s) = I(s)Ls$		$P(s) = Q(s)Is$	$F(s) = V(s)Ms$	$T(s) = \Omega(s)Js$	Impedance
Across variable storage element	$f = M \frac{dv}{dt}$ (one end must be "grounded")	$\tau = J \frac{d\omega}{dt}$	$i = C \frac{dv}{dt}$	$\phi = C \frac{d\theta}{dt}$ (one end must be "grounded")	$q = C \frac{dp}{dt}$ (one end usually "grounded")	$v = \frac{1}{K} \frac{df}{dt}$ or $\int v\,dt = \frac{1}{K} f$	$\omega = \frac{1}{K_r} \frac{d\tau}{dt}$ or $\int \omega\,dt = \frac{1}{K_r} \tau$	Push (force) storage element
Energy	$E = \frac{1}{2} Mv^2$	$E = \frac{1}{2} J\omega^2$	$E = \frac{1}{2} Cv^2$	$E = CT$ (not analogous)	$E = \frac{1}{2} Cp^2$	$E = \frac{1}{2} \frac{1}{K} f^2$	$E = \frac{1}{2} \frac{1}{K_r} \tau^2$	Energy
Impedance	The standard definition of mechanical impedance is the one on the right, based on the intuitive analogy		$V(s) = I(s) \frac{I}{sC}$	$\Theta(s) = \Phi(s) \frac{1}{sC}$	$P(s) = Q(s) \frac{1}{sC}$	$F(s) = V(s) \frac{K}{s}$	$T(s) = \Omega(s) \frac{K_r}{s}$	Impedance

87

3.3.2.   Wind Flow as an Electric Current Source

The analogy between air flow and electrical current is mathematically accurate; the momentum of a section of a gas, also called inertance, is directly analogous to electrical inductance. The compliance of a transmission vessel (hose or pipe) is directly analogous to electrical capacitance [56–59]. In this section, we will model the wind flow across the rotor as an electric current source.

Figure III-3 shows the top view of a three-blade VAWT and the different velocity components. Considering one of the blades, its shift position x_b is characterized by the rotor radius R and the angular position θ_b. Thus, the complex representation of the blade shift position x_b can be written as follows [60–62]:

$$x_b = Re^{j\theta_b} \tag{18}$$
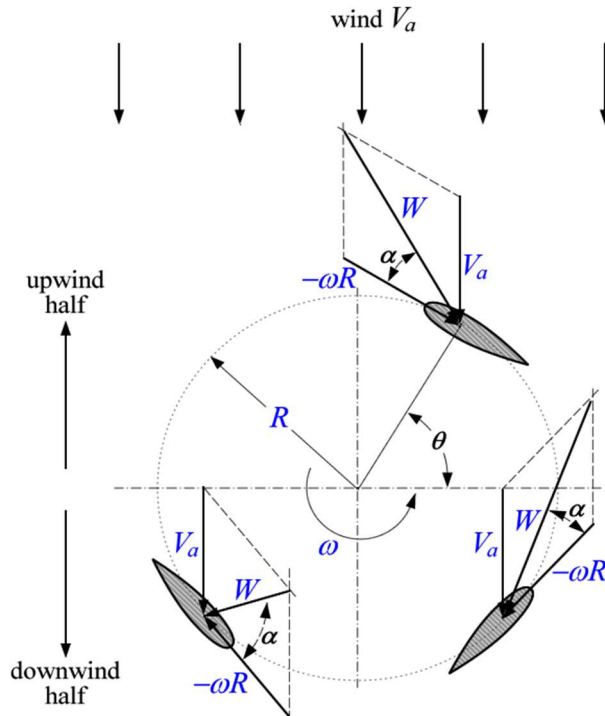
Figure III-3   Top view of a three-blade VAWT showing the velocity components relative to the blade.

The linear velocity of the blade W_b can be obtained by deriving its position with respect to time. We then have [63]:

$$W_b = \frac{d(x_b)}{dt} = j\dot{\theta}_b Re^{j\theta_b}$$

(19)

where $\dot{\theta}_b = \omega$ is the rotational speed and W_0 is the incoming wind and represents wind from any direction. The relative wind seen by the blades at any moment is given by [61,64,65]:

$$\vec{W}_r = \vec{W}_0 - \vec{W}_b = W_0 - j\omega Re^{j\theta_b}$$

(20)

As explained in [61], the angle definitions are counter-clockwise; hence, α and φ are negative for the directions of W_r and W_b (Figure III-4). Therefore, if we consider the blade reference frame, the angle of the relative wind is obtained by rotating W_r by an angle $je^{-j\theta_b}$, thereby aligning the blade motion with the negative real axis. The relative flow velocity for a blade in its own reference frame can then be defined as:

$$W_{rb} = W_r \cdot \left(je^{-j\theta_b} \right) = W_0 je^{-j\theta_b} + \omega R$$

(21)

The algebraic expression can be written as follows:

$$W_{rb} = \left(\omega R + W_0 \sin\theta_b \right) + j\left(W_0 \cos\theta_b \right)$$

(22)

89
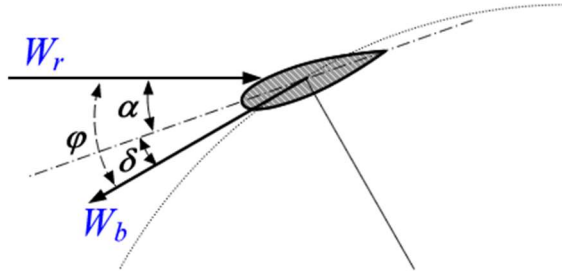
Figure III-4 Definition of angles and velocities.

The Paraschivoiu model [43] assumes that the direction of the flow does not change. Therefore, the angle of the blade relative to the vertical axis η is taken into consideration when expressing the relative wind velocity seen by the blade. Hence, from Equation (22), the relative wind seen by the blade element, and that corresponding to the streamtube i, can be expressed as follows:

$$W_{rbi} = \left(\omega R_i + W_{0i}\sin\theta_b\right) + j\left(W_{0i}\cos\theta_b\right)\cos\eta_i \tag{23}$$

where η is the angle of the blade relative to the vertical axis and is equal to zero for straight blade VAWTs ($\eta = 0$ and $\cos\eta = 1$). If the parabola shape of the blade is approximated as:

$$\frac{r}{R} = 1 - \left(\frac{z}{H}\right)^2 \tag{24}$$

then the angle of the blade relative to the vertical axes can be defined as [43,66]:

$$\eta = \tan^{-1}\left(\frac{H}{2z}\right) = \tan^{-1}\left(\frac{1}{2\sqrt{(1-r/R)}}\right) \tag{25}$$

The angle of the relative wind is the argument of W_{rb} [9,47]. Because W_0 is considered to be real, we can write:

90

$$\varphi_i = \tan^{-1}\left(\frac{\cos\theta_{bi}\cos\eta_i}{\left(\dfrac{\omega R_i}{W_{0i}}\right)+\sin\theta_{bi}}\right) = \tan^{-1}\left(\frac{\cos\theta_{bi}\cos\eta_i}{\lambda_i+\sin\theta_{bi}}\right) \tag{26}$$

where $\lambda = \dfrac{\omega R}{W_0}$ is the blade tip speed ratio.

Considering the pitch angle δ, the angle of attack α is obtained through summation of the pitch angle and that of the relative wind [23]; specifically:

$$\alpha = \varphi + \delta \tag{27}$$

Finally, the wind's angle of attack relative to a streamtube i can be written as follows:

$$\alpha = \tan^{-1}\left(\frac{\cos\theta_b\cos\eta_i}{\lambda_i+\sin\theta_b}\right)+\delta_i \tag{28}$$

For a given blade element situated at a height Z and corresponding to a given streamtube, η and δ are constant. The angle of attack (AoA) will therefore vary with the angle of the relative wind speed, that is, with the rotational angle of the blade. Figure III-5 shows the variation of the angle of attack as a function of the rotational angle of the blade for different values of the tip speed ratio λ. The results are in accordance with those obtained in [67] and show that small tip speed ratios lead to large incidence variations during a revolution.
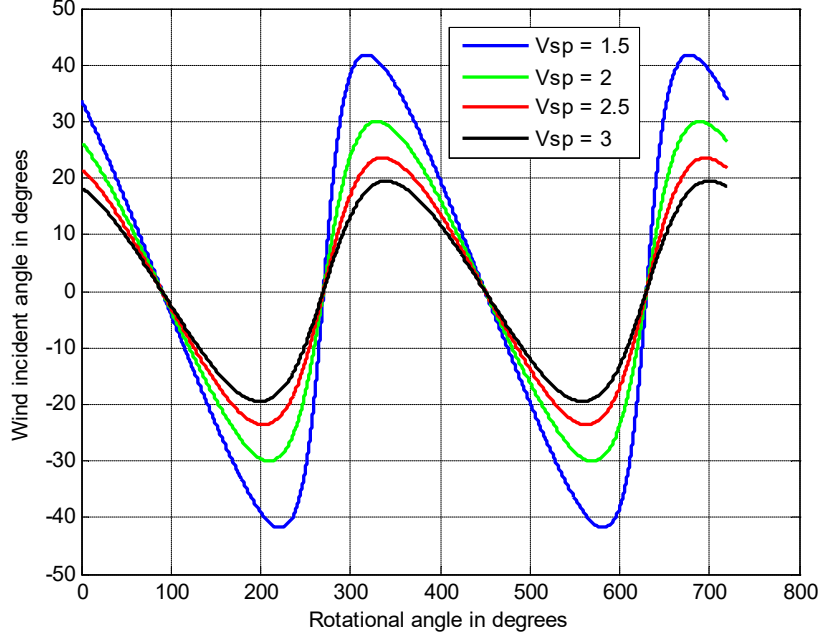
Figure III-5   Angle of attack as function of the rotational angle.

Additionally, the absolute value of the relative velocity is the modulus of the complex algebraic definition in Equation (22). Therefore, it can be written in accordance with the definition in [68]:

$$\left|W_{\mathrm{rb}}\right| = W_0 \sqrt{\left(\frac{\omega R}{W_0} + \sin\theta_{\mathrm{b}}\right)^2 + \left(\cos\theta_{\mathrm{b}}\right)^2 \left(\cos\eta\right)^2} \tag{29}$$

Broadly speaking, the incident wind at the wind turbine rotor can be written as a complex number:

$$\overline{W}_{\mathrm{rb}} = \left|W_{\mathrm{rb}}\right| \mathrm{e}^{j(\varphi+\delta)} \tag{30}$$

As stated in [56–59], an analogy can be made between the wind flow in a streamtube and an electric current. Equation (30) is similar to the complex expression of a sinusoidal current generator. Moreover, if the incident wind flow is assumed to be an electric current,

then the wind relative dynamic pressure flow $q = \frac{1}{2}\rho W_{rb}^2$ (where q is given in N/m^3 and the fluid density ρ is given in kg/m^3), which is the energy acquired by the wind due to its velocity, can be considered as an electric energy source. Referring to our system analogy table, this will be a current source. The wind relative dynamic pressure flow can therefore be written as a complex number:

$$\overline{I}_w = \overline{q} = \frac{1}{2}\rho\left(\overline{W}_{rb}\right)^2 = \frac{1}{2}\rho\left(\left|W_{rb}\right|e^{j(\varphi+\delta)}\right)^2 = \frac{1}{2}\rho\left|W_{rb}\right|^2 e^{j2(\varphi+\delta)}$$

$$\overline{I}_w = \frac{1}{2}\rho W_0^2\left(\left(\frac{\omega R}{W_0}+\sin\theta_b\right)^2 + \left(\cos\theta_b\right)^2\left(\cos\eta\right)^2\right)e^{j2(\varphi+\delta)}$$

(31)

Finally, the instantaneous expression of the current source that represents the relative wind seen by the blade is as follows:

$$i_w(t) = \Psi\cos\left(\omega t + 2\alpha\right) = \Psi\angle 2\alpha$$

(32)

where $\Psi = \frac{1}{2}\rho W_0^2\left(\left(\frac{\omega R}{W_0}+\sin\theta_b\right)^2 + \left(\cos\theta_b\right)^2\left(\cos\eta\right)^2\right)$ and $\alpha = \tan^{-1}\left(\frac{\cos\theta_b\cos\eta}{\lambda_i + \sin\theta_b}\right)+\delta\cdot\psi$

is the modulus of the current flow and varies with the rotational angle of the blade.

As shown in Figure III-6, in the double-multiple multi-streamtube models, the incoming wind speed in the upstream W_0^u disk is different than that in the downstream disk W_0^d [69]. Thus, the modulus of the corresponding current in the downwind disk is slightly lower than that in the upwind disk ($\Psi^d \prec \Psi^u$). We can therefore incorporate this into the current source definition. The new current definition is Equation (33), and the electric current source analogy for wind flow can be represented as shown in Figure III-7:

93

$$i_w(t) = \begin{cases} \Psi^{\text{u}} \sin(\omega t + 2\alpha) & \text{for} \quad -\pi/2 \leq \theta \leq \pi/2 \\ \Psi^{\text{d}} \sin(\omega t + 2\alpha) & \text{for} \quad 3\pi/2 \leq \theta \leq -\pi/2 \end{cases} \tag{33}$$
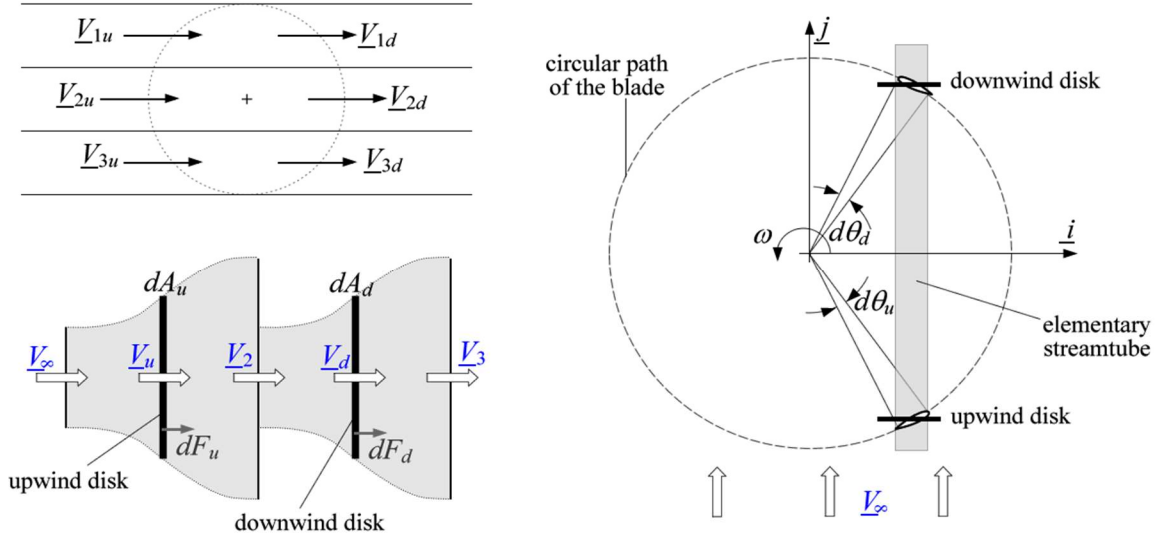
Figure III-6 Double-multiple multi-streamtube model.

Finally, the wind flow in our model is represented as follows:
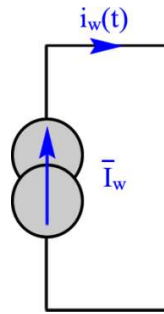
Figure III-7 Wind flow equivalent electrical model.

3.3.3. Single-Blade Electrical Equivalent Circuit (Normal, Tangential, Lift and Drag Coefficients)

The aerodynamic force coefficients acting on a cross-sectional blade element of a Darrieus wind turbine are shown in Figure III-8 [70]. The directions of the lift and drag coefficients as well as their normal and tangential components are illustrated.

94
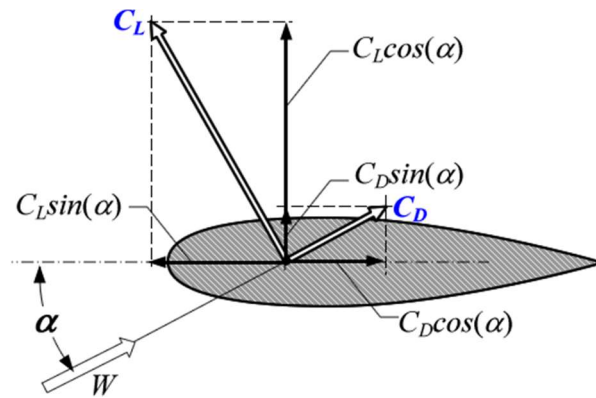
Figure III-8 Aerodynamic coefficients acting on a Darrieus WT blade element [71].

C_{L} and C_{D} denote the lift and drag coefficients, respectively. They are related to the blade profile, obtained from empirical data, and provided by the blade manufacturer. C_{L} and C_{D} are experimentally determined and depend on the incidence angle α and the Reynolds number [42]. The lift and drag coefficients for 2-*D* sections are readily available for a wide variety of wing sections at angles of attack up to the point of stall [72]. However, we performed a simulation while varying C_{L} and C_{D} as functions of the rotational angle of the blade for an NACA0012 for the full 360° range of angles. The results are presented in Figure 9 and are in agreement with data in the literature for the corresponding blade profile [17,73–75].

   a) *Writing Normal, Tangential, Lift and Drag Coefficients as Complex Numbers*

Consider a complex coordinate system defined as shown in Figure III-9.
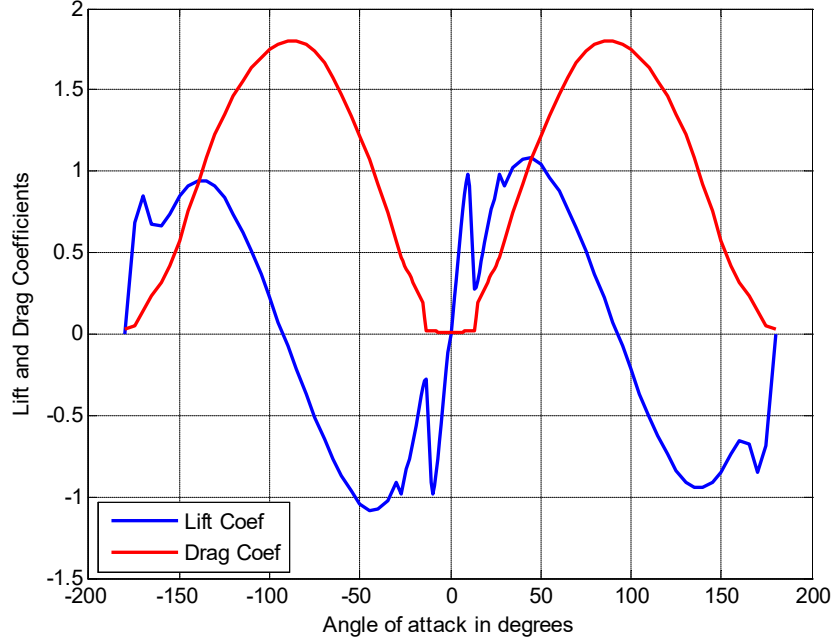
Figure III-9 Lift and drag coefficients variations as a function of the angle of attack for a NACA0012 blade profile.

The vertical axis is assumed to be real, and the horizontal axis is assumed to be imaginary. In this new complex coordinate system, the lift and drag coefficients can be written as complex numbers:

$$\begin{pmatrix} \overline{C}_{\mathrm{L}} \\ \overline{C}_{\mathrm{D}} \end{pmatrix} = \begin{pmatrix} C_{\mathrm{L}} \angle \varphi \\ C_{\mathrm{D}} \angle \dfrac{\pi}{2} - \varphi \end{pmatrix} \tag{34}$$

Using the signs of their imaginary components, $\overline{C}_{\mathrm{L}}$ can be regarded as an inductive coefficient with absolute value C_{L} and angle α, and $\overline{C}_{\mathrm{D}}$ can be seen as a capacitive coefficient with absolute value C_{D} and angle $\left(\dfrac{\pi}{2} - \varphi \right)$. We can therefore write:

$$\begin{pmatrix} \overline{C}_{\mathrm{L}} \\ \overline{C}_{\mathrm{D}} \end{pmatrix} = \begin{pmatrix} C_{\mathrm{L}} \mathrm{e}^{j\varphi} \\ C_{\mathrm{D}} \mathrm{e}^{j\left(\varphi - \frac{\pi}{2}\right)} \end{pmatrix} = \begin{pmatrix} C_{\mathrm{L}} \cos \varphi + j C_{\mathrm{L}} \sin \varphi \\ C_{\mathrm{D}} \cos \left(\varphi - \dfrac{\pi}{2} \right) + j C_{\mathrm{D}} \sin \left(\varphi - \dfrac{\pi}{2} \right) \end{pmatrix} \tag{35}$$

96

which then becomes:

$$\begin{pmatrix} \bar{C}_{L} \\ \bar{C}_{D} \end{pmatrix} = \begin{pmatrix} C_{L} \cos\varphi + jC_{L} \sin\varphi \\ C_{D} \sin\varphi - jC_{D} \cos\varphi \end{pmatrix} \tag{36}$$

The total or equivalent complex coefficients can be obtained by including the lift and drag coefficients:

$$\bar{C}_{eq} = \bar{C}_{L} + \bar{C}_{D} = \left(C_{L} \cos\varphi + jC_{L} \sin\varphi \right) + \left(C_{D} \sin\varphi - jC_{D} \cos\varphi \right) \tag{37}$$

Grouping real and imaginary components, we obtain:

$$\bar{C}_{eq} = \left(C_{L} \cos\varphi + C_{D} \sin\varphi \right) + j\left(C_{L} \sin\varphi - C_{D} \cos\varphi \right) \tag{38}$$

The tangential force coefficient C_{T} is basically the difference between the tangential components of the lift and drag forces. Similarly, the normal force coefficient C_{N} is the difference between the normal components of the lift and drag forces [25,43,76]. Thus, in the complex plane, C_{N} is real, and C_{T} is imaginary. From Equation (38):

$$\bar{C}_{eq} = C_{N} + jC_{T} \tag{39}$$

where:

$$\begin{pmatrix} C_{N} \\ C_{T} \end{pmatrix} = \begin{pmatrix} C_{L} \cos\varphi + C_{D} \sin\varphi \\ C_{L} \sin\varphi - C_{D} \cos\varphi \end{pmatrix} \tag{40}$$

The tangential coefficient characterizes the force tangential to the blade. To consider the influence of η on C_{T}, this letter is multiplied by $\kappa = \dfrac{1}{\cos\eta}$, namely, the coefficient of the blade tilt relative to the vertical axis; $\kappa = 1$ for straight-blade VAWTs [43]. Hence, the new

97

definitions of the normal and tangential coefficients that can be applied to any VAWT blade configurations are:

$$\begin{pmatrix} C_N \\ C_T \end{pmatrix} = \begin{pmatrix} C_L \cos\varphi + C_D \sin\varphi \\ \kappa\left(C_L \sin\varphi - C_D \cos\varphi\right) \end{pmatrix} = \begin{pmatrix} C_L \cos\varphi + C_D \sin\varphi \\ C_L \dfrac{\sin\varphi}{\cos\eta} - C_D \dfrac{\cos\varphi}{\cos\eta} \end{pmatrix} \tag{41}$$

The lift and drag coefficients become:

$$\begin{pmatrix} \overline{C}_L \\ \overline{C}_D \end{pmatrix} = \begin{pmatrix} C_L \cos\varphi + jC_L \dfrac{\sin\varphi}{\cos\eta} \\ C_D \sin\varphi - jC_D \dfrac{\cos\varphi}{\cos\eta} \end{pmatrix} \tag{42}$$

b)   *Normal, Tangential, Lift and Drag Impedances*

The blade is divided into *n* elements, as shown in Figure III-10. Each blade element corresponds to a given streamtube. These blade elements will experience varying flow characteristics because they may have, depending on the design, different radii, angles of relative wind speed, pitch angles, angles relative to the vertical axis, local heights, *etc.* Our approach is to calculate the characteristics for each blade element. The overall performance of the blade will then be obtained by the discrete addition of the *n* blade element characteristics along the span of the blade.

Each moving body in the air is subjected to a resisting force that tends to oppose this movement.

This resistance is a function of the air properties but also depends on the characteristics of the body itself (surface, shape, weight, *etc.*).

Kirchhoff's first law for air circuits states that the quantity of air leaving a junction must equal the quantity of air entering the junction. Kirchhoff's second law states that the sum of

the pressure drops around any closed path must be equal to zero. Pressure differences and head losses are analogous to voltage, electrical current is analogous to volumetric airflow rate and electrical resistance is analogous to airflow resistance [59,77–80]. This approach provides a useful framework when developing an equivalent electrical circuit for a blade.
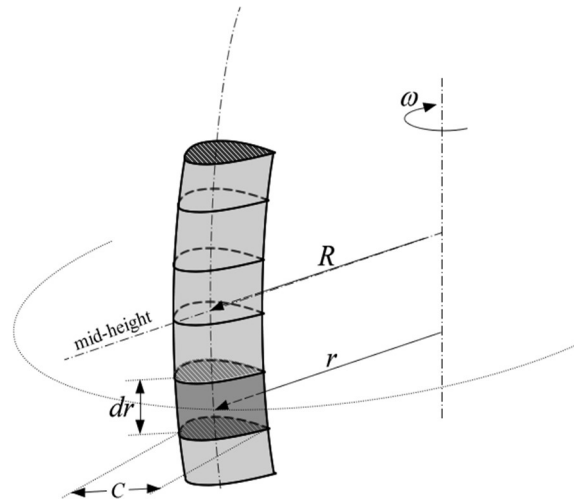
Figure III-10 Discretization of the blade into n elements.

To develop our new model, and in accordance with our mechanical-electrical analogy presented in Table III-1, the blade resistance will not represent a force; rather, it will represent the capacity of the blade to oppose the wind flow.

Thus, the blade element resistance can be defined as [57,81–84]:

$$R_i = C_{Bi} \cdot A_i \qquad (43)$$

where:

- R_i is the aerodynamic resistance of the blade element;

- C_{Bi} is the equivalent aerodynamic coefficient of the blade;

- A_i is the cord surface of the blade.

This aerodynamic resistance of the blade element can be decomposed into two components: a horizontal component (in the direction of the flow), which constitutes the drag aerodynamic resistance, and a component perpendicular to the plate, directed upwards, which is called the lift aerodynamic resistance [45].

Based on [57,58,70,85], various impedances of a blade element, because we are using a complex coordinate system, the elementary equivalent impedance of a blade element is obtained by multiplying the corresponding elementary complex coefficient by the elementary surface. Thus, we can write:

$$\overline{Z}_{Li} = A_i \overline{C}_L = c_i \cdot z_i \cdot C_{Li} \cos\varphi_i + jc_i \cdot z_i \cdot C_{Li} \frac{\sin\varphi_i}{\cos\eta_i} \tag{44}$$

From Equation (44), we can write:

$$\overline{Z}_{Li} = R_{Li} + jX_{Li} \tag{45}$$

with:

$$\begin{pmatrix} R_{Li} \\ X_{Li} \end{pmatrix} = \begin{pmatrix} c_i \cdot z_i \cdot C_{Li} \cos\varphi_i \\ c_i \cdot z_i \cdot C_{Li} \dfrac{\sin\varphi_i}{\cos\eta_i} \end{pmatrix} \tag{46}$$

where R_{Li} and X_{Li} are the resistive and inductive components of the elementary lift impedance, respectively. Because C_{Li} varies with the angle of attack α, R_{Li} and X_{Li} correspond to a variable resistor ($R_{Li} = f(\alpha_i)$) and a variable inductor ($X_{Li} = f(\alpha_i)$), respectively. The equivalent electrical diagram for the lift impedance of a blade element is as shown in Figure III-11.

Figure III-11 Equivalent electrical diagram for the lift force applied to a blade element.

Identically, the elementary drag impedance is:

$$\overline{Z}_{Di} = A_i \overline{C}_{D_i} = c_i \cdot z_i \cdot C_{Di} \sin \varphi_i - jc_i \cdot z_i \cdot C_{Di} \frac{\cos \varphi_i}{\cos \eta_i} \tag{47}$$

From Equation (47), we can write:

$$\overline{Z}_{Di} = R_{Di} - jX_{Di} \tag{48}$$

with:

$$\begin{pmatrix} R_{Di} \\ X_{Di} \end{pmatrix} = \begin{pmatrix} c_i \cdot z_i \cdot C_{Di} \sin \varphi_i \\ c_i \cdot z_i \cdot C_{Di} \dfrac{\cos \varphi_i}{\cos \eta_i} \end{pmatrix} \tag{49}$$

where R_{Di} and X_{Di} are the resistive and inductive components of the elementary drag impedance, respectively. Because C_{Di} varies with the angle of attack α, R_{Di} and X_{Di} will correspond to a variable resistor ($R_{Di} = f(\alpha_i)$) and a variable capacitor ($X_{Di} = f(\alpha_i)$), respectively. The equivalent electrical diagram for the drag impedance of a blade element is as shown in Figure III-12.
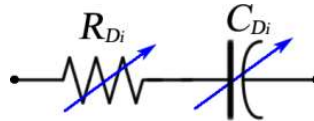

Figure III-12 Equivalent electrical diagram for the drag force applied to a blade element.

c) *Total Impedance and Equivalent Electrical Circuit of a Single Blade*

From the preceding section, the lift coefficient of the blade produces inductive impedance, and the drag coefficient is responsible for the creation of capacitive impedance. As suggested by the Aynsley resistance approach in [59], the total impedance for a blade element is obtained by adding the elementary lift and drag impedances. We have the following development:

$$\overline{Z}_{Bi} = A_i C_{Bi} = A_i \left(\overline{C}_{L_i} + \overline{C}_{L_i} \right) = \overline{Z}_{Li} + \overline{Z}_{Di} \tag{50}$$

that is:

$$\overline{Z}_{Bi} = \overline{Z}_{Li} + \overline{Z}_{Di} \tag{51}$$

We can then write:

$$\overline{Z}_{Bi} = c_i \cdot z_i \left(C_{Li} \cos \varphi_i + C_{Di} \sin \varphi_i \right) + jc_i \cdot z_i \left(C_{Li} \frac{\sin \varphi_i}{\cos \eta_i} - C_{Di} \frac{\cos \varphi_i}{\cos \eta_i} \right) \tag{52}$$

Finally:

$$\overline{Z}_{Bi} = c_i \cdot z_i \cdot C_{Ni} + jc_i \cdot z_i \cdot \frac{C_{Ti}}{\cos \eta_i} \tag{53}$$

From Equation (53), we can write:

$$\overline{Z}_{Bi} = \overline{Z}_{Ni} + \overline{Z}_{Ti} \tag{54}$$

where:

$$\begin{pmatrix} \overline{Z}_{Ni} \\ \overline{Z}_{Ti} \end{pmatrix} = \begin{pmatrix} R_i \\ jX_i \end{pmatrix} = \begin{pmatrix} R_{Li} + R_{Di} \\ j(X_{Li} - X_{Di}) \end{pmatrix} = \begin{pmatrix} C_{Li} \cos \varphi_i + C_{Di} \sin \varphi_i \\ C_{Li} \dfrac{\sin \varphi_i}{\cos \eta_i} - C_{Di} \dfrac{\cos \varphi_i}{\cos \eta_i} \end{pmatrix} \qquad (55)$$

Equations (54) and (55) show that the real component of the total elementary impedance is resistive and is generated by the normal coefficient. In the same vein, the imaginary component of the total elementary impedance is reactive and is produced by the tangential coefficient. This is in accordance with the definitions of the normal and tangential coefficients and forces found in the literature [86].

The total impedance of the entire blade is obtained by the addition of n discrete elementary impedances over the full height of the rotor [87]:

$$\overline{Z}_B = \sum_{i=1}^{n} \overline{Z}_{Bi} = \sum_{i=1}^{n} (R_i + jX_i) \qquad (56)$$

Specifically:

$$\begin{aligned} \overline{Z}_B &= \sum_{i=1}^{n} c_i z_i C_{Ni} + j \sum_{i=1}^{n} c_i z_i \frac{C_{Ti}}{\cos \eta_i} \\ &= \sum_{i=1}^{n} c_i z_i (C_{Li} \cos \varphi_i + C_{Di} \sin \varphi_i) + j \sum_{i=1}^{n} c_i z_i \left(C_{Li} \frac{\sin \varphi_i}{\cos \eta_i} - C_{Di} \frac{\cos \varphi_i}{\cos \eta_i} \right) \end{aligned} \qquad (57)$$

We can then write:

$$\overline{Z}_B = \left(\sum_{i=1}^{n} c_i z_i C_{Li} \cos \varphi_i + \sum_{i=1}^{n} c_i z_i C_{Di} \sin \varphi_i \right) + j \left(\sum_{i=1}^{n} c_i z_i C_{Li} \frac{\sin \varphi_i}{\cos \eta_i} - \sum_{i=1}^{n} c_i z_i C_{Di} \frac{\cos \varphi_i}{\cos \eta_i} \right) \qquad (58)$$

If we consider:

$$\begin{pmatrix} R_{\mathrm{L}} \\ R_{\mathrm{D}} \\ X_{\mathrm{L}} \\ X_{\mathrm{D}} \end{pmatrix} = \begin{pmatrix} \displaystyle\sum_{i=1}^{n} c_i z_i C_{\mathrm{L}i} \cos\varphi_i \\ \displaystyle\sum_{i=1}^{n} c_i z_i C_{\mathrm{D}i} \sin\varphi_i \\ \displaystyle\sum_{i=1}^{n} c_i z_i C_{\mathrm{L}i} \frac{\sin\varphi_i}{\cos\eta_i} \\ \displaystyle\sum_{i=1}^{n} c_i z_i C_{\mathrm{D}i} \frac{\cos\varphi_i}{\cos\eta_i} \end{pmatrix} \tag{59}$$

We can write:

$$\overline{Z}_B = R_B + jX_B = Z_N + jZ_T \tag{60}$$

where:

$$\begin{pmatrix} Z_{\mathrm{N}} \\ Z_{\mathrm{T}} \end{pmatrix} = \begin{pmatrix} R_{\mathrm{B}} \\ X_{\mathrm{B}} \end{pmatrix} = \begin{pmatrix} R_{\mathrm{L}} + R_{\mathrm{D}} \\ X_{\mathrm{L}} - X_{\mathrm{D}} \end{pmatrix} \tag{61}$$

For a given blade element, the equivalent electrical components are subject to the same wind flow. Thus, the equivalent electrical components of a blade are considered connected in series. Therefore, the electric equivalent circuit for a blade that is subject to a wind flow is as shown in Figure III-13.
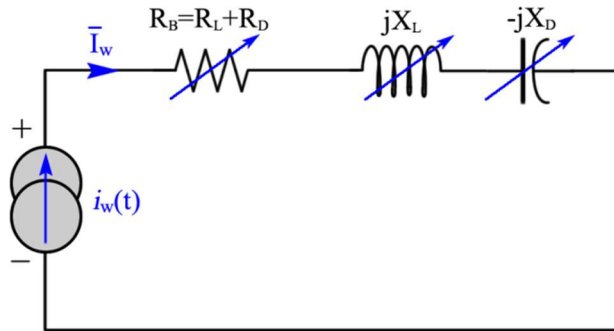

Figure III-13 Electric equivalent circuit for a blade that is subject to a wind flow.

3.4. RESULTS AND DISCUSSION

This section presents the obtained equivalent electrical model for a single blade. The simulation results for different elements of the model are also given. The simulations were conducted using data for NACA0012 that can be obtained from different sources in the literature [88–90] with Reynolds numbers ranging from 500,000 to approximately 750,000. Our selection was motivated by the fact that the NACA0012 blade profile is one of the most studied and commonly used as a rotor blade aerofoil section [89]. Finally, the simulation results were assessed using other results that can be found in the literature [91].

3.4.1. The Electrical Equivalent Model of a Single Blade

The wind flow through the blade (the current flow through the circuit) will produce lift and drag forces (lift and drag voltage) on the one hand and normal and tangential forces (normal and tangential voltage) on the other hand. The normal and tangential voltages produced by the blade can be expressed as follows:

$$\begin{pmatrix} \bar{V}_N \\ \bar{V}_T \end{pmatrix} = \begin{pmatrix} \bar{Z}_N \bar{I}_w \\ \bar{Z}_T \bar{I}_w \end{pmatrix} = \begin{pmatrix} R_B e^{i0} \\ X_B e^{i\pi/2} \end{pmatrix} (\Psi \angle 2\alpha, \Psi \angle 2\alpha) = \begin{pmatrix} \Psi R_B \angle 2\alpha \\ \Psi X_B \angle 2\alpha + \dfrac{\pi}{2} \end{pmatrix} \tag{62}$$

Following the laws of electrical circuit analyses, the total voltage across a blade can be obtained by the algebraic sum of the lift and drag voltages. We can then write:

$$\bar{V}_B = \bar{I}_w \times \bar{Z}_B = \bar{I}_w \times \left(\bar{Z}_N + j\bar{Z}_T \right) = \bar{V}_N + \bar{V}_T \tag{63}$$

Nevertheless, the torque delivered by the blade is produced only by the tangential component of the force. Therefore, only the tangential voltage will create the power in the corresponding electric circuit. Finally, the electric circuit corresponding to a single blade is

obtained. Figure III-14 shows the equivalent electric model of a single blade with voltage produce across reactive impedance that stand for blades torque.
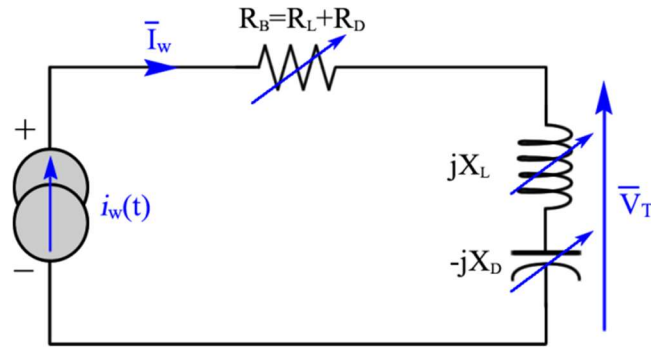
Figure III-14 The torque produced by the blade reactive impedance.

3.4.2. Simulations

The simulation characteristics of the rotor were taken from [42] and are presented in Table III-3.

Table III-3   *Blade's simulation characteristics.*

Parameter	Value/spécification
Number of blades	1
Aerofoil section	NACA0012
Average blade Reynolds number	40,000
Aerofoil chord length	9.14 cm
Rotor tip speed	45.7 cm/s
Tip speed ratio	5
Chord-to-radius ratio	0.15

a) *Variations of Coefficients and Equivalent Electric Components with the Angle of Attack*

As discussed in Section 4.2, the blade's lift and drag coefficients vary with the angle of attack of the wind, as shown in Figure III-9. These coefficients can then be used to plot the normal and tangential coefficients as a function of angle of attack using Equation (3). Furthermore, Figure 5 shows that the angle of attack changes as the blade rotates. Therefore, because the normal and tangential coefficients are obtained using lift and drag, as well as the lift and drag coefficients, the normal and tangential coefficients will vary according the blade position. The variations of the normal and tangential coefficients as functions of the angle of attack can be observed in Figure III-15. The obtained results agree with those in [43].
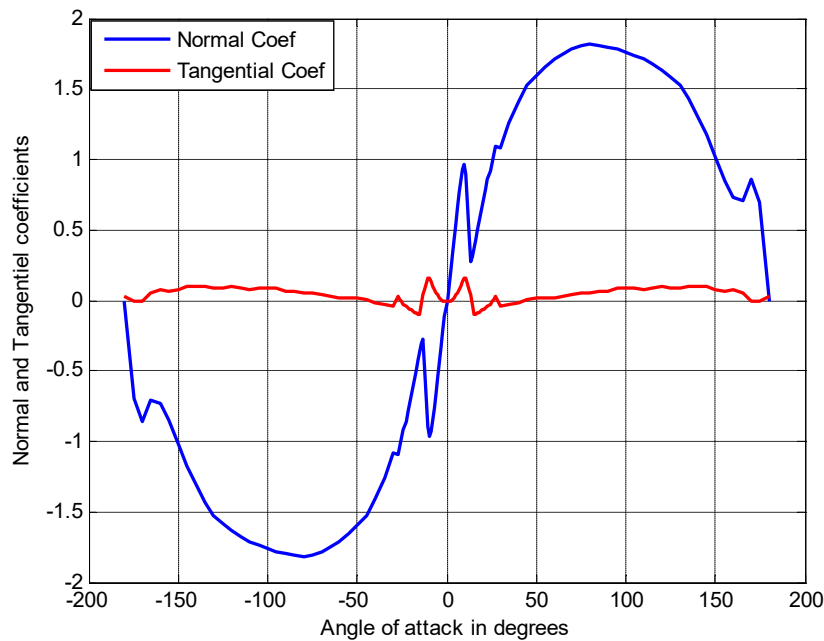
Figure III-15 Normal and tangential coefficient variations as functions of the angle of attack.

Using the relations in Equations (59) and (61), we can then find the variations in the various equivalent electrical components according to the angle of attack. The forms of the R_B and X_B curves follow those of the normal and tangential coefficients. The variations of

107

the values of electric components with the blade angle of attack are plotted on Figure III-16 and Figure III-17.

Figure III-16 Lift, drag and normal resistance variations as functions of the angle of attack.

Figure III-17 Reactive element variations as functions of the angle of attack.

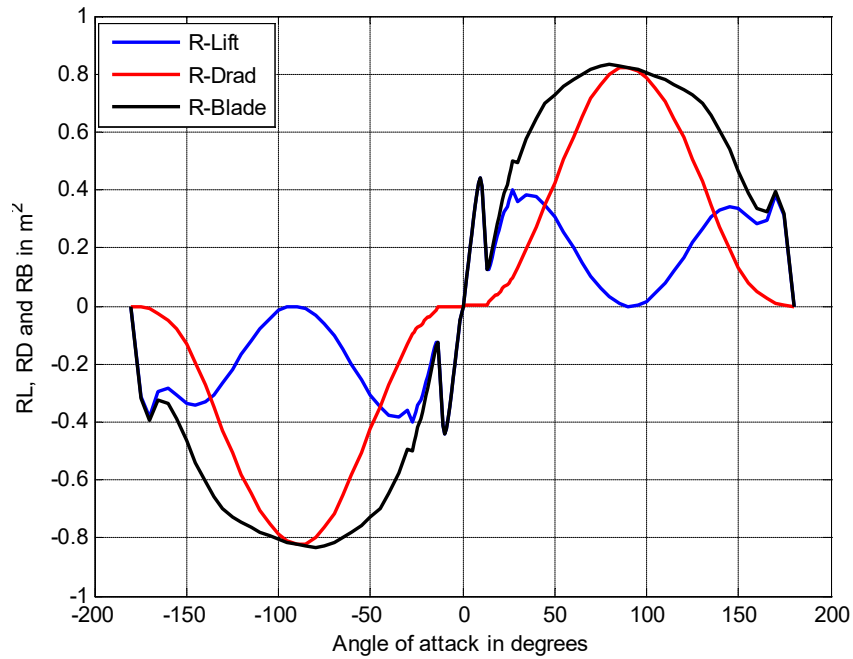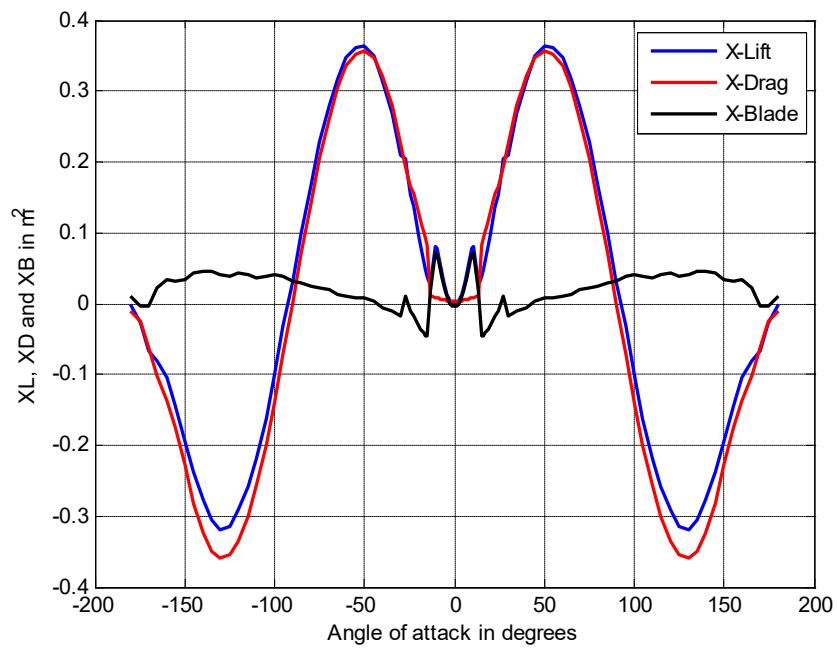### b) *Variations of Coefficients and Equivalent Electric Components with the Rotational Angle of the Blade*

The angle of attack gradually changes as the wind turbine rotor rotates. Figure 6 shows that the angle of attack varies as a function of the rotational angle of the blade; for a tip speed ratio of 1.5, the angle of attack broadly varies between −45° and 45° during a complete rotation of the turbine. Figure III-15, Figure III-16 and Figure III-17 show that only parts of the various curves, that is, for angles of attack between −50° and 50° are involved in the fluctuations of the respective coefficients and electric elements during a complete rotation of the blade. Figure III-18 and Figure III-19 simulate the variations of the coefficients as well as the equivalent electrical components according to the blade rotational angle. Our obtained results are consistent with what can be found in the relevant literature in [71].
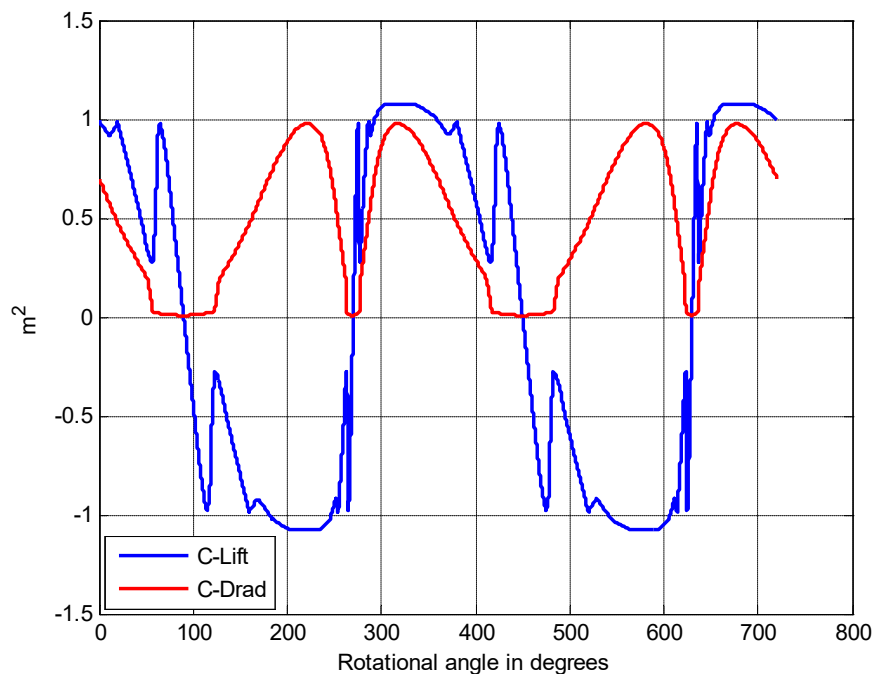

Figure III-18 Lift and drag coefficient variations as functions of rotational angle.
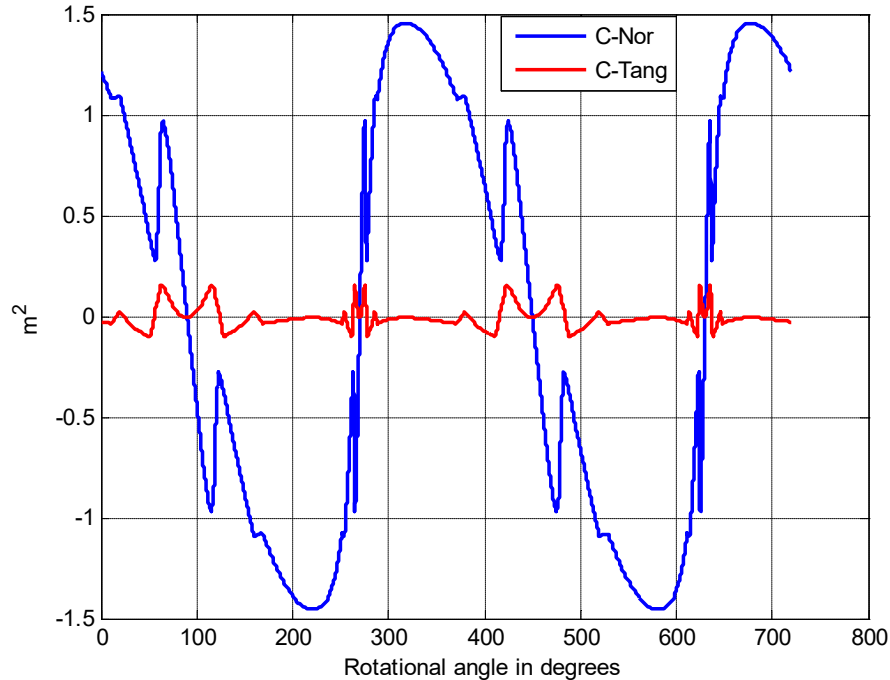
Figure III-19 Normal and tangential coefficient variations as functions of rotational angle.

The value of the lift coefficient is almost equal to that drag coefficient, in absolute value, during the rotation of the blade. Meanwhile, the blade's natural resistance as it moves through the air is nearly equivalent to the surface that opposes the blade weight by generating drag. Indeed, although the lift coefficient values alternate from positive to negative, the drag coefficient always remains positive.

The normal and tangential coefficients are non-linear combinations of the lift and drag coefficients. Both are alternative values, and the normal coefficient is much more important. The pressure of air on the surface of the blade varies widely. We can deduce that the surface of the blade that is exposed to the wind pressure varies as the blade rotate. During a complete tour, it is equal to zero for the rotational angles $\pi/2$ and $3\pi/2$. The tangential coefficient, responsible for the tangential force and thus of the power produced by the blade, is lower and alternate between positive and negative quantities.

We can now plot the variations of various equivalent electrical components with the rotational angle of the blade. The total resistance R_B is obtained by algebraic addition of the lift and drag resistances R_L and R_D. Similarly, the total reactance X_B results from the algebraic addition of the lift inductive admittance and drag capacitive admittance. Figure III-20 and Figure III-21 show that the forms of the R_B and X_B curves follow those of C_N and C_T, respectively. This finding is further evidence that the simulation results obtained using the developed model are in agreement with those obtained using existing BEM models.
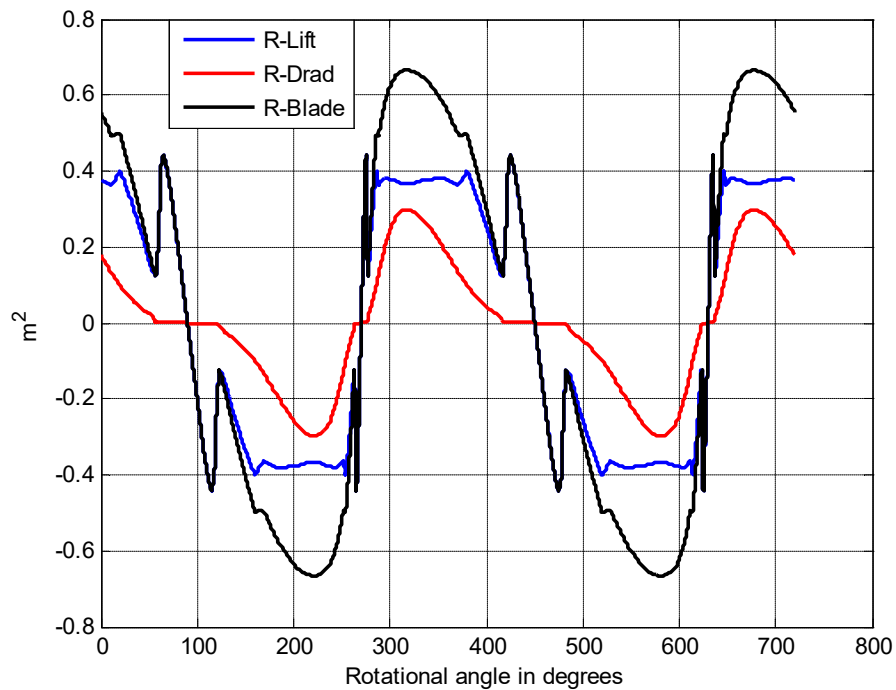
Figure III-20 Lift, drag and normal resistance variations as functions of rotational angle.
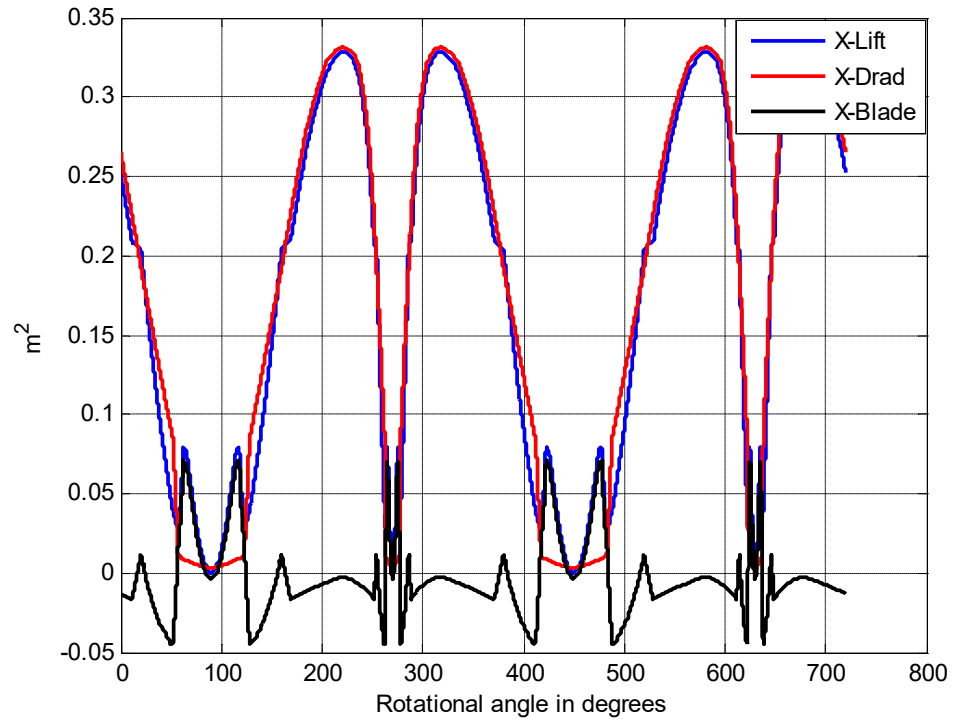
Figure III-21 Lift, drag and normal admittance variations as functions of rotational angle.

c) *Cross Validation and Comparative Analysis*

Finally, to perform the cross-validation simulation, the results of the normal and tangential forces obtained with equivalent electric model (EEM) were compared with those obtained using DMSTM. The simulation results of the normal and tangential forces using the EEM model and DMSTM of DTVAWTs are superimposed. The obtained results are shown in Figure III-22 and Figure III-23.
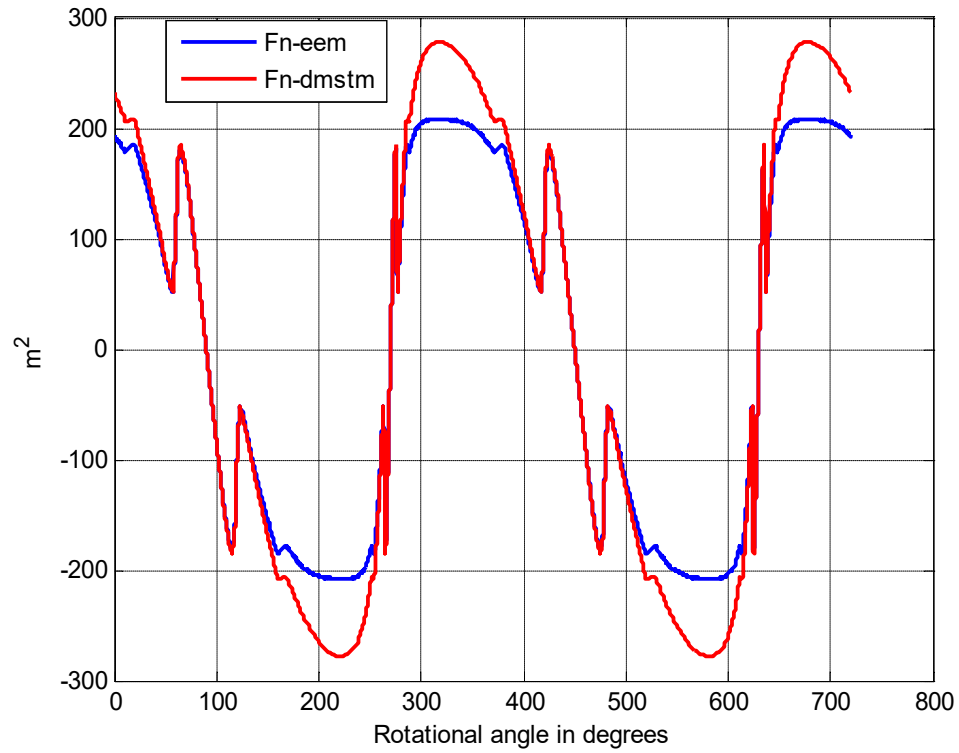
Figure III-22 Cross validation of normal force variations as functions of rotational angle.
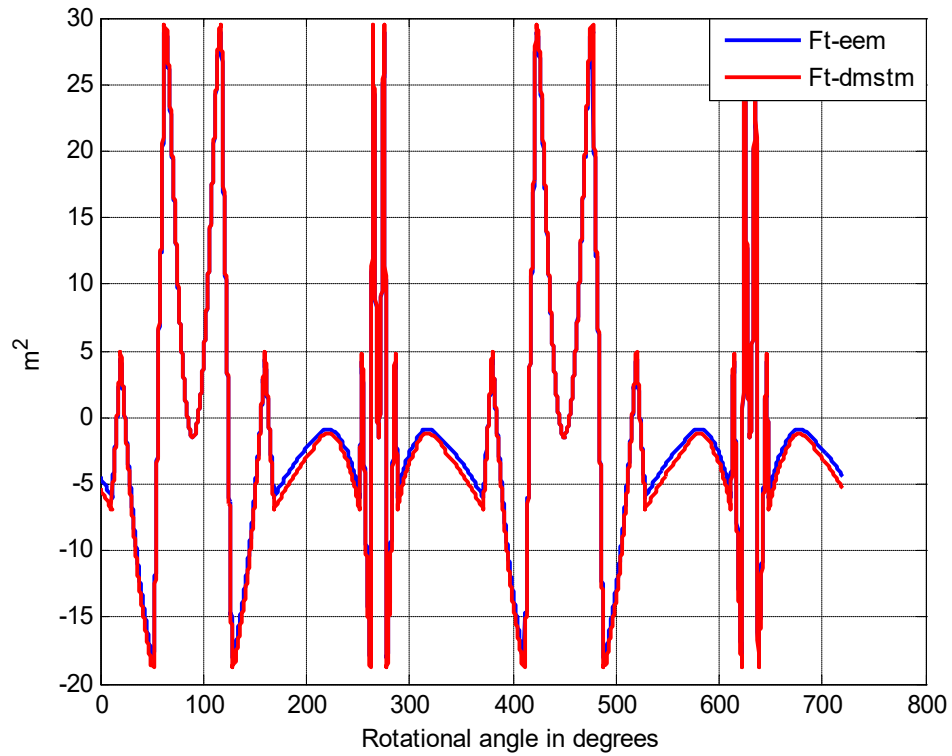
Figure III-23 Cross validation of tangential force variations as functions of rotational angle.

113

Figures 22 and 23 show that EEM produces satisfactory results as these results are in agreement with the results obtained in [43,92] for a single blade. Indeed, even though a slight distortion between the EEM and DMSTM normal forces can be observed on Figure 22. Figure 23 clearly shows that the EEM and DMSTM tangential forces strongly overlap.

3.5.   CONCLUSIONS

A new approach for modeling Darrieus-type VAWT rotors using the electric-mechanic analogy was presented. This paper provides a proof-of-concept demonstration of the approach and attests to the feasibility of such a model through both step-by-step demonstrations of the theoretical and practical concepts that underpin the new model and simulations and cross validation of a single blade model. The obtained simulation results tie in with the findings of the Paraschivoiu double-multiple streamtube model found in the literature.

An equivalent electrical model for Darrieus-type VAWTs was proven to be viable. We intend in our future work to finalize the model building process and address the electrical modeling of the blades' mechanical coupling to the shaft to generate an EEM for the full three-blade DTVAWT rotor. A comparative study of the results of the new model and those of existing models will then conducted.

The model that will emerge from this new approach is likely to be more appropriate for the design, performance prediction and optimization of Darrieus rotors. Mechanical fault diagnosis and prognosis is also an important aspect because the model could be used to simulate the rotor's behavior in the case of mechanical faults in one or more of the blades as

well as in rotor-shaft coupling elements. The model will also enable the simulation of turbine operation in the case of mechanical faults in one or more elements of the rotor.

Although further work must be conducted to build an EEM for the entire VAWT turbine, the findings of this study are encouraging and have practical applications for the determination and understanding of the aerodynamic factors that influence the performance of Darrieus-type VAWTs under different operating conditions.

In future works, the results of the EEM for DTVAWTs will be considered for extension to other types of wind turbines, including horizontal axis and Savonious types. Additionally, the EEM of rotors may be used to study the influence of wind flow turbulence on turbine vibrations. Transitional (starting) and permanent sate functioning of VAWTs may also be examined. We will also use the model to simulate the behavior of a Darrieus WT in the case of a structural break in one or more blades. Finally, as a long-term goal, the EEM of the rotor will be linked to existing models of other electrical and mechanical parts to obtain a global model of a Darrieus WECS.

Acknowledgments

Author Contributions

Pierre Tchakoua is the main author of this work. This paper provides a further elaboration on some of the results from his Ph.D. dissertation. René Wamkeue and Mohand

115

Ouhrouche supervised the project and thus supported Pierre Tchakoua's research in terms of both scientific and technical expertise. Tommy Andy Tameghe and Gabriel Ekemb participated in results analysis and interpretation. The manuscript is written by Pierre Tchakoua and revised and commented by René Wamkeue and Mohand Ouhrouche.

Conflicts of Interest

The authors declare no conflict of interest.

References

1. Scheurich, F.; Brown, R.E. Modelling the aerodynamics of vertical-axis wind turbines in unsteady wind conditions. *Wind Energy* **2013**, *16*, 91–107.

2. Howell, R.; Qin, N.; Edwards, J.; Durrani, N. Wind tunnel and numerical study of a small vertical axis wind turbine. *Renew. Energy* **2010**, *35*, 412–422.

3. Eriksson, S.; Bernhoff, H.; Leijon, M. Evaluation of different turbine concepts for wind power. *Renew. Sustain. Energy Rev.* **2008**, *12*, 1419–1434.

4. Castelli, M.R.; Grandi, G.; Benini, E. Numerical analysis of the performance of the DU91-W2-250 airfoil for straight-bladed vertical-axis wind turbine application. *World Acad. Sci. Eng. Technol.* **2012**, *6*, 742–747.

5. Ferreira, C.S.; Bussel, G.; Kuik, G.V. 2D CFD Simulation of Dynamic Stall on a Vertical Axis Wind Turbine: Verification and Validation with PIV Measurements. In Proceedings of the 45th AIAA Aerospace Sciences Meeting and Exhibit, Reno, NV, USA, 8–11 January 2007; pp. 1–11.

6. Tjiu, W.; Marnoto, T.; Mat, S.; Ruslan, M.H.; Sopian, K. Darrieus vertical axis wind turbine for power generation I: Assessment of Darrieus VAWT configurations. *Renew. Energy* **2015**, *75*, 50–67.

7. Tjiu, W.; Marnoto, T.; Mat, S.; Ruslan, M.H.; Sopian, K. Darrieus vertical axis wind turbine for power generation II: Challenges in HAWT and the opportunity of multi-megawatt Darrieus VAWT development. *Renew. Energy* **2015**, *75*, 560–571.

8. Bianchini, A.; Ferrara, G.; Ferrari, L. Design guidelines for H-Darrieus wind turbines: Optimization of the annual energy yield. *Energy Convers. Manag.* **2015**, *89*, 690–707.

9. Dixon, K.R. The Near Wake Structure of a Vertical Axis Wind Turbine Including the Development of a 3D Unsteady Free-Wake Panel Method for VAWTs. Master's Thesis, Delft University of Technology, Delft, The Netherlands, 2008.

10. Carrigan, T.J.; Dennis, B.H.; Han, Z.X.; Wang, B.P. Aerodynamic shape optimization of a vertical-axis wind turbine using differential evolution. *ISRN Renew. Energy* **2011**, *2012*, 1–16.

11. Lanzafame, R.; Mauro, S.; Messina, M. 2D CFD modeling of H-Darrieus wind turbines using a transition turbulence model. *Energy Procedia* **2014**, *45*, 131–140.

12. Tchakoua, P.; Wamkeue, R.; Tameghe, T.A.; Ekemb, G. A Review of Concepts and Methods for Wind Turbines Condition Monitoring. In Proceedings of the 2013 World Congress on Computer and Information Technology (WCCIT), Sousse, Tunisia, 22–24 June 2013; pp. 1–9.

13. Tchakoua, P.; Wamkeue, R.; Ouhrouche, M.; Slaoui-Hasnaoui, F.; Tameghe, T.; Ekemb, G. Wind turbine condition monitoring: State-of-the-art review, new trends, and future challenges. *Energies* **2014**, *7*, 2595–2630.

14. Tchakoua, P.; Wamkeue, R.; Slaoui-Hasnaoui, F.; Tameghe, T.A.; Ekemb, G. New Trends and Future Challenges for Wind Turbines Condition Monitoring. In Proceeding of the 2013 International Conference on Control, Automation and Information Sciences (ICCAIS), Nha Trang, Vietnam, 25–28 November 2013; pp. 238–245.

15. Chen, Y.; Lian, Y. Numerical investigation of vortex dynamics in an H-rotor vertical axis wind turbine. *Eng. Appl. Comp. Fluid Mech.* **2015**, *9*, 21–32.

16. Jin, X.; Zhao, G.; Gao, K.; Ju, W. Darrieus vertical axis wind turbine: Basic research methods. *Renew. Sustain. Energy Rev.* **2015**, *42*, 212–225.

17. Paraschivoiu, I. Double-multiple streamtube model for Darrieus in turbines. *Wind Turbine Dyn.* **1981**, *1*, 19–25.

18. Mohamed, M.H. Performance investigation of H-rotor Darrieus turbine with new airfoil shapes. *Energy* **2012**, *47*, 522–530.

19. Masson, C.; Leclerc, C.; Paraschivoiu, I. Appropriate dynamic-stall models for performance predictions of VAWTs with NLF blades. *Int. J. Rotat. Mach.* **1998**, *4*, 129–139.

20. Dyachuk, E.; Goude, A. Simulating dynamic stall effects for vertical Axis wind turbines applying a double multiple Streamtube model. *Energies* **2015**, *8*, 1353–1372.

21. Dai, Y.M.; Gardiner, N.; Sutton, R.; Dyson, P.K. Hydrodynamic analysis models for the design of Darrieus-type vertical-axis marine current turbines. *Proc. Inst. Mech. Eng. M J. Eng. Marit. Environ.* **2011**, *225*, 295–307.

22. Hall, T.J. Numerical Simulation of a Cross Flow Marine Hydrokinetic Turbine. Ph.D. Thesis, University of Washington, Seattle, WA, USA, 2012.

23. Islam, M.; Ting, D.S.K.; Fartaj, A. Aerodynamic models for Darrieus-type straight-bladed vertical axis wind turbines. *Renew. Sustain. Energy Rev.* **2008**, *12*, 1087–1109.

24. Beri, H.; Yao, Y. Double multiple Streamtube model and numerical analysis of vertical axis wind turbine. *Energy Power Eng.* **2011**, *3*, 262–270.

25. Zhang, L.X.; Liang, Y.B.; Liu, X.H.; Jiao, Q.F.; Guo, J. Aerodynamic performance prediction of straight-bladed vertical axis wind turbine based on CFD. *Adv. Mech. Eng.* **2015**, *5*, doi:10.1155/2013/905379.

26. Bhutta, M.M.A.; Hayat, N.; Farooq, A.U.; Ali, Z.; Jamil, S.R.; Hussain, Z. Vertical axis wind turbine—A review of various configurations and design techniques. *Renew. Sustain. Energy Rev.* **2012**, *16*, 1926–1939.

27. Edwards, J. The Influence of Aerodynamic Stall on the Performance of Vertical Axis Wind Turbines. Ph.D. Thesis, University of Sheffield, Sheffield, UK, 2012.

28. Alaimo, A.; Esposito, A.; Messineo, A.; Orlando, C.; Tumino, D. 3D CFD analysis of a vertical axis wind turbine. *Energies* **2015**, *8*, 3013–3033.

29. Verkinderen, E.; Imam, B. A simplified dynamic model for mast design of H-Darrieus vertical axis wind turbines (VAWTs). *Eng. Struct.* **2015**, *100*, 564–576.

30. Chowdhury, A.M.; Akimoto, H.; Hara, Y. Comparative CFD analysis of vertical axis wind turbine in upright and tilted configuration. *Renew. Energy* **2016**, *85*, 327–337.

31. Tilmans, H.A.C. Equivalent circuit representation of electromechanical transducers: I. Lumped-parameter systems. *J. Micromech. Microeng.* **1996**, *6*, 157–176.

32. Mason, W. An electromechanical representation of a piezoelectric crystal used as a transducer. *Proc. Inst. Radio Eng.* **1935**, *23*, 1252–1263.

33. Tilmans, H.A.C. Equivalent circuit representation of electromechanical transducers: II. Distributed-parameter systems. *J. Micromech. Microeng.* **1997**, *7*, 285–309.

34. Barakati, S.M. Modeling and Controller Design of a Wind Energy Conversion System Including a Matrix Converter. Ph.D. Thesis, University of Waterloo, Waterloo, ON, Canada, 2008.

35. Kim, H.; Kim, S.; Ko, H. Modeling and control of PMSG-based variable-speed wind turbine. *Electr. Power Syst. Res.* **2010**, *80*, 46–52.

36. Borowy, B.S.; Salameh, Z.M. Dynamic response of a stand-alone wind energy conversion system with battery energy storage to a wind gust. *IEEE Trans. Energy Conver.* **1997**, *12*, 73–78.

37. Delarue, P.; Bouscayrol, A.; Tounzi, A.; Guillaud, X.; Lancigu, G. Modelling, control and simulation of an overall wind energy conversion system. *Renew. Energy* **2003**, *28*, 1169–1185.

38. Slootweg, J.G.; de Haan, S.W.H.; Polinder, H.; Kling, W.L. General model for representing variable speed wind turbines in power system dynamics simulations. *IEEE Trans. Power Syst.* **2003**, *18*, 144–151.

39. Junyent-Ferré, A.; Gomis-Bellmunt, O.; Sumper, A.; Sala, M.; Mata, M. Modeling and control of the doubly fed induction generator wind turbine. *Simul. Model. Pract. Theory* **2010**, *18*, 1365–1381.

40. Bolik, S.M. Modelling and Analysis of Variable Speed Wind Turbines with Induction Generator during Grid Fault. Ph.D. Thesis, Aalborg University: Aalborg, Danmark, 2004.

41. Perdana, A. *Dynamic Models of Wind Turbines*; Chalmers University of Technology: Göteborg, Sweden, 2008.

42. Scheurich, F.; Fletcher, T.M.; Brown, R.E. Simulating the aerodynamic performance and wake dynamics of a vertical-axis wind turbine. *Wind Energy* **2011**, *14*, 159–177.

43. Paraschivoiu, I. *Wind Turbine Design: With Emphasis on Darrieus Concept*; Polytechnic International Press: Montréal, QC, Canada, 2002.

44. Claessens, M. The Design and Testing of Airfoils for Application in Small Vertical Axis Wind Turbines. Master's Thesis, Delft University of Technology, Delft, The Netherlands, 2006.

45. Ajedegba, J.O.; Naterer, G.; Rosen, M.; Tsang, E. Effects of Blade Configurations on Flow Distribution and Power Output of a Zephyr Vertical Axis Wind Turbine. In

Proceedings of the 3rd IASME/WSEAS International Conference on Energy & Environment, Stevens Point, WI, USA, 23 February 2008; pp. 480–486.

46. Camporeale, S.M.; Magi, V. Streamtube model for analysis of vertical axis variable pitch turbine for marine currents energy conversion. *Energy Convers. Manag.* **2000**, *41*, 1811–1827.

47. Scheurich, F. Modelling the Aerodynamics of Vertical-Axis Wind Turbines. Ph.D. Thesis, University of Glasgow, Glasgow, UK, 2011.

48. Chandramouli, S.; Premsai, T.; Prithviraj, P.; Mugundhan, V.; Velamati, R.K. Numerical analysis of effect of pitch angle on a small scale vertical axis wind turbine. *Int. J. Renew. Energy Res*. **2014**, *4*, 929–935.

49. Lewis, J.W. *Modeling Engineering Systems: PC-Based Techniques and Design Tools*; LLH Technology Publishing: Eagle Rock, VA, USA, 1994.

50. Hogan, N.; Breedveld, P. The physical basis of analogies in network models of physical system dynamics. *Simul. Ser.* **1999**, *31*, 96–104.

51. Firestone, F.A. A new analogy between mechanical and electrical systems. *J. Acoust. Soc. Am.* **1933**, *4*, 249–267.

52. Olson, H.F. *Dynamical Analogies*; D. Van Nostrand Company, Inc.: Princeton, NJ, USA, 1959.

53. Firestone, F.A. The mobility method of computing the vibration of linear mechanical and acoustical systems: Mechanical-electrical analogies. *J. Appl. Phys.* **1938**, *9*, 373–387.

54. Calvo, J.A.; Alvarez-Caldas, C.; San, J.L. *Analysis of Dynamic Systems Using Bond. Graph. Method through SIMULINK*; INTECH Open Access Publisher: Rijeka, Croatia, 2011.

55. Bishop, R.H. *Mechatronics: An Introduction*; CRC Press: Boca Raton, FL, USA, 2005.

56. Van Gilder, J.W.; Schmidt, R.R. Airflow Uniformity through Perforated Tiles in a Raised-Floor Data Center. In Proceedings of the ASME 2005 Pacific Rim Technical Conference and Exhibition on Integration and Packaging of MEMS, NEMS, and Electronic Systems collocated with the ASME 2005 Heat Transfer Summer Conference, San Francisco, CA, USA, 17–22 July 2005; pp. 493–501.

57. Pugh, L.G.C.E. The influence of wind resistance in running and walking and the mechanical efficiency of work against horizontal or vertical forces. *J. Physiol.* **1971**, *213*, 255–276.

58. Herrmann, F.; Schmid, G.B. Analogy between mechanics and electricity. *Eur. J. Phys.* **1985**, *6*, 16–21.

59. Aynsley, R.M. A resistance approach to analysis of natural ventilation airflow networks. *J. Wind Eng. Ind. Aerodyn.* **1997**, *67*, 711–719.

60. Deglaire, P. Analytical Aerodynamic Simulation Tools for Vertical Axis Wind Turbines. Ph.D. Thesis, Acta Universitatis Upsaliensis, Uppsala, Sweden, 2010.

61. Goude, A. Fluid Mechanics of Vertical Axis Turbines: Simulations and Model Development. Ph.D. Thesis, Uppsala University, Uppsala, Sweden, 2012.

62. Dyachuk, E.; Goude, A.; Bernhoff, H. Dynamic stall modeling for the conditions of vertical Axis wind turbines. *AIAA J.* **2014**, *52*, 72–81.

63. Wilson, R.E.; Walker, S.N.; Lissaman, P.B.S. Aerodynamics of the Darrieus rotor. *J. Aircr.* **1976**, *13*, 1023–1024.

64. Goude, A.; Lundin, S.; Leijon, M. A Parameter Study of the Influence of Struts on the Performance of a Vertical-Axis Marine Current Turbine. In Proceedings of the 8th European Wave and Tidal Energy Conference (EWTEC09), Uppsala, Sweden, 7–10 September 2009; pp. 477–483.

65. Wekesa, D.W.; Wang, C.; Wei, Y.; Danao, A.M. Influence of operating conditions on unsteady wind performance of vertical axis wind turbines operating within a fluctuating free-stream: A numerical study. *J. Wind Eng. Ind. Aerodyn.* **2014**, *135*, 76–89.

66. Shires, A. Development and evaluation of an aerodynamic model for a novel vertical axis wind turbine concept. *Energies* **2013**, *6*, 2501–2520.

67. Antheaume, S.; Maître, T.; Achard, J. Hydraulic Darrieus turbines efficiency for free fluid flow conditions *versus* power farms conditions. *Renew. Energy* **2008**, *33*, 2186–2198.

68. Butbul, J.; MacPhee, D.; Beyene, A. The impact of inertial forces on morphing wind turbine blade in vertical axis configuration. *Energy Convers. Manag.* **2015**, *91*, 54–62.

69. Jamati, F. Étude Numérique d'une Éolienne Hybride Asynchrone. Ph.D. Thesis, Polytechnique Montréal, Montréal, QC, Canada, 2011.

70. Batista, N.C.; Melìcio, R.; Matias, J.C.O.; Catalao, J.P.S. Self-Start Performance Evaluation in Darrieus-Type Vertical Axis Wind Turbines: Methodology and Computational Tool Applied to Symmetrical Airfoils. In Proceedings of the International Conference on Renewable Energies and Power Quality (ICREPQ'11), Las Palmas de Gran Canaria, Spain, 13–15 April 2011.

71. Patel, M.V.; Chaudhari, M.H. Performance Prediction of H-Type Darrieus Turbine by Single Stream Tube Model for Hydro Dynamic Application. *Int. J. Eng. Res. Technol.* **2013**, *2*.

72. Abbott, I.H.; Von Doenhoff, A.E. *Theory of Wing Sections, Including a Summary of Airfoil Data*; Courier Corporation: North Chelmsford, MA, USA, 1959.

73. Evans, J.; Nahon, M. Dynamics modeling and performance evaluation of an autonomous underwater vehicle. *Ocean Eng.* **2004**, *31*, 1835–1858.

74. Wu, J.; Lu, X.; Denny, A.G.; Fan, M.; Wu, J. Post-stall flow control on an airfoil by local unsteady forcing. *J. Fluid Mech.* **1998**, *371*, 21–58.

75. Castelli, M.R.; Fedrigo, A.; Benini, E. Effect of dynamic stall, finite aspect ratio and streamtube expansion on VAWT performance prediction using the BE-M model. *Int. J. Eng. Phys. Sci.* **2012**, *6*, 237–249.

76. Tala, H.; Patel, H.; Sapra, R.R.; Gharte, J.R. Simulations of small scale straight blade Darrieus wind turbine using latest CAE techniques to get optimum power output. *Int. J. Adv. Found. Res. Sci. Eng.* **2014**, *1*, 37–53.

77. Hartman, H.L.; Mutmansky, J.M.; Ramani, R.V.; Wang, Y. *Mine Ventilation and Air Conditioning*; John Wiley & Sons: San Francisco, CA, USA, 2012.

78. Aynsley, R. Indoor wind speed coefficients for estimating summer comfort. *Int. J. Vent.* **2006**, *5*, 3–12.

79. McPherson, M.J. Ventilation network analysis. In *Subsurface Ventilation and Environmental Engineering*; Springer: Amsterdam, The Netherlands, 1993; pp. 209–240.

80. Acuña, E.I.; Lowndes, I.S. A review of primary mine ventilation system optimization. *Interfaces* **2014**, *44*, 163–175.

81. Sheldon, J.C.; Burrows, F.M. The dispersal effectiveness of the achene—Pappus units of selected Compositae in steady winds with convection. *New Phytol.* **1973**, *72*, 665–675.

82. Toussaint, H.M.; de Groot, G.; Savelberg, H.H.; Vervoorn, K.; Hollander, A.P.; van Ingen Schenau, G.J. Active drag related to velocity in male and female swimmers. *J. Biomech.* **1988**, *21*, 435–438.

83. Cresswell, L.G. The relation of oxygen intake and speed in competition cycling and comparative observations on the bicycle ergometer. *J. Physiol.* **1974**, *241*, 795–808.

84. Martin, J.C.; Milliken, D.L.; Cobb, J.E.; McFadden, K.L.; Coggan, A.R. Validation of a mathematical model for road cycling power. *J. Appl. Biomech.* **1998**, *14*, 276–291.

85. Kiyoto, H.; Tosha, K. Effect of Peened Surface Characteristics on Flow Resistance. In Proceedings of the 10th International Conference on Shot Peening, Tokyo, Japan, 15–18 September 2008; pp. 535–540.

86. Crawford, C. Advanced Engineering Models for Wind Turbines with Application to the Design of a Coning Rotor Concept. Ph.D. Thesis, University of Cambridge, Cambridge, UK, 2007.

87. Mohammadi-Amin, M.; Ghadiri, B.; Abdalla, M.M.; Haddadpour, H.; de Breuker, R. Continuous-time state-space unsteady aerodynamic modeling based on boundary element method. *Eng. Anal. Bound. Elem.* **2012**, *36*, 789–798.

88. Sheldahl, R.E.; Klimas, P.C. *Aerodynamic Characteristics of Seven Symmetrical Airfoil Sections through 180-Degree Angle of attack for Use in Aerodynamic Analysis of Vertical Axis Wind Turbines*; Technical Report for Sandia National Laboratories: Albuquerque, NM, USA, 1981.

89. Critzos, C.C.; Heyson, H.H.; Boswinkle, R.W. *Aerodynamic Characteristics of NACA 0012 Airfoil Section at Angles of Attack from 0 Degree to 180 Degree*; Technical Report for National Advisory Committee for Aeronautics, Langley Aeronautical Lab: Langley Field, VA, USA, 1955.

90. Miley, S.J. *A Catalog of Low Reynolds Number Airfoil Data for Wind Turbine Applications*; Technical Rockwell International Corp: Golden, CO, USA, 1982.

91. Timmer, W.A. Aerodynamic Characteristics of Wind Turbine Blade Airfoils at High Angles-of-Attack. In Proceedings of the 3rd EWEA Conference-Torque 2010: The Science of making Torque from Wind, Heraklion, Greece, 28–30 June 2010.

92. Rathi, D. Performance Prediction and Dynamic Model Analysis of Vertical Axis Wind Turbine Blades with Aerodynamically Varied Blade Pitch. Master's Thesis, NC State University, Raleigh, NC, USA, 2012.

Chapter IV

ELECTRIC CIRCUIT MODEL FOR THE AERODYNAMIC PERFORMANCE ANALYSIS OF A THREE-BLADE DARRIEUS-TYPE VERTICAL AXIS WIND TURBINE

Electric Circuit Model for the Aerodynamic Performance Analysis of a Three-Blade Darrieus-Type Vertical Axis Wind Turbine: The Tchakoua Model

Pierre Tchakoua, René Wamkeue, Mohand Ouhrouche, Ernesto Benini and Gabriel Ekemb

Résumé

L'aérodynamique complexe et instable des éoliennes à axe vertical pose d'importants défis aux outils de simulation. D'importants efforts de recherche ont récemment porté sur le développement de nouvelles méthodes d'analyse et d'optimisation de la performance aérodynamique des éoliennes a axe vertical. Cet article présente un modèle à base de circuit électrique pour les rotors d'éoliennes à axe vertical de type Darrieus. Le nouveau modèle baptisé 'Tchakoua model' est basé sur la description mécanique donnée par le modèle à double disque et multiples tubes de vent de Paraschivoiu et utilise l'analogie mécanique électrique. Des simulations du modèle ont été effectuées avec MATLAB pour une architecture de rotor à trois pales, caractérisée par un profil NACA0012, un nombre moyen de Reynolds de 40 000 pour la pale et une vitesse spécifique de 5. Les résultats obtenus montrent une forte concordance à la fois avec les simulations de modèles aérodynamiques et ceux de modèles de dynamique des fluides issues de la littérature.

Abstract

The complex and unsteady aerodynamics of vertical axis wind turbines (VAWTs) pose significant challenges for simulation tools. Recently, significant research efforts have focused on the development of new methods for analysing and optimising the aerodynamic performance of VAWTs. This paper presents an electric circuit model for Darrieus-type vertical axis wind turbine (DT-VAWT) rotors. The novel Tchakoua model is based on the mechanical description given by the Paraschivoiu double-multiple streamtube model using a mechanical-electrical analogy. Model simulations were conducted using MATLAB for a three-bladed rotor architecture, characterized by a NACA0012 profile, an average Reynolds number of 40,000 for the blade and a tip speed ratio of 5. The results obtained show strong agreement with findings from both aerodynamic and computational fluid dynamics (CFD) models in the literature.

4.1 INTRODUCTION

Darrieus-type vertical axis wind turbines (DT-VAWTs) are nonlinear systems that operate in turbulent environments. Therefore, it is difficult to accurately characterize their aerodynamic rotor behaviour across a wide range of operating conditions using physically meaningful models. Commonly used models are either derived from wind turbine data and are presented in a "black box" format or are computationally expensive. Indeed, most of these models lack both conciseness and intelligibility and are therefore prohibitive for the routine engineering analyses of the local interaction mechanisms of wind turbines. Furthermore, none of the models with high reliability and accuracy can be efficiently coupled with models of the other mechanical and electrical parts of the wind turbine to form a global model for the wind energy conversion system (WECS).

Models are of central importance in many scientific contexts and are one of the principal instruments of modern science. Scientists spend considerable time building, testing, comparing and revising models, and many scientific publications are dedicated to introducing, applying and interpreting these valuable tools. The use of electrical circuit elements to model physical devices and systems has a long and successful history. Additionally, understanding analogies and constructing an analogue model for a given system allows the system to be studied in an environment other than that for which it is intended [1–3], thereby facilitating the study of specific system phenomena. Moreover, a model based on electrical components is accessible and quickly understood by researchers from almost all engineering fields. This wide understanding is of great importance because research and development in the wind turbine industry requires competencies from several different fields of engineering. Furthermore, the equivalent electrical model can take

128

advantage of existing resources by simultaneously capitalizing on the strengths of these resources and minimizing their respective drawbacks. In addition, such a model can be a good tool for simulating wind turbine rotor operation in the case of physical damage or structural faults on one or more blades. Finally, because electrical and other dynamic models for other parts of the wind turbine have been developed [4–11], this new rotor model can easily be linked to existing models to create an overall wind turbine model.

This paper presents an electric circuit model for three-blade DT-VAWT rotors that we named the Tchakoua model. This model is based on a recently developed approach for modelling DT-VAWT rotors using the equivalent electrical circuit analogy that is presented in [12–14]. The proposed model was built from the mechanical description given by the Paraschivoiu double-multiple streamtube model and was based on an analogy between mechanical and electrical circuits. Thus, the rotating blades and the blades' mechanical coupling to the shaft are modelled using the mechanical-electrical analogy, and the wind flow is modelled as a source of electric current.

This paper is organized as follows: Section 2 presents the context of the work and the methodology used for building the model; Section 3 presents the theoretical background and the model construction; the results are presented and discussed in Section 4; and Section 5 concludes the paper.

4.2 CONTEXT AND METHOD

4.2.1. Context

Due to their compactness, adaptability for domestic installations, omni-directionality, and other advantages, VAWTs have recently become the focus of renewed interest. Several

universities and research institutions have conducted extensive research and developed numerous designs based on aerodynamic computational models [15–17]. For example, the on-going studies at the University of Québec at Abiti-Témiscamingue could construct a new model that is more appropriate for the design and further conceptual analysis focusing on operational optimization, condition monitoring, and fault prediction and detection of DT-VAWT rotors. Figure IV-1 shows the "Cap d'Ours" three-blade VAWT that serves as a teaching and research tool at the University of Québec at Abitibi-Témiscamingue.
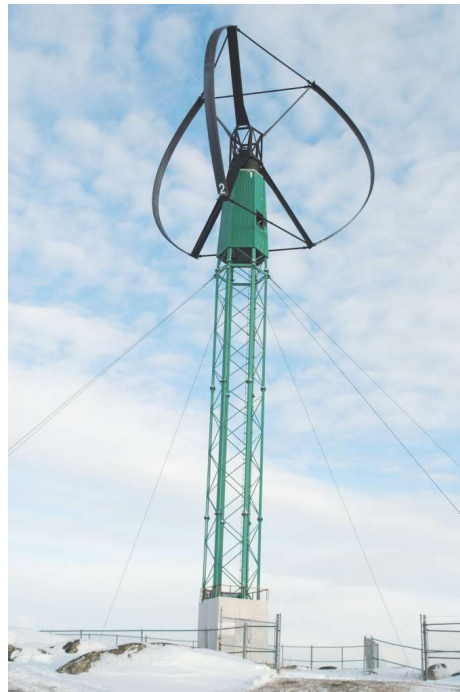
Figure IV-1   "Cap d'Ours", a curved, three-blade, Darrieus-type VAWT.

Several advances have been made in the understanding and modelling of wind turbine aerodynamics. Various models for VAWT aerodynamic simulation can be found in the literature. These models can be broadly classified into four categories: momentum models, vortex models, cascade models and computational fluid dynamic (CFD) models. A literature survey on the most used models was conducted in [12,14]. Aerodynamics are still unable to

meet the demands of various applications, although the streamtube and vortex models have seen significant improvements. However, as with all knowledge, our understanding of aerodynamics is not absolute and can be viewed as tentative, approximate, and always subject to revision. For instance, CFD solutions remain very computationally expensive and are prohibitive for routine engineering analyses of the local interaction mechanisms of wind turbines. Furthermore, none of the models with high reliability and accuracy can be efficiently coupled with the models of the other mechanical and electrical parts of the wind turbine to create a global model for the wind energy conversion system (WECS).

To overcome these problems, this paper presents a DT-VAWT model that is built using electric components. The Tchakoua model is a circuit-based model that is advantageous because it allows an electrical engineer to visualize and understand the working principles and the aerodynamics underlying the VAWT rotor functions and behaviour in a connected circuit better than a black box or a complex equation. Indeed, wind energy is a multidisciplinary domain with increasing research in the field of electrical engineering. Furthermore, the Tchakoua model could be linked to existing electric models of other mechanical and electrical parts of a wind turbine to form a global model for the WECS. Such a global circuit-based model for WECS will help users to understand the effects of various parameters on the aerodynamic blade forces and the effects of rotor structural faults on the overall WECS performance. According to [18–20], this model will contribute to constructing a global model that can be used to develop or improve the overall condition monitoring technique for WECS. Overall WTCM approaches include performance monitoring, power curve analysis, electrical signature, and supervisory control and data acquisition (SCADA) system data analysis. Compared to subsystem condition monitoring techniques, global

131

system condition monitoring techniques are nonintrusive, low cost and reliable; global monitoring techniques can be used in online monitoring to reduce downtime and OM costs [21–23]. Finally, the new model is very versatile and may therefore permit the study of various effects and phenomena, including dynamic stall effects, flow curvature effects, pitching circulation, added mass effects, interference among blades, and vibration effects.

4.2.2. Method: The Mechanical-Electrical Analogy Approach

Analogies are of greatest use in electromechanical systems when there is a connection between mechanical and electrical parts, especially when the system includes transducers between different energy domains, such as WECS.

Mechanical-electrical analogies are used to represent the function of a mechanical system as an equivalent electrical system by drawing analogies between mechanical and electrical parameters. The main value of analogies lies in the way in which mathematics unifies these diverse fields of engineering into one subject. Tools previously developed for solving problems in one field can be used to solve problems in another field. This is an important concept because some fields, particularly electrical engineering, have developed rich sets of problem-solving tools that are fully applicable to other engineering fields [24]; for example, there are simple and straightforward analogies between electrical and mechanical systems. Furthermore, analogies between mechanical systems and electrical or fluid systems are effective and commonly used.

Two valid techniques for modelling mechanical systems with electrical systems or for drawing analogies between the two types of systems can be found in the literature, and each method has its own advantages and disadvantages [25–28]. The first technique is intuitive; in this technique, current corresponds to velocity (both consist of motion), and

132

voltage corresponds to force (both provide a "push"). The second technique is the through/across analogy that uses voltage as an analogy for velocity and current as an analogy for force. The two schools of thought for modelling mechanical systems with electrical systems are presented in Table 1. Although both are valid, the through/across analogy results in a counterintuitive definition of impedance [24,29,30]. The universally applied analogy for impedance is that from the intuitive analogy listed in the corresponding section of Table IV-1. Therefore, the intuitive analogy is used in the present study.

Table IV-1   *System analogy used for developing the new model.*

Topology-Preserving Set (Book's Analogy)								
						Intuitive Analogy Set		
		⟸⟹				⟸⟹		
		Intuitive Stretch				Topology Change		
Description	Trans Mech	Rot Mech	Electrical	Thermal	Fluid	Trans Mech	Rot Mech	Description
"Through" variable	f (force)	τ (torque)	i (current)	ϕ (heat flux)	q (flow)	v (velocity)	ω (angular velocity)	Motion
"Across" variable	v (velocity)	ω (angular velocity)	v (voltage)	$T,\ \theta$	p (pressure)	f (force)	τ (torque)	Push (force)
Dissipative element	$v = \dfrac{1}{B}f$	$\omega = \dfrac{1}{B_r}\tau$	$v = iR$	$\theta = \phi R$	$p = qR$	$f = vB$	$\tau = \omega B_r$	Dissipative element
Dissipation	$f^2\dfrac{1}{B} = \dfrac{v^2}{1/B}$	$\tau^2\dfrac{1}{B} = \dfrac{\omega^2}{1/B}$	$i^2 R = v^2/R$	N/A	$q^2 R$ $= p^2/R$	$v^2 R$ $= f^2/R$	$\omega^2 B_r$ $= \tau^2/B_r$	Dissipation
Through-variable storage element	$v = \dfrac{1}{K}\dfrac{df}{dt}$ or $\int v\,dt = \dfrac{1}{K}f$	$\omega = \dfrac{1}{K_r}\dfrac{d\tau}{dt}$ or $\int \omega\,dt = \dfrac{1}{K_r}\tau$	$v = L\dfrac{di}{dt}$	N/A	$p = I\dfrac{dq}{dt}$	$f = M\dfrac{dv}{dt}$ (one end must be "grounded")	$\tau = J\dfrac{d\omega}{dt}$ (one end must be "grounded")	Motion storage element

Energy	$E = \frac{1}{2}\frac{1}{K}f^2$	$E = \frac{1}{2}\frac{1}{K_r}\tau^2$	$E = \frac{1}{2}Li^2$		$E = \frac{1}{2}Iq^2$	$E = \frac{1}{2}Mv^2$	$E = \frac{1}{2}J\omega^2$	Energy
Impedance	Standard definition is shown to the right		$V(s) = I(s)Ls$		$P(s)$ $= Q(s)Is$	$F(s)$ $= V(s)Ms$	$T(s)$ $= \Omega(s)Js$	Impedance
Across-variable storage element	$f = M\frac{dv}{dt}$ (one end must be "grounded")	$\tau = J\frac{d\omega}{dt}$	$i = C\frac{dv}{dt}$	$\phi = C\frac{d\theta}{dt}$ (one end must be "grounded")	$q = C\frac{dp}{dt}$ (one end is usually "grounded")	$v = \frac{1}{K}\frac{df}{dt}$ or $\int v dt = \frac{1}{K}f$	$\omega = \frac{1}{K_r}\frac{d\tau}{dt}$ or $\int \omega dt = \frac{1}{K_r}\tau$	Push (force) storage element
Energy	$E = \frac{1}{2}Mv^2$	$E = \frac{1}{2}J\omega^2$	$E = \frac{1}{2}Cv^2$	$E = CT$ (not analogous)	$E = \frac{1}{2}Cp^2$	$E = \frac{1}{2}\frac{1}{K}f^2$	$E = \frac{1}{2}\frac{1}{K_r}\tau^2$	Energy
Impedance	The standard definition of mechanical impedance is the one on the right, based on the intuitive analogy		$V(s)$ $= I(s)\frac{1}{sC}$	$\Theta(s)$ $= \Phi(s)\frac{1}{sC}$	$P(s)$ $= Q(s)\frac{1}{sC}$	$F(s)$ $= V(s)\frac{K}{s}$	$T(s)$ $= \Omega(s)\frac{K_r}{s}$	Impedance

4.3 MODEL CONSTRUCTION

4.3.3. Theoretical Background

DT-VAWTs are lift-based machines, i.e., their driving torque is mainly generated by the lift force, and they consist of two or more aerofoil-shaped blades attached to a rotating vertical shaft. The interaction between the wind and the rotating blades creates a system of lift and drag forces over the blades themselves. The instantaneous resultant of these forces is dominated by the lift effect that is responsible for the aerodynamically generated mechanical torque. If we consider a Darrieus-type VAWT, as shown in Figure IV-2, the aerofoil blade is characterized by the height $2H$, the rotor radius R, the number of blades $N_b = 3$ and the blade chord c. For a given point on any of the blades, r and z are the local radius and height, respectively. When the rotor is subject to an instantaneous incoming wind speed $W_0(t)$, it turns at a rotational speed $\omega(t)$.
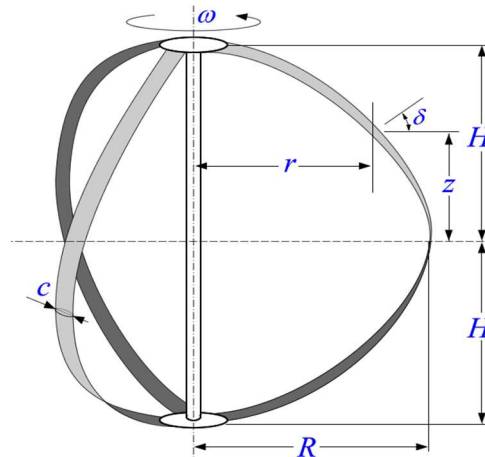

Figure IV-2 Schematic of a curved, three-blade DT-VAWT.

Figure IV-3 shows the aerodynamic forces and the three velocity vectors acting on DT-VAWT blade elements at a random position [31,32]. F_L and F_D are the lift and drag force,

respectively. As the blade rotates, the local angle of attack α varies with the relative velocity W_r. The incoming wind speed W_0 and the rotational velocity of the blade ω govern the orientation and magnitude of W_r [33,34]. In turn, the forces F_L and F_D acting on the blade vary. The magnitude and orientation of the lift and drag forces vary along with the resultant force. The resultant force can be decomposed into a normal force F_N and a tangential force F_T. The tangential force component drives the rotation of the wind turbine and produces the torque necessary to generate electricity [35].
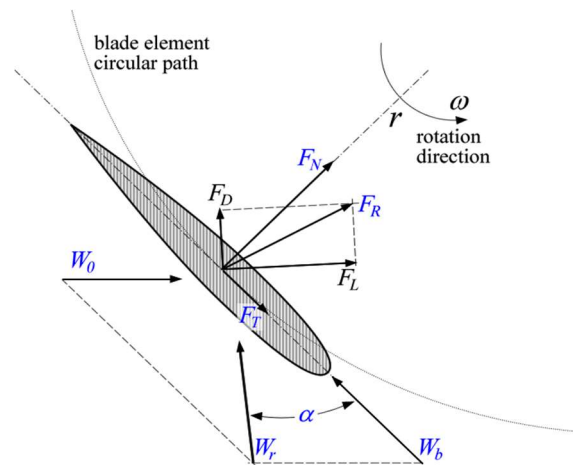

Figure IV-3   Velocity and force components for a DT-VAWT.

A new approach for modelling DT-VAWT rotors using the electric-mechanic analogy was presented in [12–14]. These works provide a proof-of-concept demonstration of the approach and verify the feasibility of such a model through step-by-step demonstrations of the theoretical and practical concepts that underpin the new model as well as simulations and cross-validation of a single-blade model.

4.3.4. **Wind Flow as a Current Source**

As stated in [12,14], an analogy can be made between the wind flow in a streamtube and an electric current. If the incident wind flow is assumed to be an electric current, then

the wind's relative dynamic pressure flow can be defined as $q = \dfrac{1}{2}\rho W_{rb}^2$ (where q is given in N/m^2 and the fluid density ρ is given in kg/m^3), which is the energy of the wind due to its velocity, that can be considered an electric energy source. Thus, the instantaneous expression of the current source that represents the relative wind seen by the blade is as follows:

$$i_w(t) = \begin{cases} \Psi^u \sin(\omega t + 2\alpha) & \text{for} \quad -\pi/2 \le \theta \le \pi/2 \\ \Psi^d \sin(\omega t + 2\alpha) & \text{for} \quad 3\pi/2 \le \theta \le -\pi/2 \end{cases} \tag{1}$$

where $\Psi = \dfrac{1}{2}\rho W_0^2 \left(\left(\dfrac{\omega R}{W_0} + \sin\theta_b \right)^2 + (\cos\theta_b)^2 (\cos\eta)^2 \right)$

and $\alpha = \tan^{-1}\left(\dfrac{\cos\theta_b \cos\eta}{\lambda_i + \sin\theta_b} \right) + \delta$.

Ψ is the modulus of the current flow that varies with the rotational angle of the blade. For the Double-multiple multi-streamtube model shown in Figure IV-4, the modulus of the corresponding current in the downwind disk is slightly lower than that in the upwind disk, that is ($\Psi^d \prec \Psi^u$).
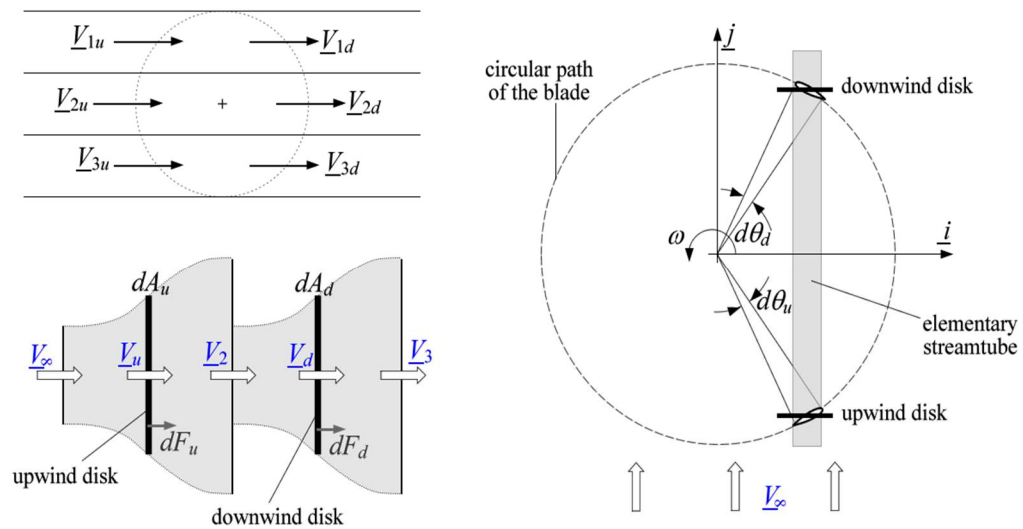

Figure IV-4 Double-multiple multi-streamtube model.

138

As described in [12,14], the airflow in a streamtube can be compared to wind flow on a thin flat disc that is parallel to the airstream. In such conditions, the resistance to the airflow due to air friction on both sides of the plate is minimal, and the wind driving pressure difference from one point of the streamtube to another is approximately zero. Thus, the resistance to wind flow is zero, meaning that the electric resistance parallel to the current source tends to infinity such that the total current produced by the current generator flows in the blade. The improved equivalent electric model for wind flow in a double-multiple multi-streamtube model is shown in Figure IV-5.
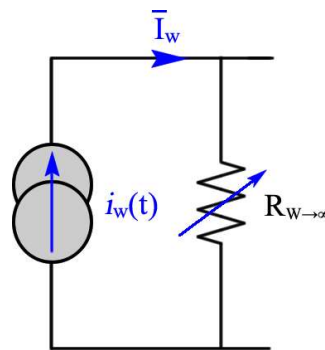

Figure IV-5 Electric circuit model for wind flow.

4.3.5. **Electric Circuit Model for a Single Blade**

The aerodynamic force coefficients acting on a cross-sectional blade element of a Darrieus wind turbine are shown in Figure IV-6. The directions of the lift and drag coefficients as well as their normal and tangential components are illustrated in this figure. The effort variable is voltage, while the flow variable is electrical current. The ratio of voltage to current is the electrical resistance (Ohm's law). The ratio of the effort variable to the flow variable in other domains is also described as resistance. Oscillating voltages and currents with a phase difference between them provide the concept of electrical impedance. Impedance can be considered an extension to the concept of resistance: resistance is

139

associated with energy dissipation, while impedance encompasses both energy storage and energy dissipation.
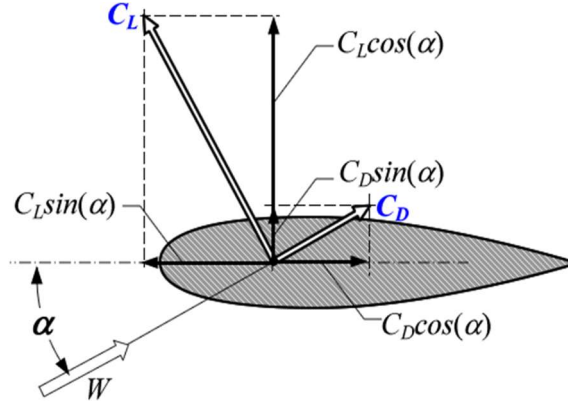
Figure IV-6 Aerodynamic coefficients acting on a Darrieus wind turbine blade element [36].

We consider a complex coordinate system as shown in Figure 6, where the vertical axis is assumed to be real and the horizontal axis is assumed to be imaginary. Then, the lift and drag coefficients can be written as follows:

$$\begin{pmatrix} \overline{C}_L \\ \overline{C}_D \end{pmatrix} = \begin{pmatrix} C_L \cos\varphi + jC_L \dfrac{\sin\varphi}{\cos\eta} \\ C_D \sin\varphi - jC_D \dfrac{\cos\varphi}{\cos\eta} \end{pmatrix} \tag{2}$$

The total impedance for a blade element is obtained by adding the elementary lift and drag impedances. We can then write:

$$\overline{Z}_B = R_B + jX_B = Z_N + jZ_T \tag{3}$$

where

$$\begin{pmatrix} Z_{\mathrm{N}} \\ Z_{\mathrm{T}} \end{pmatrix} = \begin{pmatrix} R_{\mathrm{B}} \\ X_{\mathrm{B}} \end{pmatrix} = \begin{pmatrix} R_{\mathrm{L}} + R_{\mathrm{D}} \\ X_{\mathrm{L}} - X_{\mathrm{D}} \end{pmatrix} \tag{4}$$

and

$$\begin{pmatrix} R_{\mathrm{L}} \\ R_{\mathrm{D}} \\ X_{\mathrm{L}} \\ X_{\mathrm{D}} \end{pmatrix} = \begin{pmatrix} \sum_{i=1}^{n} c_i z_i C_{\mathrm{L}i} \cos \varphi_i \\ \sum_{i=1}^{n} c_i z_i C_{\mathrm{D}i} \sin \varphi_i \\ \sum_{i=1}^{n} c_i z_i C_{\mathrm{L}i} \dfrac{\sin \varphi_i}{\cos \eta_i} \\ \sum_{i=1}^{n} c_i z_i C_{\mathrm{D}i} \dfrac{\cos \varphi_i}{\cos \eta_i} \end{pmatrix} \tag{5}$$

where R_{Li} and X_{Li} are the resistive and inductive components of the lift impedance, respectively, while $R_{\mathrm{D}i}$ and $X_{\mathrm{D}i}$ are the resistive and inductive components of the elementary drag impedance, respectively. Because C_{Li} varies with the angle of attack α, R_{Li} and X_{Li} correspond to a variable resistor ($R_{\mathrm{L}i} = f(\alpha_i)$) and a variable inductor ($X_{\mathrm{L}i} = f(\alpha_i)$), respectively. Similarly, because C_{D} varies with the angle of attack α, $R_{\mathrm{D}i}$ and $X_{\mathrm{D}i}$ correspond to a variable resistor ($R_{\mathrm{D}i} = f(\alpha_i)$) and a variable capacitor ($X_{\mathrm{D}i} = f(\alpha_i)$), respectively.

Figure IV-7 shows the enhanced equivalent electric model of a single blade. The normal and tangential voltages produced by the blade can be expressed as follows:

$$\begin{pmatrix} \overline{V}_{\mathrm{N}} \\ \overline{V}_{\mathrm{T}} \end{pmatrix} = \begin{pmatrix} \overline{Z}_{\mathrm{N}} \overline{I}_{\mathrm{w}} \\ \overline{Z}_{\mathrm{T}} \overline{I}_{\mathrm{w}} \end{pmatrix} = \begin{pmatrix} R_{\mathrm{B}} e^{i0} \\ X_{\mathrm{B}} e^{i\pi/2} \end{pmatrix} (\Psi \angle 2\alpha, \Psi \angle 2\alpha) = \begin{pmatrix} \Psi R_{\mathrm{B}} \angle 2\alpha \\ \Psi X_{\mathrm{B}} \angle 2\alpha + \dfrac{\pi}{2} \end{pmatrix} \tag{6}$$
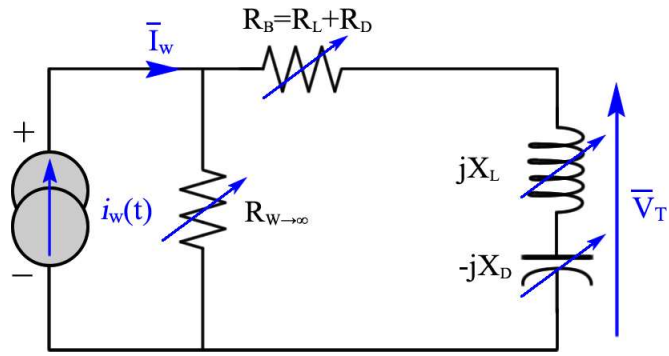
141

Figure IV-7 Electric circuit model for a single blade.

The variation of the lift, drag and normal resistances as well as those of the lift, drag and tangential reactances are shown in Figure IV-8 and Figure IV-9, respectively [14]. These resistances and reactances are obtained considering a blade element; therefore, they are given per unit of blade height.
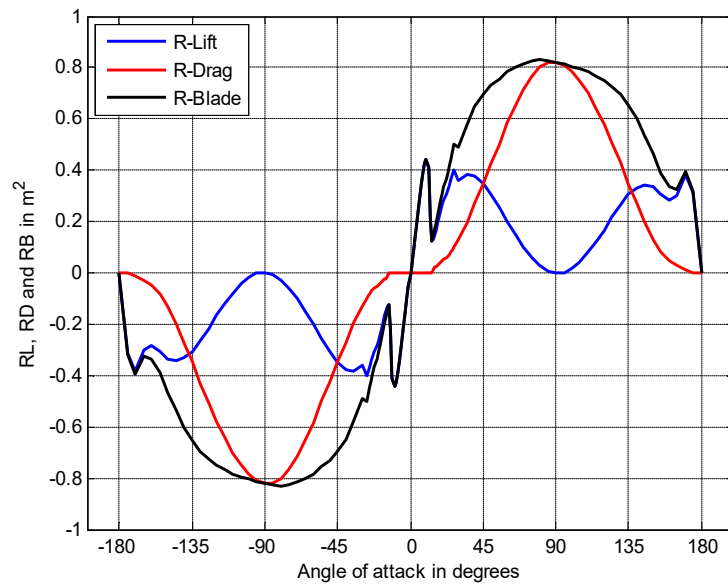

Figure IV-8 Lift, drag and normal resistance variations as functions of the angle of attack.
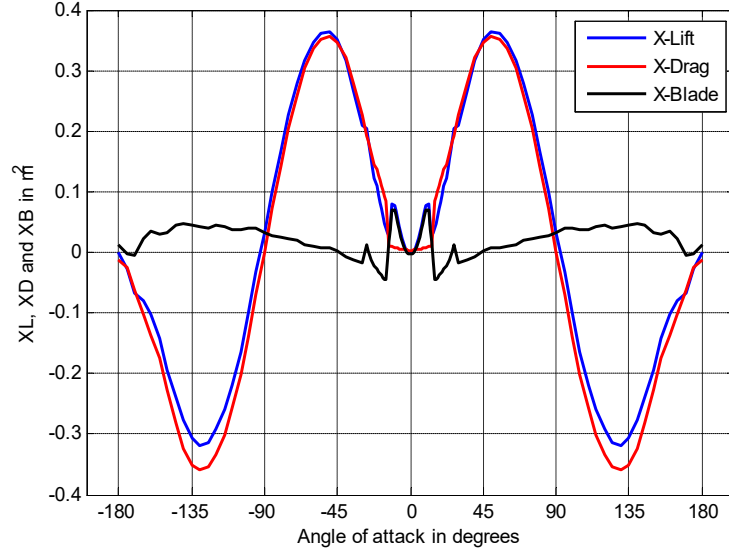
Figure IV-9 Lift, drag and tangential reactance variations as functions of the angle of attack.

Following the laws of electrical circuit analysis, the branch with $R_{W \to \infty}$ can be assumed to be an open circuit, and the total voltage across a blade can be obtained from the algebraic sum of the lift and drag voltages. We can then write:

$$\overline{V}_B = \overline{I}_w \times \overline{Z}_B = \overline{I}_w \times \left(\overline{Z}_N + j\overline{Z}_T\right) = \overline{V}_N + \overline{V}_T \tag{7}$$

When the blade is turning, the elementary work (or elementary amount of mechanical energy) is produced when an elementary force is exerted on an elementary linear distance $rd\theta$ covered by the blade. Furthermore, because the torque varies with the azimuth angle of the blade, the torque produced by a blade element is obtained by integrating with respect to the rotational angle. Then, the total torque produced by the entire blade for a complete revolution of the turbine is obtained by adding n discrete elementary torques over the full height of the rotor:

$$T_B = \sum_{i=1}^{n} T_{Bi} = \sum_{i=1}^{n} \left(\frac{r_i}{2\pi} \int_0^{2\pi} \Psi X_{Bi} d\theta \right) = \frac{1}{2\pi} \int_0^{2\pi} \left(\sum_{i=1}^{n} r_i \Psi X_{Bi} \right) d\theta \cdot \tag{8}$$

143

The final expression of the total torque is then obtained;

$$T_B = \frac{1}{2\pi}\int_0^{2\pi}\Psi\left(\sum_{i=1}^{n}r_i c_i z_i\left(C_{Li}\frac{\sin\varphi_i}{\cos\eta_i} - C_{Di}\frac{\cos\varphi_i}{\cos\eta_i}\right)\right)d\theta. \tag{9}$$

4.3.6. **Electric Circuit Model for the Blades' Mechanical Coupling to the Shaft**

The wind turbine shaft is connected to the centre of the rotor; this shaft supports the rotor (hub and blades) and transmits the rotary motion and torque moments of the rotor to the gearbox and/or generator. When the rotor spins, the shaft spins as well. In this way, the rotor transfers its rotational mechanical energy to the shaft and then to an electrical generator on the other end. If we assume that the rotor's mechanical coupling to the shaft is ideal, then it would be electrically equivalent to an ideal transformer. Figure IV-10 shows the equivalent electric diagram for a single blade coupled to the shaft.
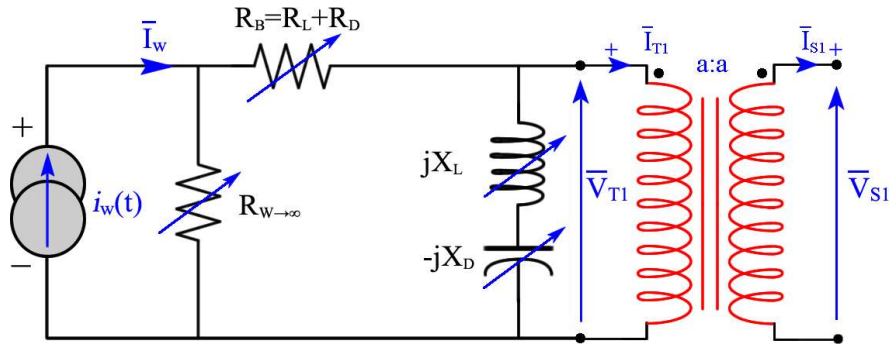

Figure IV-10 Equivalent diagram for a single blade coupled to the shaft.

At this stage of the WECS (shaft), we no longer consider fluid mechanics; instead, we address translation and/or rotation mechanics. Assuming an ideal autotransformer, the voltage at the primary side is equal to that at the secondary side, i.e., $V_{Si} = V_{Ti}$. The current

produced by the source corresponds to the relative wind seen by the blades at any moment. That is, for each blade:

$$\bar{I}_B = \bar{I}_w = \frac{1}{2}\rho V_0^2 \left(\left(\frac{\omega R}{V_0} + \sin\theta_b \right)^2 + \left(\cos\theta_b \right)^2 \left(\cos\eta \right)^2 \right) e^{j2(\varphi+\delta)} \qquad (10)$$

$$\bar{I}_B = \Psi e^{j2\alpha} \qquad (11)$$

where $\qquad \Psi = \frac{1}{2}\rho W_0^2 \left(\left(\frac{\omega R}{W_0} + \sin\theta_b \right)^2 + \left(\cos\theta_b \right)^2 \left(\cos\eta \right)^2 \right) \qquad$ and

$\alpha = \tan^{-1}\left(\dfrac{\cos\theta_b \cos\eta}{\lambda_i + \sin\theta_b} \right) + \delta$.

We can then obtain:

$$\bar{V}_T = \Psi X_B e^{i(2\alpha+\pi/2)}. \qquad (12)$$

Because the mechanical coupling of a single blade I to the shaft can be modelled as an ideal autotransformer, we can then write:

$$\begin{cases} V_{Ti} = V_{Si} \\ I_{Ti} = I_{Si} \end{cases} \qquad (13)$$

Assuming that the rotor mechanical coupling of three blades to the shaft is ideal, this coupling can be electrically modelled as multiple ideal primary transformers, as shown in Figure IV-11.
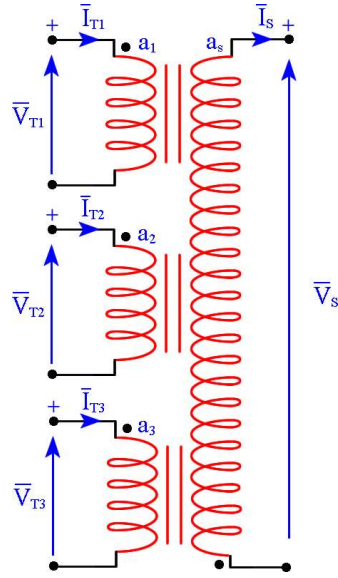
Figure IV-11 Rotor coupling of three blades modelled as an electric transformer.

The windings of the corresponding transformer are made so that the following is true:

$$\frac{V_{T1}}{a_1} + \frac{V_{T2}}{a_2} + \frac{V_{T3}}{a_3} = \frac{V_R}{a_R} \tag{14}$$

Because we have $a_1 = a_2 = a_3 = a_R$, we can write:

$$\vec{V}_R = \vec{V}_{T1} + \vec{V}_{T2} + \vec{V}_{T3} \tag{15}$$

The voltage at the secondary of the transformer can be obtained by vector addition of the three primary voltages because $\vec{V}_{T1}$, $\vec{V}_{T2}$ and $\vec{V}_{T2}$ have variable moduli and phases while the phase difference from one blade to another remains constant. At any instant, the three voltages behave as if in an unbalanced three-phase system.

As suggested in the intuitive analogy, the rotational speed of the shaft ω is analogous to the electrical current. Finally, the rotational speed of the shaft can be assumed to be equivalent to the electric current at the secondary of the transformer, i.e., $I_S = \omega$. We can therefore write the following relations:

146

$$\begin{cases} I_S = I_{S1} + I_{S2} + I_{S3} = \omega \\ I_{S1} = I_{S2} = I_{S3} = \dfrac{\omega}{3} \end{cases} \tag{16}$$

4.4 RESULTS AND DISCUSSION

4.4.1. Electric Circuit Model for Three-Blade DT-VAWT Rotors: The Tchakoua Model

We can now construct the equivalent electric model for the whole three-blade turbine. The equivalent circuits for various blades are brought together and are coupled based on the developments presented in Section 3. Figure IV-12 presents the Tchakoua model, which is the global equivalent electric model for a three-blade DT-VAWT.
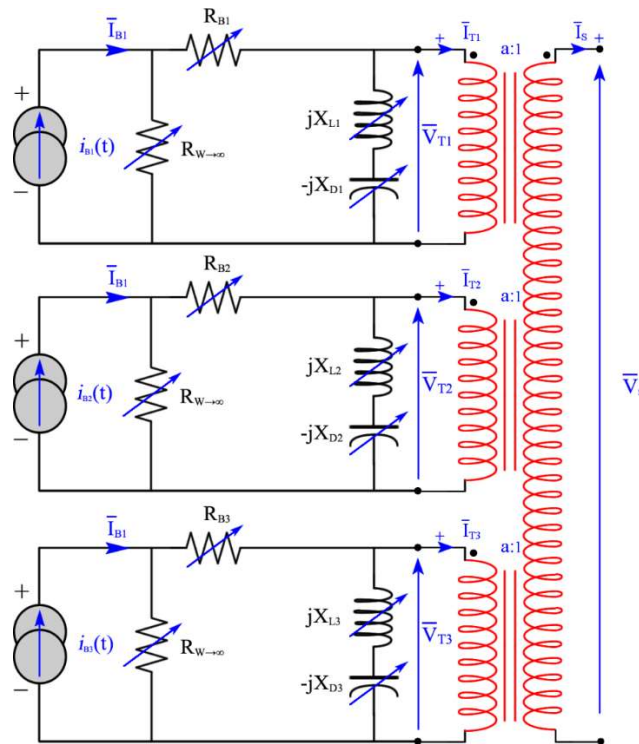

Figure IV-12 Equivalent electric diagram for a three-blade DT-VAWT.

Because the rotor has three blades, the angle between two blades is $\frac{2\pi}{3}$. If we assume

a constant wind flow, then the blades are subject to the same current vector with their

respective phase delays. Assuming that the rotor turns in the forward rotational direction, we

can write:

$$\left|\overline{I}_{B1}\right|=\left|\overline{I}_{B2}\right|=\left|\overline{I}_{B3}\right|;\ \arg\left(\overline{I}_{B2}\right)=\arg\left(\overline{I}_{B1}\right)-\frac{2\pi}{3}\ \text{and}\ \arg\left(\overline{I}_{B3}\right)=\arg\left(\overline{I}_{B1}\right)+\frac{2\pi}{3}.$$

Then, the following matrix can be obtained:

$$\begin{pmatrix}\overline{V}_{B1}\\\overline{V}_{B2}\\\overline{V}_{B3}\end{pmatrix}=\mathrm{Im}\begin{pmatrix}\overline{Z}_{B_1}&0&0\\0&\overline{Z}_{B_2}&0\\0&0&\overline{Z}_{B_3}\end{pmatrix}\begin{pmatrix}\overline{I}_{B1}\\\overline{I}_{B2}\\\overline{I}_{B3}\end{pmatrix} \tag{17}$$

Considering the operator $\overline{a}=1\angle120$, we have $\overline{I}_{B2}=\overline{a}^2\cdot\overline{I}_{B1}$ and $\overline{I}_{B3}=\overline{a}\cdot\overline{I}_{B1}$. Thus,

the voltage vectors for the three-blade rotor can be written as follows:

$$\begin{pmatrix}\overline{V}_{B1}\\\overline{V}_{B2}\\\overline{V}_{B3}\end{pmatrix}=\mathrm{Im}\begin{pmatrix}\overline{Z}_{B_1}&0&0\\0&\overline{Z}_{B_2}&0\\0&0&\overline{Z}_{B_3}\end{pmatrix}\begin{pmatrix}1\\\overline{a}^2\\\overline{a}\end{pmatrix}\overline{I}_{B1} \tag{18}$$

$$\begin{pmatrix}\overline{S}_{B1}\\\overline{S}_{B2}\\\overline{S}_{B3}\end{pmatrix}=\begin{pmatrix}\overline{V}_{B1}\\\overline{V}_{B2}\\\overline{V}_{B3}\end{pmatrix}\times\begin{pmatrix}\overline{I}_{S1}^*\\\overline{I}_{S2}^*\\\overline{I}_{S3}^*\end{pmatrix}=\begin{pmatrix}\overline{V}_{B1}\\\overline{V}_{B2}\\\overline{V}_{B3}\end{pmatrix}\times\begin{pmatrix}1\\\overline{a}^2\\\overline{a}\end{pmatrix}\overline{I}_{S1}^* \tag{19}$$

Following Figure 4, the apparent power representing the contribution of the whole

rotor to the shaft power can be obtained by adding the power produced by the three blades

separately:

$$\overline{S}_T = \overline{V}_T \overline{I}_S^* = (\overline{V}_{B1} + \overline{V}_{B1} + \overline{V}_{B1})\overline{I}_S^*$$

(20)

Finally:

$$\overline{S}_T = \left(\overline{Z}_{B_1} + \overline{Z}_{B_2}\overline{a}^2 + \overline{Z}_{B_3}\overline{a}\right)\left|\overline{I}_S\right|^2$$

(21)

The voltage produced by a sectional element of a single blade varies with its azimuth position and relative radius and height. The curved blade is discretized into n blade elements, as suggested in [14], and the average power produced by a blade element for a complete revolution of the turbine is obtained by integrating the elementary power with respect to θ.

$$S_B = \frac{1}{2\pi}\int_0^{2\pi} \overline{s}(\omega t)d(\omega t)$$

(22)

For different blades, the blades elements at the same high will produce the same power. We can then write:

$$S_B = S_{B1} = S_{B2} = S_{B3} = \frac{1}{2\pi}\int_0^{2\pi}\left((r\omega)(X_D - X_L)\Psi\right)d\theta_b$$

(23)

That is:

$$S_B = \frac{1}{2\pi}\int_0^{2\pi}\left[(r\omega)(X_D - X_L)\left(\frac{1}{2}\rho W_0^2\left(\left(\frac{\omega R}{W_0} + \sin\theta_b\right)^2 + \left(\cos\theta_b\right)^2\left(\cos\eta\right)^2\right)\right)\right]d\theta_b .$$

(24)

We the obtain:

$$S_B = \frac{1}{2}\rho W_0^2 \cdot \frac{r\omega}{2\pi}\int_0^{2\pi}\left[(X_{D_i} - X_{L_i})\left(\left(\frac{\omega R}{W_0} + \sin\theta_b\right)^2 + \left(\cos\theta_b\right)^2\left(\cos\eta\right)^2\right)\right]d\theta_b$$

(25)

149

Finally, the total average power produced by sectional element of the rotor is obtained by adding the power from each of the three blades.

$$S_T = 3S_B = \frac{3}{2}\rho W_0^2 \cdot \frac{r\omega}{2\pi} \int_0^{2\pi} \left[\left(X_{D_i} - X_{L_i}\right)\left(\left(\frac{\omega R}{W_0} + \sin\theta_b\right)^2 + \left(\cos\theta_b\right)^2 \left(\cos\eta\right)^2\right)\right] d\theta_b \tag{26}$$

4.4.2. Simulation Results

This section presents the results of the Tchakoua model for a three-blade DT-VAWT. The simulations were performed in MATLAB using data for NACA0012 that was obtained from different literature sources [37–39] with Reynolds numbers ranging from 500,000 to approximately 750,000. We choose the NACA0012 blade profile because it is one of the most studied and most commonly used profiles [39] Finally, the simulation results were assessed using results from the literature [40].

The simulation characteristics of the rotor were taken from [34] and are presented in Table IV-2.

Table IV-2   Blade simulation characteristics.

Number of Blades	3
Aerofoil section	NACA0012
Blade's average Reynolds number	40,000
Aerofoil chord length	9.14 cm
Rotor tip speed	45.7 cm/s
Tip speed ratio	5
Chord-to-radius ratio	0.15

a) *Simulation Results for Current Sources*

Figure IV-13 shows the current variations for each blade. These variations are similar to those of AOA as a function of the rotational angle of the blade. In addition, the incident current for a given blade is at a maximum when its AOA is at a maximum; similarly, the incident current is minimal or zero when the AOA is minimal or zero. Furthermore, the incident currents appear similar to the alternating current of a symmetric three-phase power supply system with the same frequency and voltage amplitudes relative to a common reference but with a phase difference that is one-third of the period.
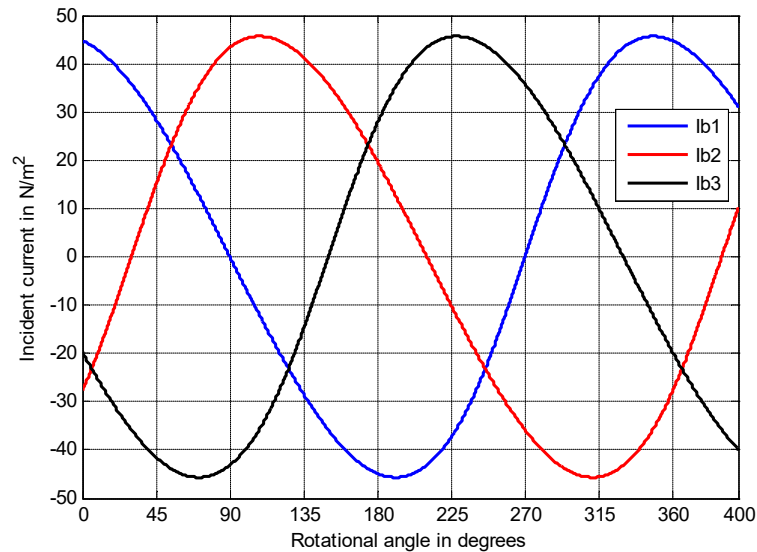

Figure IV-13 Incident current variations as functions of the rotational angle.

b) *Variations of the Resistances and Reactances in the Model*

The total normal and resistive components of the blade impedance R_b and the total tangential and reactive components of the blade impedance X_b are plotted using the relations in Equations (4) and (5). Figure IV-14 and Figure IV-15 show the variations of R_b and X_b for the three blades as functions of the rotational angle.
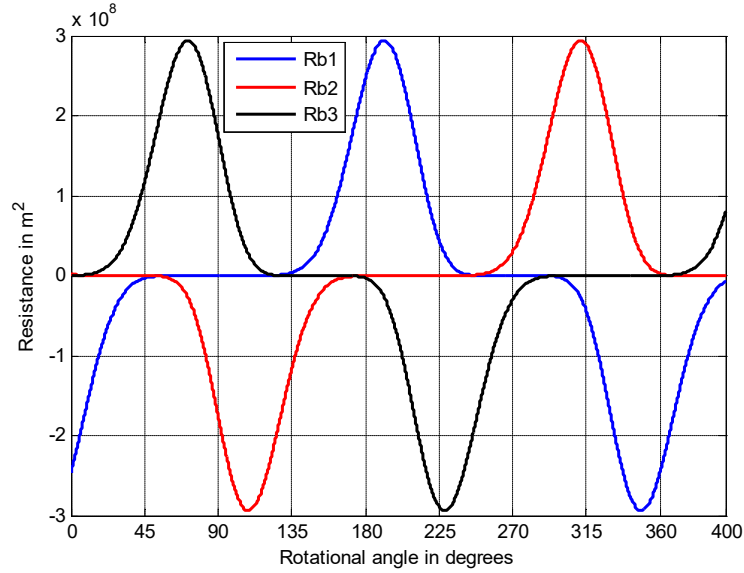
Figure IV-14 Variations of the blade total resistance as a function of the rotational angle.
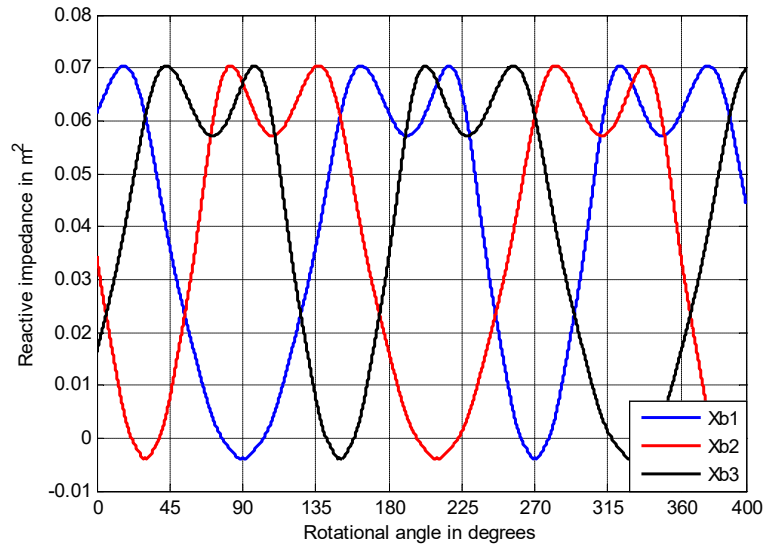
Figure IV-15 Variations of the blade reactance as a function of the rotational angle.

For a given blade, the resistance is zero when the blade rotational angle corresponds

to wind incident angle equal to zero, that is a shortly before $\theta = \dfrac{\pi}{2}$ and $\theta = \dfrac{3\pi}{2}$ for B1. At these

positions, the blade is parallel to the wind flow streamtubes, and the incident angle is

therefore zero. In addition, the blade's B1 resistance is at a maximum when corresponding

wind incident angle is minims, which corresponds to a position close to 190° from the reference point for these blade positions, the blades are perpendicular to the wind flow streamtubes, and the incident angle is at its maximum. Furthermore, the resistances vary between positive and negative quantities. According to our model inspired from double-multiple multi-streamtube models, the resistance of the blade to the wind flow is considered to be positive in the upwind disk and negative in the downwind disk.

The reactance of B1 is minimal when it is at $\theta = \dfrac{\pi}{2}$ and $\theta = \dfrac{3\pi}{2}$. At these positions, the blade is parallel to the wind flow streamtubes, and the incident angle is therefore zero; thus, the contribution of the wind to the torque production is negligible. Starting from $\theta = \dfrac{\pi}{2}$, the blade reactance continues to increase reaching two maximums respectively at 160° and 220°. At between 160° and 220°, a valley appears that is caused by dynamic stall, which occurs when an aerofoil, operating in unsteady flow, overcomes the static stall angle. For a VAWT with a fixed blade geometry in unsteady flow and a given induction factor, the angle of attack is a function of the azimuth angle; for $\lambda < 5$, the angle of attack can overcome the static stall angle, causing dynamic stall. During dynamic stall, large leading edge separated vortices are formed, delaying lift loss until they are convected over the surface results in a rapid decrease in lift.

c) *Variations of the Normal and Tangential Voltages*

Figure IV-16 and Figure IV-17 plot the normal and tangential voltage variations as functions of the blade position, respectively.

The normal voltage produced by the blade during a complete rotation varies from zero to a minimal value. All the normal voltages are negative quantities at any instant of

blade rotation because they stem from the drag coefficient and constitute obstructions to the blade rotation, meaning that they are negative contributions to the torque production. During a complete rotation of the reference blade, there are two minimums at rotational angles for which the angle of attack is zero at 190° and 350°. The negative value of the resistance matches the contribution of this impedance element in the blade movement and thus in the torque production.
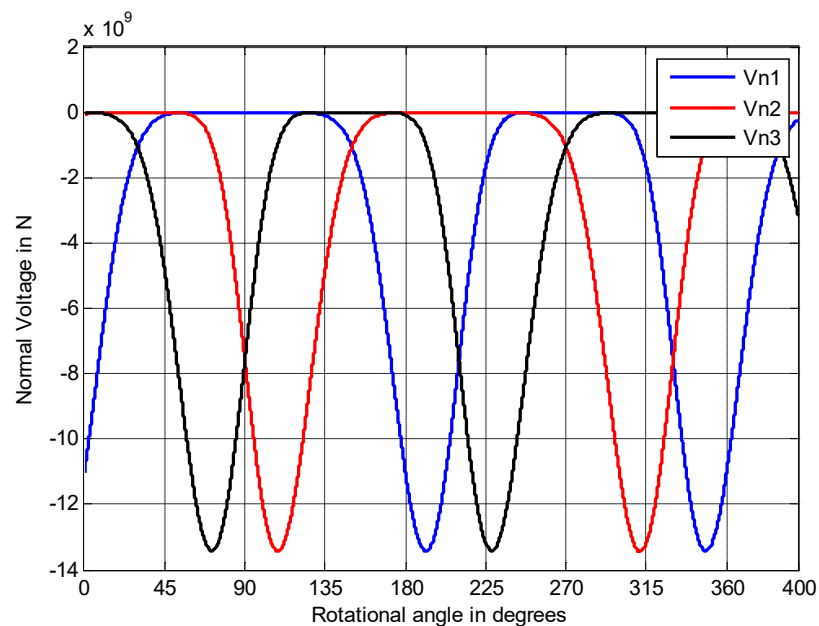

Figure IV-16 Normal voltage variations of the blade as a function of the rotational angle.

The tangential voltage produced by the blade during a complete rotation varies following an alternative and 2π periodic signal. During a complete rotation of the blade, the tangential voltage is equal to zero at $\frac{\pi}{2}$ and $\frac{2\pi}{3}$; these points are also inflexion points that correspond to angles for which the tangential impedance is zero. Similar to the tangential impedance, a valley occurs between 160° and 220° due to dynamic stall. The total voltage produced by the rotor is obtained by adding the voltages produced by the blades. As shown

in Figure 17, the total voltage is an alternative and $\frac{2\pi}{3}$ periodic signal is not equal to zero because at any moment, the blade voltage is an unbalanced three-phase system. The effect of dynamic stall can also be observed for the total voltage at $\frac{\pi}{2}$ and every $\frac{2\pi}{3}$ after this point.
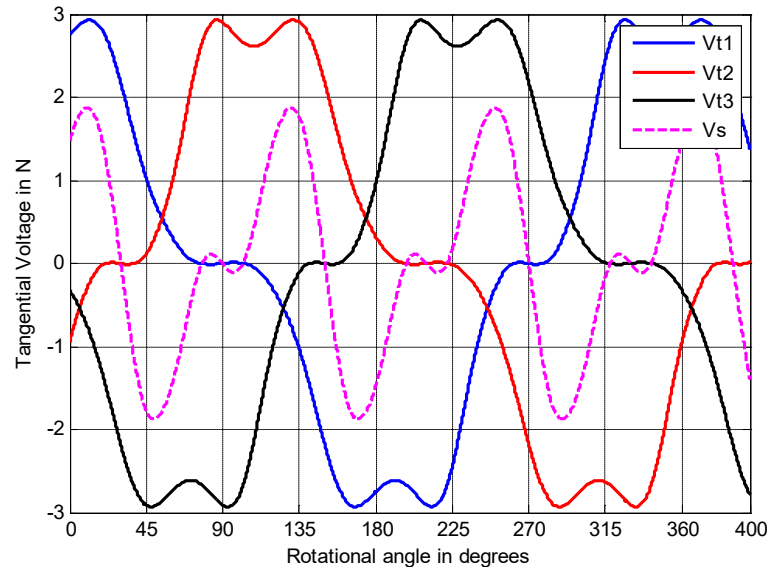

Figure IV-17 Tangential voltage variations of the blades as a function of the rotational angle.

d) *Power Variations Produced as a Function of the Rotational Angle*

The power produced by individual blades and the total power produced by the whole rotor are plotted in Figure IV-18. These results agree with findings in [32,35,41-43]. The power produced by each blade is always positive and is a variable and periodic quantity with a period of π. The power produced by a blade varies similar to the reactance with negative reactance producing positive power. A phase difference of $\frac{2\pi}{3}$ exists between the powers of the three blades. The total power for the rotor is always a positive quantity; is variable and periodic with a period of $\frac{2\pi}{3}$. The results obtained show strong agreement with results from both aerodynamic and CFD models in the literature.
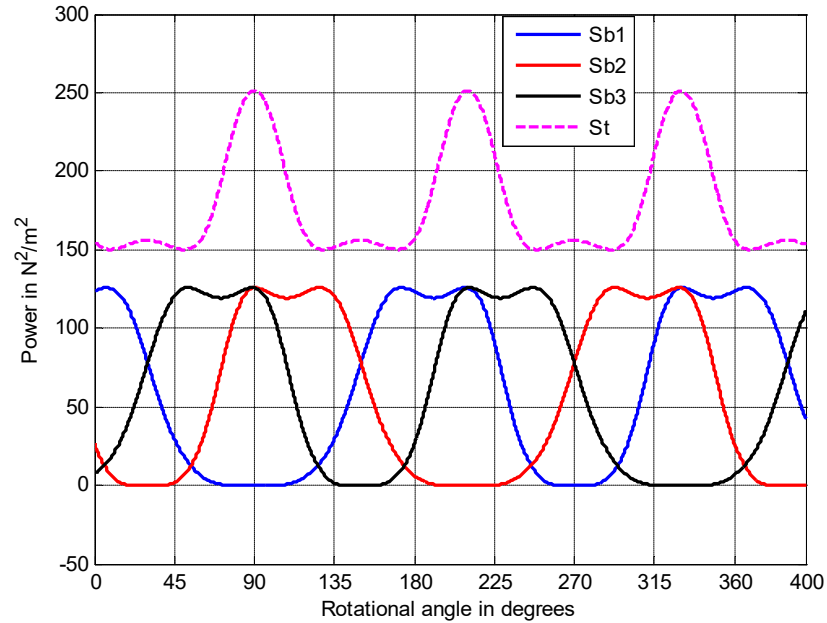
155

Figure IV-18 Power produced by the blades as a function of the rotational angle.

The normal and tangential voltages are both periodic values that undergo important variations during rotor rotation. The total tangential voltage produces the total torque.

4.5 CONCLUSIONS

In this paper, an electric circuit model for a three-blade DT-VAWT rotor is proposed. The new Tchakoua model is based on a new approach for modelling DT-VAWT rotors using the mechanical-electrical analogy. Indeed, the construction of this novel model is further to the proof-of-concept demonstration of the relevancy of modelling VAWTs rotors using electrical equivalent circuit analogy that was performed in previous research work. The model is based on an analogy with the double multiple streamtube model and was obtained by combining the equivalent electrical models for the wind, the three blades and the mechanical coupling. For validation, simulations were conducted using MATLAB for a three-bladed rotor. Results obtained for models outputs such as voltages and power are

consistent with findings of the Paraschivoiu double-multiple streamtube model as well as Frank Scheurich among others.

The Tchakoua model is more appropriate for the design, performance prediction and optimization of Darrieus rotors. Mechanical fault diagnosis and prognosis are also important because the model can be used to simulate rotor behaviour in the event of mechanical faults in one or more of the blades or in the rotor-shaft coupling elements. The model can also simulate turbine operation in the event of mechanical faults in one or more rotor elements. The simulations were conducted in MATLAB, and the results show high accuracy with the Paraschivoiu model as well as other results in the literature.

Despite the very simple design philosophy of VAWTs, their aerodynamics presents several challenges. The main feature of VAWTs is that the effective angle of attack "seen" by the blades undergoes a very large variation that in moderate to low tip speed conditions drives the blades into stall for both negative and the positive angles of attack. In future works, we intend to implement the Tchakoua model in simulation tools such as MATLAB Simulik or P-SPICE to study the effects of varying angles of attack within the post-stall region on flow unsteadiness and dynamic stall phenomena. The model could be extended to other types of wind turbines including horizontal axis wind turbines, Savonious-type VAWTs and hybrid Darrius-Savonius VAWTs. Additionally, the Tchakoua model will be used to study the influence of wind flow turbulence on turbine vibrations. Transitional (starting) and permanent sate functioning of VAWTs may also be examined. Finally, we intend to use the model to study the impact of structural faults in one or more blades on a DT-VAWT. As a long-term goal, the Tchakoua model will be linked to existing models of other electrical and mechanical wind turbine parts to obtain a global Darrieus-type WECS model.

Author Contributions: Pierre Tchakoua is the main author of this work. This paper further elaborates on some of the results from his Ph.D. dissertation. René Wamkeue and Mohand Ouhrouche supervised the project and supported Pierre Tchakoua's research in terms of both scientific and technical expertise. Gabriel Ekemb and Ernesto Benini assisted in the results analysis and interpretation. The manuscript was written by Pierre Tchakoua and was reviewed and revised by René Wamkeue, Mohand Ouhrouche and Ernesto Benini.

Conflicts of Interest: The authors declare no conflicts of interest.

Reference

1. Tilmans, H.A. Equivalent circuit representation of electromechanical transducers: I. Lumped-parameter systems. *J. Micromech. Microeng.* **1996**, *6*, 157–176.

2. Mason, W. An electromechanical representation of a piezoelectric crystal used as a transducer. *Proc. Inst. Radio Eng.* **1935**, *23*, 1252–1263.

3. Tilmans, H.A. Equivalent circuit representation of electromechanical transducers: II. Distributed-parameter systems. *J. Micromech. Microeng.* **1997**, *7*, 285–309.

4. Barakati, S.M. Modeling and Controller Design of a Wind Energy Conversion System Including a Matrix Converter. Ph.D. Thesis, University of Waterloo, Waterloo, ON, Canada, 2008.

5. Kim, H.-W.; Kim, S.-S.; Ko, H.-S. Modeling and control of PMSG-based variable-speed wind turbine. *Electr. Power Syst. Res.* **2010**, *80*, 46–52.

6. Borowy, B.S.; Salameh, Z.M. Dynamic response of a stand-alone wind energy conversion system with battery energy storage to a wind gust. *IEEE Trans. Energy Conve.* **1997**, *12*, 73–78.

7. Delarue, P.; Bouscayrol, A.; Tounzi, A.; Guillaud, X.; Lancigu, G. Modelling, control and simulation of an overall wind energy conversion system. *Renew. Energy* **2003**, *28*, 1169–1185.

8. Slootweg, J.; Haan, S.D.; Polinder, H.; Kling, W. General model for representing variable speed wind turbines in power system dynamics simulations. *IEEE Trans. Power Syst.* **2003**, *18*, 144–151.

9. Junyent-Ferré, A.; Gomis-Bellmunt, O.; Sumper, A.; Sala, M.; Mata, M. Modeling and control of the doubly fed induction generator wind turbine. *Simul. Model. Pract. Theory* **2010**, *18*, 1365–1381.

10. Bolik, S.M. *Modelling and Analysis of variable Speed Wind Turbines with induction Generator during Grid Fault;* Aalborg Universitet: Aalborg, Denmark, 2004.

11. Perdana, A. *Dynamic Models of Wind Turbines;* Chalmers University of Technology: Göteborg, Sweden, 2008.

12. Tchakoua, P.; Ouhrouche, M.; Tameghe, T.A.; Ekemb, G.; Wamkeue, R.; Slaoui-Hasnaoui, F. Basis of theoretical formulations for new approach for modelling darrieus-type vertical axis wind turbine rotors using electrical equivalent circuit analogy. In proceedings of the 2015 IEEE 3rd International Renewable and Sustainable Energy Conference, Marrakech & Ouarzazate, Morocco, 10–13 December 2015; pp. 1–7.

13. Tchakoua, P.; Ouhrouche, M.; Tameghe, T.A.; Ekemb, G.; Wamkeue, R.; Slaoui-Hasnaoui, F. Development of equivalent electric circuit model for darrieus-type vertical axis wind turbine rotor using mechanic-electric analogy approach. In proceeding of the 2015 IEEE 3rd International Renewable and Sustainable Energy Conference, Marrakech & Ouarzazate, Morocco, 10–13 December 2015; pp. 1–8.

14. Tchakoua, P.; Wamkeue, R.; Ouhrouche, M.; Tameghe, T.A.; Ekemb, G. A new approach for modeling Darrieus-type vertical axis wind turbine rotors using electrical

equivalent circuit analogy: Basis of theoretical formulations and model development. *Energies* **2015**, *8*, 10684–10717.

15. Eriksson, S.; Bernhoff, H.; Leijon, M. Evaluation of different turbine concepts for wind power. *Renew. Sustain. Energy Rev.* **2008**, *12*, 1419–1434.

16. Tjiu, W.; Marnoto, T.; Mat, S.; Ruslan, M.H.; Sopian, K. Darrieus vertical axis wind turbine for power generation I: Assessment of Darrieus VAWT configurations. *Renew. Energy* **2015**, *75*, 50–67.

17. Bedon, G.; Castelli, M.R.; Benini, E. Optimal spanwise chord and thickness distribution for a Troposkien Darrieus wind turbine. *J. Wind Eng. Ind. Aerodyn.* **2014**, *125*, 13–21.

18. Tchakoua, P.; Wamkeue, R.; Tameghe, T.A.; Ekemb, G. A review of concepts and methods for wind turbines condition monitoring. In Proceedings of the 2013 IEEE World Congress on Computer and Information Technology (WCCIT), Sousse, Tunisia, 22–24 June 2013; pp 1–9.

19. Tchakoua, P.; Wamkeue, R.; Slaoui-Hasnaoui, F.; Tameghe, T.A.; Ekemb, G. New trends and future challenges for wind turbines condition monitoring. In Proceeding of the 2013 IEEE International Conference on Control, Automation and Information Sciences (ICCAIS), Nha Trang, Vietnam, 25–28 November 2013; pp. 238–245.

20. Tchakoua, P.; Wamkeue, R.; Ouhrouche, M.; Slaoui-Hasnaoui, F.; Tameghe, T.A.; Ekemb, G. Wind turbine condition monitoring: State-of-the-art review, new trends, and future challenges. *Energies* **2014**, *7*, 2595–2630.

21. Yang, W.; Tavner, P.J.; Crabtree, C.J.; Wilkinson, M. Cost-effective condition monitoring for wind turbines. *IEEE Trans. Ind. Electron.* **2010**, *57*, 263–271.

22. Yang, W.; Jiang, J.; Tavner, P.; Crabtree, C. Monitoring wind turbine condition by the approach of Empirical Mode Decomposition. In Proceedings of the 2008 International Conference on Electrical Machines and Systems (ICEMS), Wuhan, China, 17–20 October 2008; pp 736–740.

23. Yang, W.; Tavner, P.; Crabtree, C.; Wilkinson, M. Research on a simple, cheap but globally effective condition monitoring technique for wind turbines. In Proceedings of

the 2008 International Conference on Electrical Machines and Systems (ICEMS), Wuhan, China, 17–20 October 2008; pp 1–5.

24. Lewis, J.W. *Modeling Engineering Systems: PC-Based Techniques and Design Tools*; High Text Publications: San Diego, CA, USA, 1994.

25. Hogan, N.; Breedveld, P. The physical basis of analogies in network models of physical system dynamics. *Simul. Ser.* **1999**, *31*, 96–104.

26. Olson, H.F. *Dynamical Analogies;* Van Nostrand: Princeton, NJ, USA, 1958.

27. Firestone, F. The mobility method of computing the vibration of linear mechanical and acoustical systems: mechanical-electrical analogies. *J. Appl. Phys.* **1938**, *9*, 373–387.

28. Calvo, J.A.; Alvarez-Caldas, C.; San, J.L. *Analysis of Dynamic Systems Using Bond Graph Method through SIMULINK*; INTECH Open Access Publisher: Rijeka, Croatia, 2011.

29. Firestone, F. A new analogy between mechanical and electrical systems. *J. Acoust. Soc. Am.* **1933**, *4*, 249–267.

30. Bishop, R.H. *Mechatronics: An Introduction*; CRC Press: Boca Raton, FL, USA, 2005.

31. Zhang, L.; Liang, Y.; Liu, X.; Jiao, Q.; Guo, J. Aerodynamic performance prediction of straight-bladed vertical axis wind turbine based on CFD. *Adv. Mech. Eng.* **2013**, *5*, doi:10.1155/2013/905379.

32. Paraschivoiu, I. *Wind Turbine Design: With Emphasis on Darrieus Concept*; Presses Inter Polytechnique: Montreal, QC, Canada, 2002.

33. Islam, M.; Ting, D.S.-K.; Fartaj, A. Aerodynamic models for Darrieus-type straight-bladed vertical axis wind turbines. *Renew. Sustain. Energy Rev.* **2008**, *12*, 1087–1109.

34. Scheurich, F.; Fletcher, T.M.; Brown, R.E. Simulating the aerodynamic performance and wake dynamics of a vertical-axis wind turbine. *Wind Energy* **2011**, *14*, 159–177.

35. Beri, H.; Yao, Y. Double multiple streamtube model and numerical analysis of vertical axis wind turbine. *Energy Power Eng.* **2011**, *3*, 262–270.

36. Claessens, M.C. The Design and Testing of Airfoils for Application in Small Vertical Axis Wind Turbines. Master's Thesis, Delft University of Technology, Delft, The Netherlands, 2006.

37. Sheldahl, R.E.; Klimas, P.C. *Aerodynamic Characteristics of seven Symmetrical Airfoil Sections through 180-Degree Angle of Attack for Use in Aerodynamic Analysis of Vertical Axis Wind Turbines;* Technical Report; Sandia National Labs: Albuquerque, NM, USA, 1981.

38. Critzos, C.C.; Heyson, H.H.; Boswinkle, R.W. *Aerodynamic Characteristics of NACA 0012 Airfoil Section at Angles of Attack from 0 to 180 Degrees*; National Advisory Committee for Aeronautics: Washington, DC, USA, 1955.

39. Miley, S.J. *A Catalog of Low Reynolds Number Airfoil Data for Wind Turbine Applications*; National Technical Information Service: Alexandria, VA, USA, 1982.

40. Timmer, W. *Aerodynamic Characteristics of Wind Turbine Blade Airfoils at High Angles-of-Attack*; European Wind Energy Association: Brussels, Belgium, 2010.

41. Li, S.; Li, Y. Numerical study on the performance effect of solidity on the straight-bladed vertical axis wind turbine. In Proceedings of the 2010 Asia-Pacific Power and Energy Engineering Conference (APPEEC), Chengdu, China, 28–31 March 2010; pp 1–4.

42. Attia, E.; Saber, H.; Gamal, H.E. Analysis of straight bladed vertical axis wind turbine. *Int. J. Eng. Res. Technol.* **2015**, *4*, doi:10.1007/s11630-014-0712-8.

43. Scheurich, F.; Brown, R.E. Modelling the aerodynamics of vertical-axis wind turbines in unsteady wind conditions. *Wind Energy* **2013**, *16*, 91–107.

Chapter V

CONCLUSION AND RECOMMENDATIONS

5.1. Conclusion

The aerodynamic characteristics of vertical-axis wind turbines are somewhat more complex compared to those of horizontal-axis configurations and are partially responsible for the fact that industrial and academic research has focused primarily on horizontal-axis turbines in the past decades. This has had the result that vertical-axis wind turbines are still relatively poorly understood compared to horizontal-axis wind turbines. However, vertical-axis wind turbines are becoming ever more important in wind power generation thanks to their compactness and adaptability for domestic installations. Furthermore, it is well known that VAWTs have poor efficiency, especially compared to HAWTs.

The blades are governing the turbine's efficiency and their power output is primarily given by their design. The challenges in vertical axis wind turbines have not yet been all mastered. The accurate modelling of the aerodynamics of vertical-axis wind turbines poses a significant challenge as past experiences showed that good rotor modelling for accurate condition monitoring has not reached a matured and reliable state of the art. The cyclic motion of the turbine induces large variations in the angle of attack on the blades of the rotor that result in significant unsteadiness in the blade aerodynamic loading and can manifest as dynamic stall. In addition, aerodynamic interactions occur between the turbine blades and the wake that is generated by the rotor.

Commencing this research, an inventory and classification of WTCMTs highlighted the fact that a combination of preventive and reactive maintenance strategies can improve reliability, availability, and maintainability of WTs while reducing maintenance costs. Also, a quick literature survey was performed on most used models and presented the relevant features as well as the advantages and shortcoming for each model category.

The object of the current PhD thesis was to contribute to the development of new tools, techniques and methods to improve the design, optimization, diagnosis, prognosis and monitoring of Darrieus vertical axis wind turbines to better ensure their maintenance.

A new approach for modeling Darrieus-type VAWT rotors using the electric-mechanic analogy was presented based on double multiple streamtube model. A proof-of-concept demonstration of the approach attested the feasibility of such a model through both step-by-step demonstrations of the theoretical and practical concepts that underpin the new model and simulations and cross validation of a single blade.

Then, an electric circuit model for a three-blade DT-VAWT rotor was developed. The so called Tchakoua model was obtained by combining the equivalent electrical models for the wind, the three blades and the mechanical coupling. For validation, simulations were for single blade using MATLAB and cross validation was done with findings of existing models. Various simulations for the VAWT three-bladed rotor were also perform in MATLAB. Outputs variables such as voltages and power are consistent with findings of the Paraschivoiu double-multiple streamtube model as well as Frank Scheurich among others.

5.2. RECOMMENDATIONS

The new model built in this thesis could be more suitable for the supervision and diagnosis of AVEs for better maintenance. However, as any new model, this model can be improved and upgrade to make it more realistic. Because not all the objectives of the project were fulfilled, some future work is necessary to be done:

- Upgrade the model by improving wind modeling. Indeed, the current modulization considers wind flow to be of constant direction and intensity which is far from reality. An improved wind model would consider the different turbulences in the wind flow.

- Use the new model to study the effects of varying angle of attack in the aerodynamic stall region and the instability generated.

- Use the model to study the impact of structural faults on one or more blades on the quality of wind turbine electrical production.

- Build default models for VAWTs rotors including for cases of mass imbalance and blades aerodynamic asymmetry.

- Finally, as a long-term goal, the model will be assembled with existing electrical models of other electrical and mechanical parts of VAWTs to build a global equivalent electrical model of the wind-energy conversion system. This global model will open the way for the study of certain phenomena from a macroscopic point of view. It would also be interesting to extend this modeling approach and apply it to other types of wind turbines such as horizontal axis wind turbines, Savonious wind turbines and Darrieus Savonius hybrid wind turbines.

Appendix A

The research work done in this PhD thesis has already broth to the publication of the following papers.

❖ **Conference papers**

- TCHAKOUA, Pierre, WAMKEUE, René, TAMEGHE, Tommy Andy, Gabriel Ekenb. A review of concepts and methods for wind turbines condition monitoring. In :Computer and Information Technology (WCCIT), 2013 World Congress on. IEEE, 2013. p. 1-9.

- TCHAKOUA, Pierre, WAMKEUE, René, Fouad, Slaoui-Hasnaoui, F., Tameghe, T. A., & Ekemb, G., New trends and future challenges for wind turbines condition monitoring. In :Control, Automation and Information Sciences (ICCAIS), 2013 International Conference on. IEEE, 2013. p. 238-245.

- TCHAKOUA, Pierre, WAMKEUE, René, SLAOUI-HASNAOUI, Fouad, et al. Basis of Theoretical Formulations for New Approach for Modelling Darrieus-Type Vertical Axis Wind Turbine Rotors using Electrical Equivalent Circuit Analogy. In : 2015 3rd International Renewable and Sustainable Energy Conference (IRSEC). 10-13 Décembre 2015 Marrakech, Morocco.

- TCHAKOUA, Pierre, WAMKEUE, René, SLAOUI-HASNAOUI, Fouad, et al. Development of Equivalent Electric Circuit Model for Darrieus-Type Vertical Axis Wind Turbine Rotor using Mechanic - Electric Analogy Approach. In : 2015 3rd International Renewable and Sustainable Energy Conference (IRSEC). 10-13 Décembre 2015 Marrakech, Morocco.

- Tchakoua, P.; Wamkeue, R.; Ouhrouche, M.; Tameghe, T.A.; Ekemb, G. An Electric Circuit Model for Darrieus-Type Vertical Axis Wind Turbine Rotors: The Tchakoua Model . In : 2016 4th International Renewable and Sustainable Energy Conference (IRSEC). 14-17 November 2016 Marrakech, Morocco

❖ **Journal papers**

- TCHAKOUA, Pierre, WAMKEUE, René, OUHROUCHE, Mohand, Slaoui-Hasnaoui, F., Tameghe, T. A., & Ekemb, G., Wind turbine condition monitorage:

State-of-the-art review, new trends, and future challenges. Energies, 2014, vol. 7, no 4, p. 2595-2630.

- Tchakoua, P.; Wamkeue, R.; Ouhrouche, M.; Tameghe, T.A.; Ekemb, G. A New Approach for Modeling Darrieus-Type Vertical Axis Wind Turbine Rotors Using Electrical Equivalent Circuit Analogy: Basis of Theoretical Formulations and Model Development. Energies 2015, 8, 10684-10717.
- Tchakoua, P.; Wamkeue, R.; Ouhrouche, M.; Benini, E.; Ekemb, G. Electric Circuit Model for the Aerodynamic Performance Analysis of a Three-Blade Darrieus-Type Vertical Axis Wind Turbine: The Tchakoua Model. Energies 2016, 9, 820.

❖ **Book chapter**

- Tchakoua, P., Wamkeue, R., Ouhrouche, M., Slaoui-Hasnaoui, F., Tameghe, T. A., & Ekemb, G., "Wind turbine condition monitoring: State-of-the-art review, new trends, and future challenges" dans "Wind Ressource and Future Enwergy Security: Enviromental, Social, and Econimic Issues", Edited by Muyiwa Adaramola, Apple Academic Press 2015, pp. 283 – 330